United Arab Emirates University

Scholarworks@UAEU

12-2019

MODELLING AND FAULT DIAGNOSIS APPROACH FOR PROTON EXCHANGE MEMBRANE FUEL CELL SYSTEMS INCORPORATING AMBIENT CONDITIONS

Saad Saleem Khan

United Arab Emirates University

College of Engineering

MODELLING AND FAULT DIAGNOSIS APPROACH FOR PROTON EXCHANGE MEMBRANE FUEL CELL SYSTEMS INCORPORATING AMBIENT CONDITIONS

Saad Saleem Khan

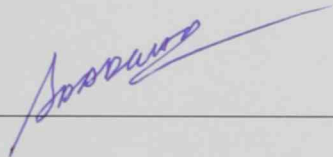This dissertation is submitted in partial fulfilment of the requirements for the degree of Doctor of Philosophy

Under the Supervision of Dr. Hussain Shareef

December 2019

Declaration of Original Work

I, Saad Saleem Khan, the undersigned, a graduate student at the United Arab Emirates University (UAEU), and the author of this dissertation entitled. "*Modelling and Fault Diagnosis Approach for Proton Exchange Membrane Fuel Cell Systems Incorporating Ambient Conditions*," hereby, solemnly declare that this dissertation is my own original research work that has been done and prepared by me under the supervision of Associate Professor Dr. Hussain Shareef, in the College of Engineering at UAEU. This work has not previously been presented or published, or formed the basis for the award of any academic degree, diploma or a similar title at this or any other university. Any materials borrowed from other sources (whether published or unpublished) and relied upon or included in my dissertation have been properly cited and acknowledged in accordance with appropriate academic conventions. I further declare that there is no potential conflict of interest with respect to the research, data collection, authorship, presentation and/or publication of this dissertation.

Student's Signature: _____   Date: ___8/12/2019___

Approval of the doctorate dissertation

This Doctorate Dissertation is approved by the following Examining Committee Members:

1) Advisor (Committee Chair): Dr. Hussain Shareef
    Title: Associate Professor
    Department of Electrical Engineering
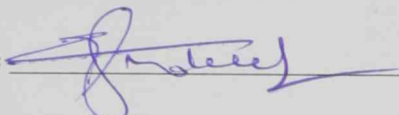   College of Engineering

    Signature _____   Date 8/12/2019

2) Member: Dr. Mohammad Shakeel
    Title: Professor
    Department of Electrical Engineering
    College of Engineering

    Signature _____   Date 8-12-2019

3) Member: Dr. Yaser E. Greish
    Title: Professor
    Department of Chemistry
    College of Science

    Signature _____   Date 8/12/2019

4) Member (External Examiner): Dr. Bahman Shabani
    Title: Associate Professor
    Department of Mechanical and Automotive Engineering
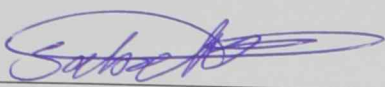   Institution: Royal Melbourne Institute of Technology (RMIT) Australia
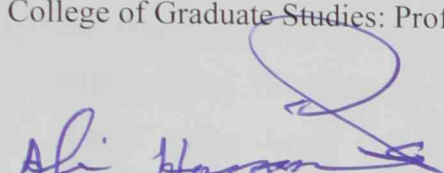
    Signature _____   Date 8/12/2019

This Doctorate Dissertation is accepted by:

Dean of the College of Engineering: Professor Sabah Alkass

Signature _____ Date _22/1/2020_

Dean of the College of Graduate Studies: Professor Ali Al-Marzouqi

Signature _____ Date _23/1/2020_

Copy _2_ of _5_

Advisory Committee

1) Advisor: Dr. Hussain Shareef

Title: Associate Professor

Department of Electrical Engineering

College of Engineering

2) Co-advisor: Dr. Addy Wahyudie

Title: Associate Professor

Department of Electrical Engineering

College of Engineering

Abstract

Proton exchange membrane fuel cell (PEMFC), as a source of electrical power, provides numerous benefits such as zero carbon emission and high reliability as compared to wind and solar energy. PEMFC operates at very low temperature, high power density and has very high durability as compared to other fuel cells. Being a non-linear power source with high sensitivity to ambient conditions variation, the prediction of PEMFC voltage and temperature is a complicated issue. The most common PEMFC models are classified as mechanistic model, semi-empirical model and purely empirical methods. The mechanistic models are complex and requires differential equations to predict the voltage and temperature of PEMFC. However, the semi-empirical models are less complicated and can be used easily for online prediction of PEMFC outputs. Therefore, the first part of this thesis attempt to model the voltage of PEMFC using simple and effective semi-empirical equations. The initial feature of the proposed technique is to incorporate the features of mechanistic model with less complex equations. The model considers the internal currents and the internal voltage drop associated with the PEMFC. Besides, activation and concentration voltage drops are addressed based on theoretical functions. Thus, the proposed model provides an additional benefit that not only output voltage model satisfy the voltage for both loaded and unloaded conditions but also the component voltage drops waveforms match with the theoretical waveforms given in the mechanistic models. The second part of the thesis focuses on modelling the PEMFC temperature. Previously most temperature models use complex equations incorporating PEMFC output voltage which is not a good option as the temperature must be predicted using only load current and ambient temperature. The model proposed in this thesis is developed through an algorithm which tracks the online changes in the load current and ambient temperature. It provides accurate temperature of PEMFC by using simple first order equation with the help of tracking algorithm. Quantum lightening search algorithm (QLSA) is used for optimization of constant parameters for both voltage and temperature models. The PEMFC performance is affected by factors such as variations in ambient temperature, pressure and air relative humidity and thus they are vital for predicting PEMFC performance. The thesis also attempts to directly predict the variations in PEMFC

voltage under varying ambient conditions at different load resistance. For this purpose, statistical analysis is used to propose empirical equations that can predict the variations in PEMFC voltage for varying ambient conditions. In this context of the model development, the parameters which are significantly varying with ambient changes are identified with the help of statistical regression analysis, and represented as ambient temperature and air relative humidity dependent parameters. The enhanced semi-empirical voltage model is verified by performing experiments on both the Horizon and NEXA PEMFC systems under different conditions of ambient temperature and relative humidity with root mean square error (RMSE) less than 0.5. Results obtained using the enhanced model is found to closely approximate those obtained using PEMFCs under various operating conditions, and in both cases, the PEMFC voltage is observed to vary with changes in the ambient and load conditions. Inherent advantages of the proposed PEMFC model include its ability to determine membrane-water content and water pressure inside PEMFCs. The membrane-water content provides clear indications regarding the occurrence of drying and flooding faults. For normal conditions, this membrane water content ranges between 12.5 to 6.5 for Horizon PEMFC system. Based on simulation results, a threshold membrane-water-content level is suggested as a possible indicator of fault occurrence under extreme ambient conditions. Limits of the said threshold are observed to be useful for fault diagnosis within the PEMFC systems.

Keywords: Proton exchange membrane fuel cell, modelling, semi-empirical, fault diagnosis, flooding, drying and algorithm.

Title and Abstract (in Arabic)

النمذجة والنُهُج الخاطئة للتشخيص في أنظمة الخلايا البروتينية للتبادل العضوي في االوقود ، بما في ذلك الشروط الطموحة

الملخص

تستخدم خلية وقود غشاء التبادل البروتوني (PEMFC) كمصدر للطاقة الكهربائية. إنه يوفر فوائد عديدة مثل الانبعاثات الكربونية الصفرية والموثوقية العالية بالمقارنة مع طاقة الرياح والطاقة الشمسية.مقارنة بخلايا الوقود الأخرى كونه مصدر الطاقة غير الخطية مع حساسية عالية لتباين الظروف المحيطة. تعمل PEMFC في درجات حرارة منخفضة للغاية وكثافة عالية للطاقة ولديها متانة عالية مقارنة بخلايا الوقود الأخرى. كونه مصدر الطاقة غير الخطية مع حساسية عالية لتغير الظروف المحيطة ، والتنبؤ PEMFC الجهد ودرجة الحرارة هي قضية معقدة. تصنف نماذج PEMFC الأكثر شيوعًا كنموذج ميكانيكي ونموذج شبه تجريبي وطرق تجريبية بحتة. النماذج الميكانيكية معقدة وتتطلب معادلات تفاضلية للتنبؤ بجهد ودرجة حرارة PEMFC. ومع ذلك ، فإن النماذج شبه التجريبية أقل تعقيدًا ويمكن استخدامها بسهولة للتنبؤ بنتائج PEMFC عبر الإنترنت. ومع ذلك ، فإن النماذج شبه التجريبية أقل تعقيدًا ويمكن استخدامها بسهولة للتنبؤ بنتائج PEMFC عبر الإنترنت. الميزة الأولى للتقنية المقترحة هي دمج ميزات النموذج الميكانيكي مع معادلات أقل تعقيدًا. يأخذ النموذج في الاعتبار التيارات الداخلية وانخفاض الجهد الداخلي المرتبط بـ PEMFC. إلى جانب ذلك ، تتم معالجة قطرات الجهد والتركيز استنادًا إلى الوظائف النظرية. وبالتالي ، يوفر النموذج المقترح فائدة إضافية ، حيث لا يفي نموذج الجهد الناتج فقط بالجهد لكل من الظروف التي تم تحميلها وتفريغها ، ولكن أيضًا أشكال موجات قطرات الجهد الكهربي تتطابق مع الأشكال الموجية النظرية الواردة في النماذج الميكانيكية. يركز الجزء الثاني من الرسالة على نمذجة درجة حرارة PEMFC. في السابق ، تستخدم معظم نماذج درجات الحرارة معادلات معقدة تشتمل على جهد إخراج PEMFC ، وهو ليس خيارًا جيدًا حيث يجب التنبؤ بدرجات الحرارة باستخدام درجة حرارة الحمل الحالية فقط. تم تطوير النموذج المقترح في هذه الرسالة من خلال خوارزمية تتعقب التغييرات عبر الإنترنت في درجة حرارة الحمل الحالية ودرجة الحرارة المحيطة. يوفر درجة حرارة دقيقة من PEMFC باستخدام معادلة بسيطة من الدرجة الأولى بمساعدة تتبع خوارزمية. تستخدم خوارزمية البحث عن البرق الكمومي (QLSA) لتحسين المعلمات الثابتة لكلا الطرازين ودرجات الحرارة. يتأثر أداء PEMFC بعوامل مثل

الاختلافات في درجة الحرارة المحيطة والضغط والرطوبة النسبية للهواء وبالتالي فهي ضرورية للتنبؤ بأداء PEMFC. تحاول الأطروحة أيضًا أن تتنبأ بشكل مباشر بالتغيرات في جهد PEMFC في ظل ظروف محيطة مختلفة في مقاومة تحميل مختلفة. لهذا الغرض ، يتم استخدام التحليل الإحصائي لاقتراح معادلات تجريبية يمكنها التنبؤ بالتغيرات في جهد PEMFC لمختلف الظروف المحيطة. في هذا السياق من تطوير النموذج ، يتم تحديد المعلمات التي تختلف اختلافًا كبيرًا مع التغيرات المحيطة بمساعدة تحليل الانحدار الإحصائي ، ويتم تمثيلها كمعلمات تعتمد على درجة الحرارة المحيطة والرطوبة النسبية للهواء. يتم التحقق من نموذج الجهد شبه التجريبي المحسن من خلال إجراء تجارب على كل من أنظمة Horizon و NEXA PEMFC في ظل ظروف مختلفة من درجة الحرارة المحيطة والرطوبة النسبية مع خطأ مربع الجذر المتوسط (RMSE) أقل من 0.5. تم العثور على النتائج التي تم الحصول عليها باستخدام النموذج المحسّن بشكل تقريبي لتلك التي تم الحصول عليها باستخدام PEMFCs في ظل ظروف التشغيل المختلفة ، وفي كلتا الحالتين ، لوحظ أن الجهد PEMFC يختلف مع التغيرات في الظروف المحيطة وظروف التحميل. تشمل الميزات المتأصلة في نموذج PEMFC المقترح قدرته على تحديد محتوى الماء الغشائي وضغط الماء داخل PEMFCs. يوفر محتوى الماء الغشائي مؤشرات واضحة فيما يتعلق بحدوث أخطاء التجفيف والفيضانات. بالنسبة للظروف العادية ، يتراوح محتوى الماء الغشائي بين 12.5 إلى 6.5 لنظام Horizon PEMFC. بناءً على نتائج المحاكاة ، يُقترح مستوى محتوى الغشاء المائي العتبة كمؤشر محتمل لحدوث العيوب في الظروف المحيطة القاسية. لوحظ أن حدود محتوى الماء الغشائي مفيدة لتشخيص الأعطال ضمن أنظمة PEMFC.

مفاهيم البحث الرئيسية: خلية وقود غشاء التبادل البروتوني ، النمذجة ، شبه التجريبية ، تشخيص الأعطال ، الفيضانات ، التجفيف ،الخوارزمية.

Acknowledgements

Dedication

To my beloved mother

Table of Content

List of Tables

List of Figures

List of Abbreviations

α	Charge Transfer Coefficient
α_i	Axial Points
A_{H2O}	Pressure of Water Constant
A_{cell}	Area of PEMFC
B_1	First Exchange Current Density Coefficient
B_2	Second Exchange Current Density Coefficient
β_{no}	Ratio of Concentration of Gases
C_f	Compensation Factor
C_1	Ionic Resistance Constant
C_{H2}	Specific Heat Capacity of Hydrogen
C_{O2}	Specific Heat Capacity of Oxygen
C_{H2O}	Specific Heat Capacity of Water
C_{FC}	Heat Capacity of Fuel Cell
CCD	Central Composite Design
E_{stack}	Emf of Stack
FC	Fuel Cell
ΔG	Gibbs Free Energy
h_{cell}	Convective Heat Transfer Coefficient
I_{lim}	Limiting Current
i_o	Exchange Current Density
LSA	Lightening Search Algorithm
l_m	Membrane Thickness
M_{FC}	Mass of Fuel Cell
N	Number of Fuel Cells in a Stack
N_{H2}	Rate of Consumption of Hydrogen
N_{O2}	Rate of Consumption of Oxygen
P_{air}	Ambient Air Pressure
P_{O2}	Partial Pressure of Oxygen
P_{H2}	Partial Pressure of Hydrogen
P_{N2}	Partial Pressure of Nitrogen
P_{H2O}	Pressure of Liquid Water

P_{an}	Anode Pressure
P_{vap}	Vapour Pressure
PSO	Particel Swarm Optimization
PEMFC	Proton Exchange Membrane Fuel Cell
q_{net}	Net Heat Energy
q_{chem}	Heat Energy Produced by Chemical Reaction
q_{loss}	Heat Energy Loss
q_{elec}	Electrical Energy
QLSA	Quantum Lightening Search Algorithm
R_{ionic}	Ionic Resistance
R_e	Electronic Resistance
RH_{air}	Relative Humidity of Air
R_c	Output Resistance
T_{amb}	Ambient Temperature in Kelvin
$T_{amb,c}$	Ambient Temperature in Celsius
T_{mod}	Modelled Temperature
V_{out}	Output Voltage
V_{act}	Activation Voltage Drop
V_{ohm}	Ohmic Voltage Drop
V_{conc}	Concentration Voltage Drop
V_{exp}	Experimental Voltage
$V_{no\text{-}load}$	No-load Voltage
V_{int}	Voltage Drop due to Internal Currents
x_{N_2}	Concentration of Nitrogen
x_{O_2}	Concentration of Oxygen
λ	Membrane Water Content
λ_b	Box-Cox Transformation Constant
φ	Relative Humidity of Fuel Cell

Chapter 1: Introduction

1.1 Research background

There are various energy sources that have been explored to date. Most of them are exhaustible energy sources such as oil, natural gas, and coal. Due to the increasing demand of energy and serious climate change threats, the world has decided to move towards renewable and alternate energy sources. By considering the serious threats to climate, a global agreement has been made in Paris to reduce the use of fossil fuels by all its member countries. The fossil fuel reserves in 2016 are given in Figure 1 for various countries/regions. (Johnsson, Kjärstad and Rootzén, 2018)
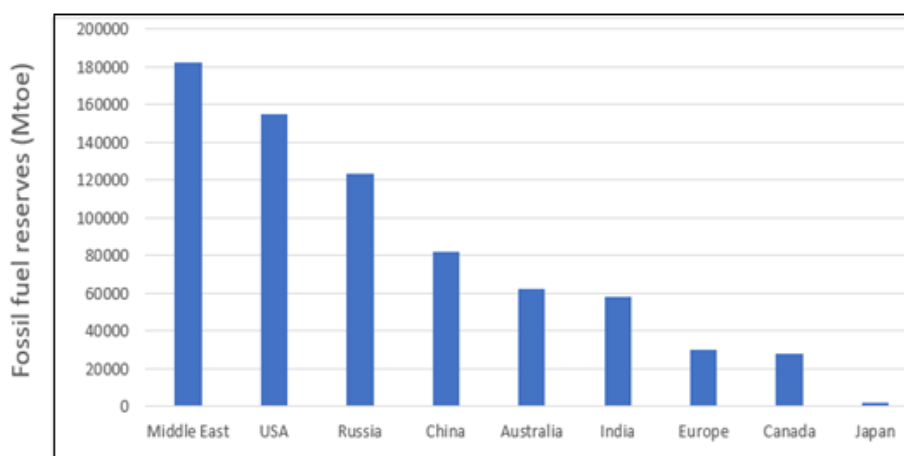
Figure 1: Fossil fuel reserves comparison for different countries/regions

UAE in 2010 was completely extracting its power from fossil fuels but by 2030 the plan is to extract most of the power from renewable/alternate energy sources. The report of International Renewable Energy Agency (IRENA) reveals the plan of UAE to move its energy demand from fossil fuels to renewable energy sources (Said, Alshehhi and Mehmood, 2018). Based on the plan, nuclear energy will take the major

portion of renewable electricity generation in UAE by 2030. Almost 44 Twh (terra-watt-hour) energy is planned to extract from nuclear energy sources (Said, Alshehhi and Mehmood, 2018). Due to high temperature produced in nuclear energy this energy can be used to produce Hydrogen from water in the process. Hydrogen is a very useful energy source because of its highest energy content by weight, so it is engaged as fuel in various applications such as power generation, electric vehicles (EV), aircraft and rockets, etc. (Manoharan et al., 2019; Yildiz and Kazimi, 2006). The efficient processes for Hydrogen production with the help of nuclear energy has been discussed in Figure 2 (Yildiz and Kazimi, 2006).
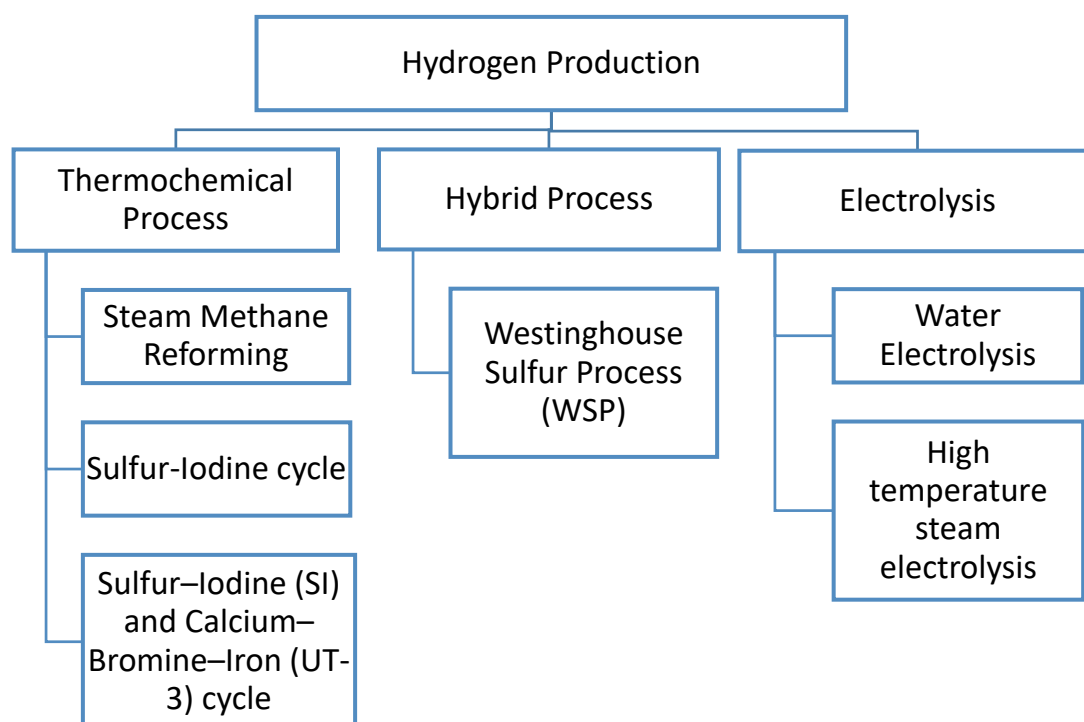
Figure 2: Hydrogen production processes through nuclear energy

The best equipment to harness the Hydrogen energy without having harmful effects on the environment are the fuel cells. Fuel cells are one of the promising alternative energy sources like wind and photovoltaic systems. Unlike wind and solar

energy systems, fuel cells are the most reliable alternative energy sources. There are different types of fuel cells. Many fuel cell technologies mainly depend on the electrolyte material used, such as proton exchange membrane fuel cells (PEMFCs), direct methanol fuel cells, alkaline fuel cells (AFC), molten carbonate fuel cells, and solid oxide fuel cells. Except for AFC and PEMFC, other fuel cell temperatures are higher than 100°C and may reach up to 500°C, especially in molten carbonate and solid oxide fuel cells. Table 1 explains the type of fuel cells along-with their detail description of operating temperature and electrolyte used. (Gamalath, Wijewardena and Peiris, 2012).

Table 1: Description of fuel cell types along-with their operating temperature range

No.	Fuel Cell Type	Electrolyte	Operating Temperature (°C)
1	Alkaline fuel cell (AFC)	KOH solution	60-120
2	Phosphoric-acid fuel cell (PAFC)	Phosphoric acid	160-200
3	Molten carbonate fuel cell (MCFC)	Molten carbonate	500-650
4	Solid oxide fuel cell (SOFC)	Ceramic compound	600-1000
5	Proton exchange membrane fuel cell (PEMFC)	Solid polymer	20-180

Among all fuel cells, PEMFCs are the most effective technologies for portable and transportation applications because of their simple assembly and low operating temperature (Motapon, Tremblay and Dessaint, 2012). Besides, PEMFC is the most commonly used type of fuel cell in almost all major applications because of its low cost, durability, and compactness. It has a high power density and the best efficiency among all other fuel cell variants. However, there are many issues related to the mass

utilization of PEMFC systems because of their high cost and short lifetime (Petrone et al., 2013). PEMFCs are fed continuously with fuel (Hydrogen) at the anode and an oxidant (air) at the cathode side. The electrolyte materials of PEMFCs are sulfonated polymers (Nafion), which allow the reaction of Hydrogen and Oxygen from both electrodes to produce electricity and water. Voltage and current are produced through a complex electrochemical system. The membrane of PEMFC is an integral part of the PEMFC system which allows the Hydrogen ions to pass from anode to cathode. Proper hydration of the membrane is necessary. Any unbalance in membrane water content produces drying and flooding of the membrane which affects the performance of the PEMFC system. Figure 3 shows the working principle of PEMFC, where Hydrogen and Oxygen are inputs while water and excess Hydrogen discharges from the PEMFC system and electrical energy is the main output (Salim et al., 2015).
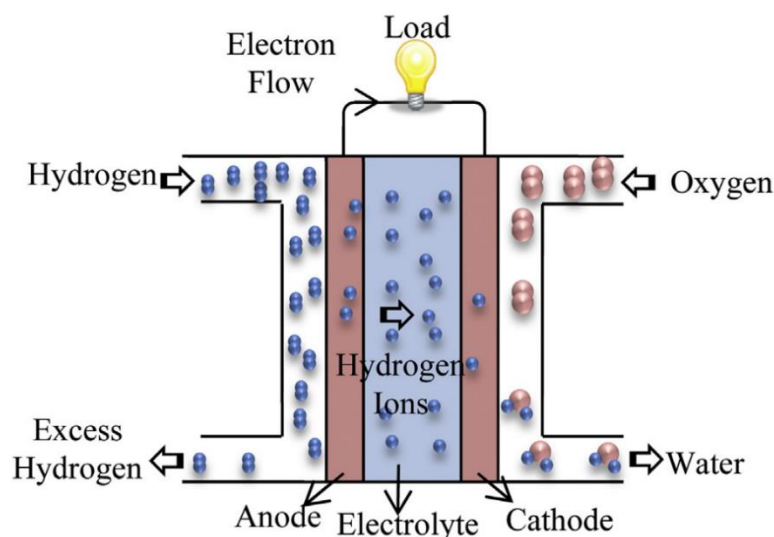
Figure 3: PEMFC schematic diagram

The PEMFC ionic conductivity depends majorly on gas fuel transport with the help of water molecules. However, the mass transport phenomena in the PEMFC

system are very complex and require a lot of complex calculations. The equations in the mechanistic (theoretical) model, however, explain the flow of gases, water production and how internal pressures vary in the presence of water vapor (Amphlett et al., 1995; Petrone et al., 2013). The complexity of these equations and also failing to fulfill general models' requirement of PEMFC, especially in case PEMFC stack models, has brought researchers to semi-empirical (half mechanistic and half empirical) modeling of PEMFC. The semi-empirical models explain the performance of the PEMFC mathematically and fit the experimental models to a good extent. The literature review of semi-empirical models will be explained in detail in Chapter 2.

Since PEMFC is mainly affected by ambient and operating conditions, its voltage and current vary with change in ambient temperature and pressure (Al-Zeyoudi, Sasmito and Shamim, 2015; Dyantyi et al., 2019; Pratt, Brouwer and Samuelsen, 2007; Werner et al., 2015). The inlet humidity level is also an important factor that affects the PEMFC voltage/current values. Proper water/vapor balance is required in the PEMFC system. Water is already produced in PEMFC but deficiency of water may occur due to drying and also excess water may also be produced in the PEMFC system due to flooding in PEMFC. The inlet fuel gases are sometimes humidified to inhibit from drying conditions and a water drain system is provided in the PEMFC system to protect from flooding. The flooding and drying faults must be attended at the earliest and quick actions are needed before it can cause serious damage to PEMFC. PEMFC models that have the ability to determine temperature and voltage may have the inherent advantage of diagnosing flooding/drying faults as a part of water management and fault diagnostics in the PEMFC system. This is called the model-based fault diagnosis.

1.2 Statement of the problem

Although PEMFC is a very useful alternate energy source, it has a very short life due to the sensitivity of the membrane. The life-span of PEMFC can be enhanced if it is handled with care and faults are avoided with the help of quick and reliable fault diagnosis. The most common occurring faults in the PEMFC system are flooding and drying faults. These faults occur due to improper water management in the PEMFC system. For a quick diagnosis of these faults, a reliable fault diagnosis method has to be adopted. Currently, there are a lot of fault diagnosis techniques that have been developed which can be categorized into two parts: (i) model based fault diagnosis techniques (ii) non-model based fault diagnosis techniques (Petrone et al., 2013; Zheng et al., 2013). The non-model based technqiues are not generic but the model-based techniques have the advantage of being generic fault diagnosis technique i.e. it can be applied to all similar types of PEMFC system, the model based techniques developed to date doesn't incorporate ambient conditions which is a major deficiency.

Though there are several techniques for modeling the PEMFC system, the most effective, quick and reliable technique is the use of semi-empirical models (Akimoto and Suzuki, 2018; Ettihir et al., 2014). These models are the combination of theoretical and empirical equations and are preferred techniques for the online diagnosis of the PEMFC system (Salim et al., 2015). The semi-empirical models are usually less complex and they have high computational efficiency with remarkable precision and reliability (Hou, Zhuang and Wan, 2007).

The semi-empirical model discussed in (Salim et al., 2015) is appropriate and models both voltage and temperature of PEMFC. But the voltage and temperature models are interconnected and used each other outputs as feedback. The similar semi-

empirical models have been witnessed in (Del-Real, Arce and Bordons, 2007; Moore et al., 2018) where modeled temperature and voltage are in a feedback loop. These types of techniques usually take time to settle because of the feedback system and cannot be used for a quick fault diagnosis system. Moreover, in most of the techniques, the waveforms of component voltage drops of the PEMFC model have not been witnessed, as in many cases, they don't follow the exact theoretical pattern although they provide an acceptable output voltage. Due to this deficiency in the existing models, an attempt should be made to properly incorporate the component voltage.

Considering the development of more robust PEMFC models and their fault diagnostic abilities, it has been revealed that many models with diagnostic capabilities haven't incorporated ambient conditions such as ambient temperature, pressure, and air relative humidity directly. The semi-empirical models usually take normal air pressure and fuel cell temperature as inputs. In some cases, the PEMFC temperature is modelled based on ambient temperature, load current, and voltage of PEMFC. The inlet air humidity has also been discussed in the semi-empirical model mentioned in (Labach, Rallières and Turpin, 2017), but the ambient temperature has not been added explicitly. Instead, PEMFC temperature measured with the help of internal sensors is commonly used. So, there is a need to model voltage and temperature simultaneously when modelling the semi-empirical PEMFC model. Meanwhile temperature model should not require a voltage of PEMFC as feedback.

The ambient conditions have significant effects on PEMFC performance which has been mentioned in (Al-Zeyoudi, Sasmito and Shamim, 2015; Hottinen et al., 2003). The severe dry and humid ambient conditions affect water management in PEMFC as discussed in (Ji and Wei, 2009). Thus, the change in ambient conditions

must be incorporated into the model while analyzing the PEMFC hydration state with the help of the PEMFC model. Besides, all the parameters cannot be fixed for all types of PEMFC system, an adjustment may be required for using the same model parameters for different PEMFC systems using the different number of fuel cells in the stack. This must be very time consuming for the operators and researchers to re-optimize the parameters with suitable limits. A compensation factor must be introduced to adjust the model parameters based on the number of fuel cells in the stack.

1.3 Objectives of the research

The objectives of the research are as follows:

1- To develop an effective non-complex PEMFC semi-empirical voltage model that has the ability to access PEMFC hydration conditions.

2- To study the effect of ambient conditions and model the voltage variations of PEMFC with respect to ambient conditions change through empirical equations.

3- To develop the non-complex PEMFC temperature model based on the current and ambient temperature.

4- To enhance and validate the proposed semi-empirical voltage model for possible drying and flooding fault diagnosis by directly incorporating the ambient.

1.4 Scope and methodology of the research

The initial work done in this research properly focuses on the development of the voltage model of PEMFC through semi-empirical equations. Currently, very few

researches have emphasized the importance of no-load voltage variations of PEMFC. This distinctive feature of this research has been achieved by considering the effect of internal currents in PEMFC which is missing in most of the semi-empirical models. The no-load voltage of PEMFC has been validated experimentally, where variations in the no-load voltage of PEMFC is expected to achive through variations of internal pressure of Hydrogen gas and temperature of PEMFC. Moreover, the on-load voltage variations will be modelled through semi-empirical equations and various voltage drops of PEMFC requires separate plotting with a current variation. This procedure is expected to help researchers to achieve a more generic model of PEMFC.

After the semi-empirical voltage model development, the temperature model is developed. This temperature model is expected to have inherent advantage of using only load current and ambient temperature variations. Together voltage and temperature model of PEMFC is expected to account for the complete model of PEMFC system. The parameters for both voltage and temperature models can be extracted using quantum lightening search algorithm (QLSA). QLSA is the updated version of lightening search algorithm (LSA), this technique is based on natural phenomena of lightening. QLSA is most accurate and fast among all renowned optimization techniques that are presented to date.

In this research work, the PEMFC performance with the change in ambient conditions will also be studied. For this purpose, additional empirical equations will be extracted using previously validated models of PEMFC and with the help of statistical analysis approach. This is expected to bring a novel electrical equivalent model that can access the variations in ambient conditions as well. As a part of this study, the starting voltage characteristics with the change in ambient conditions will

also be modelled through statistical analysis based on experiments performed on PEMFC. Central composite design (CCD) has been used as statistical analysis (by using Minitab® software) for extracting the second-order regression equation.

After observing the serious changes in PEMFC performance with ambient conditions for different types of PEMFC, the semi-empirical model parameters may require updating to incorporate ambient temperature and relative humidity of the air. While the number of fuel cells variation in the stack can be introduced through a compensation factor. The model must show good precision after the up-gradation, this model will be used in the experimentation for fault diagnosis of drying and flooding faults by monitoring the membrane water content calculated with the help of model equations. A certain pattern must be pointed out for the variations in membrane water content i.e. upper and lower threshold limits of membrane water content. These limit setting procedures can be done through simulations on Matlab® software, as real flooding and drying faults in PEMFC may damage the PEMFC system permanently.

The brief methodology of the work is stated as:

1- Experimental study of PEMFC voltage and temperature at both loading and non-loading conditions.

2- Experimental characterization of ambient conditions effects on PEMFC voltage.

3- Identification and quantification of possible fault conditions in PEMFC for extreme ambient conditions.

4- Development of generic dynamic semi-empirical PEMFC model for predicting voltage and temperature of PEMFC by directly incorporating the change in ambient conditions.

5- Validation of proposed models against experimental results.

6- Obtain model-based health monitoring and diagnosis system for flooding and drying faults in PEMFC.

1.5 Organization of the research

The research consists of six chapters, which are organized as follows:

Chapter II gives an overview of the voltage and temperature modelling techniques of PEMFC. The details about PEMFC water management, ambient conditions effects, and fault diagnosis techniques are provided. Moreover, the importance of a semi-empirical model-based diagnosis has been highlighted in this chapter.

Chapter III highlights the complete description of the dynamic semi-empirical PEMFC voltage model along-with its use in model-based fault diagnosis and empirical model for predicting the change in PEMFC voltage with ambient conditions.

Chapter IV describes the development of PEMFC temperature model, where the novel algorithm has been introduced which tracks the changes of current and ambient temperature by using model equations. Quantum lightening search algorithm (QLSA) has also been described in detail.

Chapter V illustrates the results and discussions. Both experiments' experimental results and the models' validation are detailed in this chapter. The experiments are performed to validate the voltage and temperature models. The experiments are also done at varying ambient conditions to improve the voltage model

in case of varying ambient conditions. Finally, after the validation, the voltage model has been tested for possible fault diagnosis.

Chapter VI provides the conclusion of the study.

Chapter 2: Literature review

This chapter provides the literature review of fuel cell modelling techniques, fault diagnosis methods and the study on the effect of the ambient condition for PEMFC. Section 2.1 provides a detailed literature review of the voltage modelling techniques of PEMFC from white box to black box modelling and their limitations are highlighted. The later sections also provides a comprehensive review of water management in PEMFC and the faults in PEMFC. They also enlightens the effect of the ambient condition on PEMFC, the advantages and disadvantages of fault diagnosis techniques by mentioning almost all possible fault diagnosis techniques in PEMFC presented to date. The importance of temperature model is also mentioned by considering the best approach for temperature modelling.

2.1 PEMFC models overview

Modelling of PEMFC is important as its characteristics of PEMFC are nonlinear. Modelling of the PEMFC is therefore very important, because the output voltage prediction of PEMFC under different loading conditions is required for the operators before using PEMFC in real-time applications. There are some linear (ohmic) and non-linear (activation and concentration) voltage drops with in the PEMFC system (Andrea et al., 2006). Figure 4 gives the details of V-I (voltage-current) characteristics of PEMFC.
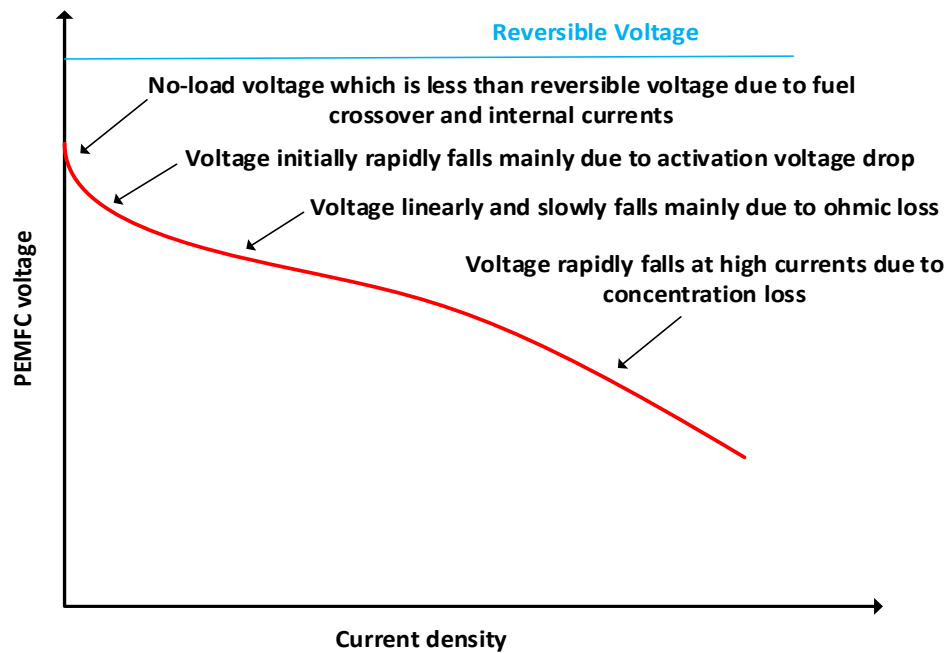
Figure 4: PEMFC V-I characteristics

The ohmic losses appear due to internal resistance of the PEMFC which comprises the membrane, anode, cathode and the associated connections. The internal resistance of the PEMFC reduces based on the membrane hydration level. However, over-hydration may also cause system faults. The activation losses depend upon the reaction speed and it can be improved by increasing the catalyst contact area where the reaction occurs. Due to the leakage of electrons through the membrane, there are some amount of internal currents. They also produce a voltage drop in the PEMFC system. The gas concentration usually changes at the surface of electrodes and causes a concentration voltage drop in PEMFC (Andrea et al., 2006; Salim et al., 2015).

However, most of these voltage drops are difficult to calculate as some of the model parameters such, the internal current (i_{int}), the exchange current density (i_o) and the charge transfer coefficient (α) for PEMFC vary with temperature and loading

conditions of PEMFC. In addition, these voltage and internal resistance vary with the number of fuel cells used in the stack (Atifi, Mounir and El-Marjani, 2014)

Various voltage models of the PEMFC system have been proposed by many types of research. The electrochemical models (referred to as mechanistic models) presented in most researches are very complex and requires very sophisticated and expensive laboratory testing facilities. Most of these models are based on theoretical electrochemical equations of PEMFC with the complete elaboration of mass transport phenomena in PEMFC. The problem with these single-cell models is that they require a lot of information from the manufacturer. PEMFCs are used in the stack where the number of fuel cells are attached in series for higher voltages, thus these models require tuning for stack systems. So, for the sake of simplicity other modelling techniques have been referred by the researchers. A complete review on all modelling techniques are discussed in detail (Moreira and Da-Silva, 2009).

2.1.1 Mechanistic models

The mechanistic models of PEMFC are based on complex electrochemical equations of PEMFC system. It describes the mass transport phenomena of fuel cell gases and water in the fuel cell through anode and cathode, gas diffusion layer, catalyst layers and membrane. The models in (Amphlett et al., 1995; Bernardi and Verbrugge, 1992; Springer, Zawodzinski and Gottesfeld, 1991) are one-dimensional models which considers the gas flow in one direction. That is from cathode to anode and vice versa. The Stefan-Maxwell equation, Nernst-Planck equation, Schlogl's velocity equation and Butler-Volmer equation are commonly used to explain the mass transport, its diffusion and its flow velocity in the PEMFC system. The solution of these equations is obtained based on the boundary conditions namely the distance travelled by masses.

This distance varies from one PEMFC to another. Also, the geometry of the PEMFC system is not the same for all fuel cells. The voltage models are mainly based on Ohm's law where internal resistance is measured based on mass transport and the hindrance offered to the masses. The electromotive force (emf) produced by PEMFC is taken from the Nernst equation which depends upon temperature, partial pressure of fuel gases in the PEMFC. Besides, the thermal models are commonly developed according to energy balance over time.

The models in (Dannenberg, Ekdunge and Lindbergh, 2000; Gurau, Liu, and Kakaç, 1998; Pisani et al., 2002; Sharma, Birgersson and Khor, 2014; Xing et al., 2017) has the major focus of mass transport in two-dimension considering the gas flow in the direction towards the membrane of PEMFC and also along the membrane. The models use the Navier-Stokes equation and the partial differential equations with special boundary conditions. The voltage drops are considered separately based on the activation, ohmic and concentration of masses phenomena.

Three dimensional-flow of masses are also considered in (Le et al., 2012) and are based on Darcy's law of mass and momentum equations but the third dimension is usually redundant in the design and will account for more complexity. The modern (Abdollahzadeh et al., 2018; Atyabi and Afshari, 2018; Gamalath, Wijewardena and Peiris, 2012; Headley et al., 2016; Lim et al., 2019; Min et al., 2019; Zhang and Xie, 2019) mechanistic models majorly includes three-dimensional flow, the model considers modern PEMFC auxiliary system such as humidifiers, pumps, and special cooling systems are incorporated. This deep study of PEMFC further elaborated the mechanistic designs while considering even those processes in PEMFC system that were neglected in previous researches. The main issue with mechanistic models is that

no matter how detailed information has been considered, the desired information of PEMFC system is usually not given by the manufacturers. The detail information that is difficult to obtain is the combination of diffusity factors, layers thickness, membrane thickness, internal geometry, materials used, fuel stoichiometry etc. The mechanistic models are good for insight studies but are difficult to adopt for fault diagnosis or performance monitoring models.

2.1.2 Semi-empirical models

The semi-empirical models on the other hand uses the combination of theoretical and empirical equations to resolve the issue of generality in PEMFC models (Al-Baghdadi, 2005; Hou, Zhuang and Wan, 2007; Nalbant, Colpan and Devrim, 2018; San, Dursun and Yazici, 2019; Xu, Wang and Wang, 2019). Also, they require very basic information which are easily available from datasheet/nameplate of any type of PEMFC system. The advantage of these models is that they don't require laborious calculations, as the equations used are simpler especially in most of the modern models. The parameters are optimized using various optimization techniques such as particle swarm optimization, lightening search algorithm and back-tracking search algorithm etc. Some semi-empirical models that are discussed in (Marr and Li, 1999; Pisani et al., 2002) are very close to mechanistic models and use the same mass transport equations as that of the mechanistic models. The empirical equations are used but the complete model is still complicated and not general at all. The models discussed in (Correa et al., 2005; Moreira and Da-Silva, 2009; Wishart, Dong and Secanell, 2006) are simpler and use less complex equations. In these models the equations model both stack and single cell. The voltage and thermal models are

interdependent and can be used as feedback for simulating both models simultaneously.

The semi-empirical models described in (Hyun-Il et al., 2010) uses very simple equations for modelling voltage and temperature. The model performance was found acceptable for steady-state and dynamic load changes. The semi-empirical model in (Jee-Hoon, Ahmed and Enjeti, 2011; Restrepo et al., 2015) developed an auxiliary system model as well such as external cooling/humidification techniques. The model in (Jee-Hoon, Ahmed and Enjeti, 2011) is also implemented for real-time simulation on Matlab ® software. The models give both voltage and thermal equations. The model in (Ariza et al., 2018; Fathy and Rezk, 2017; Geem and Noh, 2016; Giner-Sanz, Ortega and Pérez-Herranz, 2015; Salim et al., 2015; Sun et al., 2015) has been the simplest among all previous models discussed, it has been implemented for haphazard load changes and fit the experimental waveforms for the voltage and temperature. The models have been implemented on software for online applications with the help of given equations. The voltage model in all the research mentioned above is comparatively simple by making component voltage drops such as activation, ohmic, concentration in a better way. Though the equations are simple, still improvements are required to make them simpler. The equations for activation, ohmic and concentration voltage drops are present in almost all the research mentioned above have some variations in the parameters and equations. Besides, the dependency on PEMFC temperature and current lies in almost all models. The simpler the model the more chances are that they are not applicable to all fuel cells and all operating conditions. So, the trade-off is there while modelling fuel cells. No perfect model of PEMFC exists that is applicable to all operating conditions and for all types of PEMFC systems. It is

needed that the separate waveforms of component voltage drop such as activation,

concentration, and ohmic voltage drop have also been revealed and check whether the

waveform matches the pattern given in {Formatting Citation}. This makes the model

more effective and the model validity must be checked with more than one PEMFC

system with the different number of fuel cells in series. Different ambient conditions

must also be checked to incorporate the ambient changes in the PEMFC model. If these

steps have been taken, then the model will surely hold the property of generality and

it must be applicable to all PEMFC systems with the same auxiliary system.

2.1.3 Electrical equivalent models

The electrical equivalent models are the models that use the electrical circuit

to model the PEMFC system. The active and passive elements of the circuit are given

specific values or calculated through specific equations, based on the transient

behavior of PEMFC. These models have the advantage of designing the auxiliary

power electronics equipment with PEMFC in order to regulate PEMFC voltage. These

models are mentioned in (Aglzim et al., 2014; Azri et al., 2017; Becherif et al., 2011;

Choi, Howze and Enjeti, 2006; Hinaje et al., 2012; Taieb, Mukhopadhyay and Al-

Othman, 2019), where different approaches predominantly electrochemical impedance

electroscopy (EIS) has been used to design the electrical equivalent model. Most of

these models lack generality. The majority of these models are specific to specific

types of PEMFC and do not consider the changes in ambient conditions in the design.

In this research, the model in (Aglzim et al., 2014) model is updated by incorporating

the ambient conditions which are presented in detail in Chapter 5.

2.1.4 Other PEMFC models (black-box models)

The other modelling techniques in PEMFC system are signal processing based models, control technique based models, purely empirical models and artificial intelligence type of models mentioned in (Akbari and Dahari, 2019; Barzegari, Alizadeh and Pahnabi, 2017; Kurz et al., 2008; Laribi et al., 2019; Liu et al., 2018; Puranik, Keyhani and Khorrami, 2010; Restrepo et al., 2016; San, Dursun and Yazici, 2019). Model in (Akbari and Dahari, 2019) uses the adaptive neuro-fuzzy technique for modelling fuel cell, while (Barzegari, Alizadeh and Pahnabi, 2017; Kurz et al., 2008) used predictive control methods to model PEMFC. The (Laribi et al., 2019; Puranik, Keyhani and Khorrami, 2010) PEMFC models uses artificial neural networks. Finally the model in (Restrepo et al., 2016) uses input/output diffusive approach to model PEMFC. These models are very specific, lots of modifications are required for using any model on different type of PEMFC system. They also can give very erroneous results for different operating conditions especially while changing ambient conditions.

2.2 Water management in PEMFC system

The water transport in the PEMFC system is shown in Figure 5. In the chemical reaction happening in the PEMFC, the Hydrogen is oxidized at anode and the protons produced are conducted through the membrane. In cathode, the Oxygen is reduced to make water as a by-product (Burheim et al., 2014; Hogarth and Benziger, 2006; Ji and Wei, 2009; Wong et al., 2011). This water transport is called electro-osmatic drag when moves from the anode to the cathode while it is called back-diffusion when the water molecules move from cathode to anode.

2.2.1 Electro-osmatic drag and back-diffusion

In PEMFC when protons are formed and transported, they drag the water molecules along with them from anode to cathode. This phenomenon is called electro-osmatic drag. This is necessary for ions transport as protons move in the hydrated parts of the ionomer.

The dry ionomer doesn't conduct protons. Due to electro-osmatic drag, the water is accumulated in the cathode. As cathode has its own water production and water molecules coming from the anode. At high currents, the electro-osmatic drag will prevail. As the water concentration increases in cathode after water production and electro-osmatic drag. This water concentration increment will cause the water molecules to diffuse back to anode called back-diffusion. The number of water molecules transported doesn't only depend upon the amount of water in cathode but also depends upon membrane characteristics, inlet gases humidification and temperature of PEMFC (Nishida, Hosotani and Asa, 2019). At low currents, the back diffusion will prevail. Figure 5 explains the complete water transport phenomena in PEMFC (Ji and Wei, 2009).
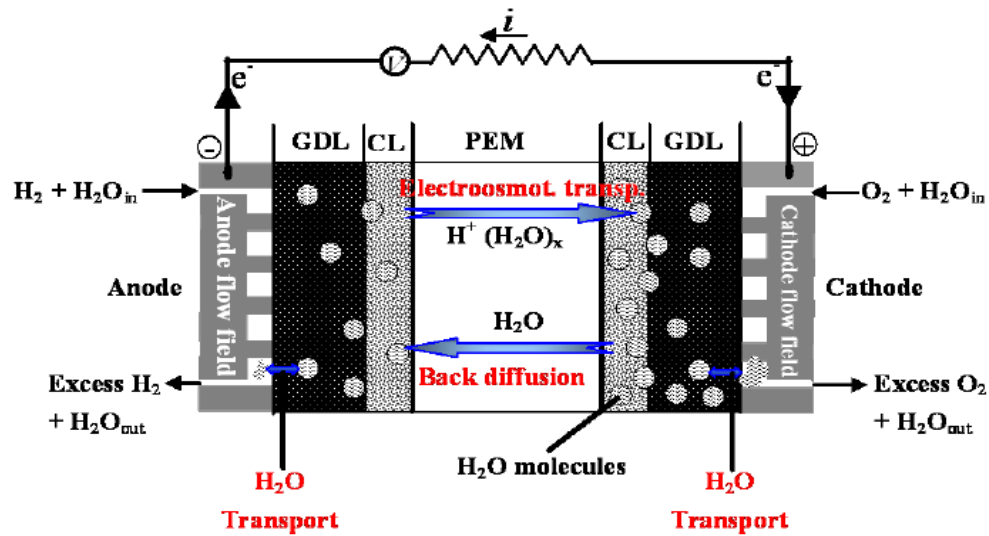
Figure 5: Water transport in PEMFC system

2.2.2 Issues in water management of PEMFC

The balance of water in anode and cathode is very important for the smooth operations of PEMFC. If this equilibrium is affected, then the PEMFC system will undergo from drying or flooding faults. These faults are usually temporary in a self-humidified PEMFC commercial system but it may cause permanent damages as well if it is persisted for a longer time (Kim, Cha and Kim, 2015; Le-Canut, Abouatallah and Harrington, 2006).

The next section explains the flooding and drying faults of PEMFC, it also highlights the reason for the occurrence of these faults.

2.2.3 PEMFC drying and flooding

PEMFC drying is considered as drying of the membrane of the PEMFC system. This fault is more severe than flooding fault. It may cause irreversible damage to the PEMFC system in just approximately 100 s if the membrane is severely dry. The

reasons for drying of the membrane are (i) feeding fuel gas with dry reactant gases (ii) water formation at cathode doesn't fulfill the requirement (iii) electro-osmatic drag at high current prevails back-diffusion which usually happens for a step increase in current by a significant amount. The flooding fault occurs at anode, cathode and flow channels separately. The cathode flooding is more frequent due to the following reasons (i) water formation due to Oxygen reduction reaction (ii) due to electro-osmatic drag (iii) over humidified reactant gas at the cathode or liquid water injection for cooling. (Ji and Wei, 2009; Maggio, Recupero and Pino, 2001; Murugesan and Senniappan, 2013; Steiner et al., 2011)

This flooding will stop the flow of Oxygen and the lack of Oxygen leads to under stoichiometry or starvation of gas, in this case, the protons are transporting in a regular manner from anode but the lack of Oxygen in cathode not only increases internal resistance but in worst case scenario the proton ions undergo reduction at cathode and this produces the negative potential across cathode. The anode flooding is rare but at low current densities and lower temperatures the back-diffusion prevails, and excess water comes to the anode. Also, excess humidification or water cooling can also be responsible for anode flooding. This will also lead to anode gas starvation which also increase PEMFC internal resistance. In flow channels of gases, the flooding also occurs if the excess water is not removed regularly. Usually the use of multiple gas channels is common and some of channels are blocked due to flooding. This also brings the gas starvation phenomena in fuel cell. Flooding may cause permanent damages but its impacts are less adverse and slow as compared to drying (Ji and Wei, 2009; Le-Canut, Abouatallah and Harrington, 2006) .

2.3 Experimental characterization of water management faults

There is a list of experimental methods that can monitor PEMFC water content which is discussed in this section (Yousfi-Steiner et al., 2008).

The first method is the use of comparing polarization curves (current-voltage curve) of PEMFC operated with air and pure oxygen. This is used to analyze the mass transfer limitations at the cathode side which has a direct link to flooding fault. It is pointed out in various research that liquid water has more influence in cell performance than fuel gases in the channels, so monitoring a single cell voltage for each cell in the stack can indicate the water management issues. But not all commercial PEMFCs give this facility to obtain each cell voltage easily (Ralph and Hogarth, 2002).

The hysteresis in the current (increasing and decreasing of current) can be used to indicate drying and flooding faults. In a flooding and drying situation, the polarization curve follows a different pattern if the current is raised from zero to maximum and vice versa (Wensheng, Gua and Nguyen, 2004). This pattern is discussed in detail in (Yousfi-Steiner et al., 2008) for flooding and drying faults.

Membrane resistance can be measured by inserting probes inside PEMFC, but this is an unrealistic method in commercial PEMFC systems. Current interruption method i.e interrupting current while measuring the voltage at the high sample rate. The change in voltage is associated with the membrane hydration state (Mennola, 2004).

The measure of fuel gas pressures at inlet and outlet channels of PEMFC can also indicate water management faults in PEMFC. The variation in pressure at all inlet and outlet are measured with the help of sensors. The difference in inlet and outlet

channel pressure is a good indicator of water management faults (Yousfi-Steiner et al., 2008).

The experimental methods for characterization of water management faults are a very expensive process and a lot of care is required while performing experiments. Installing new sensors within PEMFC is not a good option as it is very costly and may affect the PEMFC badly while opening and closing the commercial PEMFC system. Also, special performing special experiments for fault characterization hinder the normal operation of PEMFC.

2.4 Fault diagnosis of drying and flooding faults

The fault diagnosis methods are mentioned in this section. Procedures for PEMFC water-management fault diagnosis as a result of major events such as flooding and drying have been presented in detail using non-model and model-based techniques.

The model-based approach is mainly categorized as a mechanistic modelling approach and semi-empirical modelling approach (Benmouna et al., 2017).

2.4.1 Non-Model approach for fault diagnosis

The non-model approach mainly includes the following approach for fault diagnosis (Benmouna et al., 2017):

1. Artificial intelligence method
2. Statistical method
3. Signal processing method

The artificial intelligence methods mainly include the fuzzy logic, neural network, and expert system, etc. The statistical method does statistical analysis on the voltage disturbances, polarization curve, data received after performing electrochemical impedance spectroscopy (EIS), and spatial current density, etc. The third approach process the signals received mainly through magnetic resonance imaging, acoustic emission, neutron radiography and other types of analyzers.

A lot of work has been done in this field, for example, a non-model-based method (Cauffet, Chadebec and Rouveyre, 2019) used various sensors and proved that the current distribution among the cells could be responsible for faults in the PEMFC stack. In this work, magnetic tomography was used to identify the change in current distribution which in turn is helpful for fault diagnosis of the PEMFC. The magnetic field sensing method requires a number of sensors and expensive equipment (Mao, Jackson, and Davies, 2017). This research also emphasizes the use of humidity sensors inside the PEMFC to aid fault diagnosis. Other researchers proposed the use of artificial intelligence for fault diagnosis (Li et al., 2018; Liu et al., 2018). However, this technique may only be applicable to one type of PEMFC system and requires a huge amount of training data before it could be applied to other types of PEMFC system. A fault diagnostic technique, which is based on signal processing (Benne, Grondin-Perez and Bessa, 2015), and which involves empirical mode decomposition. This is an intuitive, direct, and empirical method based on signal processing (adaptive), without pre-determined basis functions. A signal processing technique for fault diagnosis (Ibrahim et al., 2015), which diagnoses faults based on wavelet transform, whereas the technique of (Hoon et al., 2019) uses the time-domain analysis of the step response of voltage. The most accurate and reliable fault diagnosis non-model

techniques entail the use of the electrochemical impedance spectrum (EIS) of PEMFC (Araya et al., 2019; Chamagne et al., 2017; Lu et al., 2019), but this technique is extremely expensive to implement. (Maizia et al., 2017) used the statistical analysis of noise in the voltage signal of the PEMFC for fault diagnosis; however, although electrochemical noise analysis can be highly effective for fault diagnosis, this technique requires a very high sampling rate for data collection. The fault diagnosis technique adopted by (Salim, Noura and Fardoun, 2017) uses the numerical analysis approach to calculate the residuals. Five residuals were generated from mathematical calculations using the stack voltage, current, pressure of fuel gases, and temperature of the PEMFC.

2.4.2 Model-based approach for fault diagnosis

The model-based approach mainly includes the following models for fault diagnosis.

1. Mechanistic model approach

2. Electrical equivalent model approach

3. Semi-empirical model approach

The mechanistic model can diagnose faults, lots of studies have been conducted and most studies concluded the change in pressure at cathode and anode due to flooding and drying faults. The pressure drop is not limited to faults, sometimes operating conditions are the main factors such as PEMFC temperature, current and inlet pressure of gases. Also the amount of pressure drop varies with the geometry of PEMFC. The pressure drop is mainly reviewed based on theoretical equations of PEMFC extracted from Darcy's law, Bernoulli's equation, and two-phase flow

multiplier. The equations require a flow rate of the reactant, fuel stoichiometry ratio, surface area and depth/width of channels, etc which isn't easily available for all commercial PEMFC systems. (Pucheng et al., 2016)

The electrical equivalent model approach has been used for fault diagnosis in (Andres, Hissel and Rachid, 2010; Forrai et al., 2005), but this approach has not been popular because of their complexity and less accuracy as compared to other techniques.

The research in (Salim, Noura and Fardoun, 2017) the variable water content of the membrane, which is actually the ratio of the number of water molecules in the PEMFC membrane to the number of charge sites in the membrane. The membrane water content was measured in that research by using Siemens LMS AMESim software for the PEMFC stack and it is very helpful for the diagnosis of drying and flooding faults in the PEMFC. The membrane water content is also calculated in some semi-empirical model-based fault diagnosis techniques, which have the inherent advantage of being generic, especially mechanistic and semi-empirical models. Semi-empirical models are less complex and can easily be implemented for online diagnosis (Petrone et al., 2013). In addition, fault diagnosis techniques based on these models can also be used for prognostic and health monitoring of PEMFC systems (Lechartier et al., 2015). Another approach involved calculating the water content of the membrane (Murugesan and Senniappan, 2013) but this requires the volume of the anode and cathode along with the dry density and weight of the membrane, which are not available for all commercial PEMFCs. More complex computational procedures to determine the water content of the membrane (Görgün, Arcak and Barbir, 2005; Hinaje et al., 2012; Hogarth and Benziger, 2006) require the inlet and outlet flow of

mass at both the anode and cathode and this requires the use of special flow sensors at the inlet/outlet of the PEMFC.

None of the reported fault diagnosis techniques (among all mentioned techniques) directly incorporate the effect of ambient changes on the PEMFC which clearly have significant effects on PEMFC performance as mentioned earlier.

2.5 Effect of ambient conditions on PEMFC

The studies conducted in (Al-Zeyoudi, Sasmito and Shamim, 2015; Dyantyi et al., 2019; Hottinen et al., 2003; Pratt, Brouwer and Samuelsen, 2007; Werner et al., 2015) discussed that the ambient conditions such as temperature, pressure, and humidity in the air affect the PEMFC performance. Since the emf of the PEMFC directly depends upon the pressure of Oxygen (usually taken from air) and the temperature of PEMFC, these two factors can be largely affected by ambient temperature and pressure. In aeronautical and outdoor applications of PEMFC in distributed generation, the ambient conditions vary greatly. The voltage models based on the change of ambient has been indirectly discussed in most semi-empirical and mechanistic models. The explicit voltage modelling of ambient variation has been discussed in (Pessot et al., 2018), where efforts have been made to model directly the variation voltages using previous model equations. The major effect of the change in ambient was witnessed in water management inside the PEMFC system. The water balance is of vital importance in the PEMFC system (Ji and Wei, 2009; Wong et al., 2011).

The ambient conditions (ambient temperature, pressure, and air humidity) effect have not been separately modelled for PEMFC voltage in the previous research

work. Empirical models of PEMFC regarding variation in ambient conditions may be very helpful for the researchers. The empirical model mentioned in Chapter 3 will predict the change in PEMFC voltage for the variation in ambient conditions.

2.5.1 Models of PEMFC considering ambient conditions

Most of the mechanistic models can incorporate ambient conditions and are also very helpful if the ambient conditions are to be changed. Majority of semi-empirical models such as (Moreira and Da-Silva, 2009; Salim et al., 2015) have considered ambient conditions like in (Salim et al., 2015) thermal modeling, the room temperature has been used as the modelling factor. In (Moreira and Da-Silva, 2009) the partial pressure of Oxygen in PEMFC has been calculated from ambient air pressure. The other semi-empirical models (Giner-Sanz, Ortega, and Pérez-Herranz, 2015; Mo et al., 2006) use ambient condition indirectly as the pressure of Oxygen and PEMFC temperature has been taken from sensors which clearly changes with ambient.

The recent model developed in (Pessot et al., 2018) have modelled the PEMFC voltage variations with ambient conditions by using statistical analysis technique. The model in (Pessot et al., 2018) is more descriptive and it is based on experiments performed in aeronautical conditions. The model has some errors especially at high currents, but a compensation has been proposed using empirical laws to reduce the errors. The summary of models of PEMFC considering flooding and drying fault diagnosis based upon models outputs is given in Figure 6.
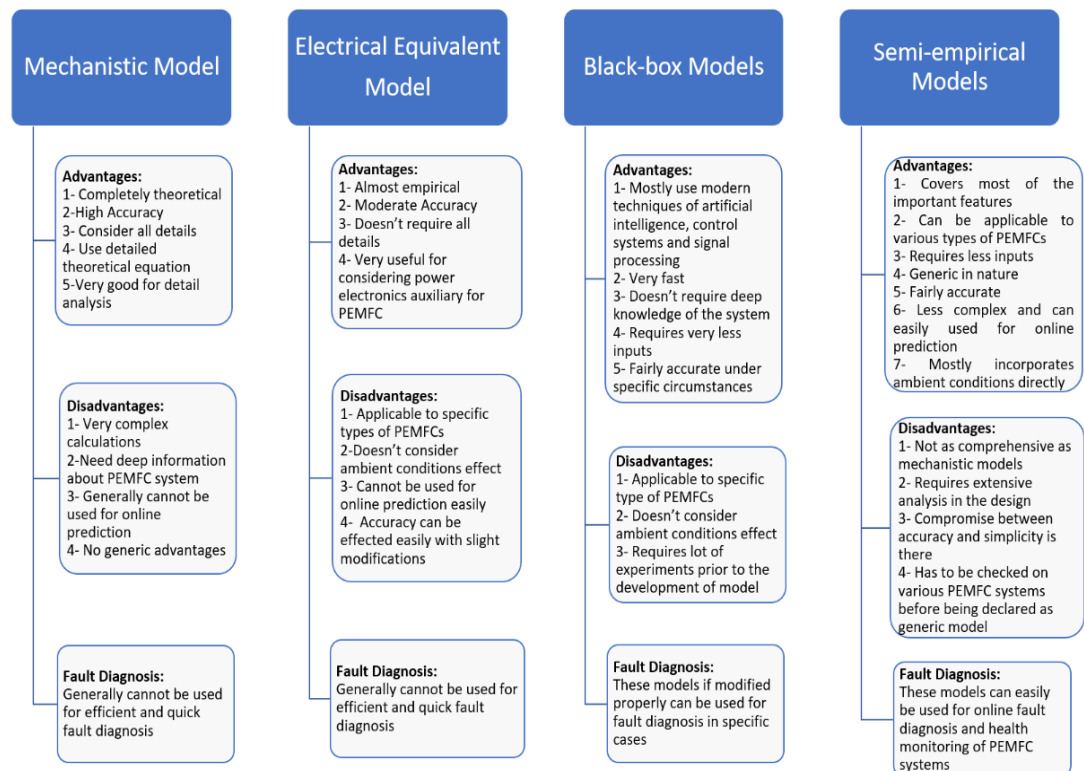
Figure 6: Summary of models of PEMFC and their affectivity in diagnosis for temporary PEMFC faults

2.5.2 Ambient condition considering water balance in PEMFC system

The ambient conditions such as air humidity, ambient temperature, and ambient air pressure affect fuel cell performance by a great deal. The ambient conditions greatly affect the water balance in the PEMFC system. The study in (Hottinen et al., 2003) describes the impact of ambient conditions on the performance of PEMFC. The ambient temperature and air humidity were controlled in a climate chamber. The variation in ambient temperature and humidity effects the PEMFC voltage by a significant amount. The PEMFC performance at high altitude has been tested in (Pratt, Brouwer and Samuelsen, 2007; Werner et al., 2015), by varying ambient pressure, ambient temperature along-with air humidity level. The membrane water content has also been discussed by considering the pressure of water and vapor.

The PEMFC performance for hot and dry weather on PEMFC has been studied in (Al-Zeyoudi, Sasmito and Shamim, 2015), in hot and dry conditions the significant changes in PEMFC electrical performance has been witnessed due to variation in the water content of PEMFC and it is proposed that external humidification through anode will make the performance better. It is concluded in (Ustinov et al., 2016) that lower ambient temperature (15-25°C) with appropriate inlet air humidity results in better performance of PEMFC. Too low temperatures, especially in freezing conditions, have adverse effects i.e. the water inside PEMFC may solidify into ice and it has the ability to destroy the cell (Ji and Wei, 2009).

2.6 Temperature model of PEMFC review

According to literature, most recent voltage models depend upon PEMFC temperature (Ay, Midilli and Dincer, 2006; Chavan and Talange, 2017; Del-Real, Arce and Bordons, 2007; Fouquet et al., 2006; Kumar et al., 2017; Moore et al., 2018; Moreira and Da-Silva 2009; Salim et al., 2015). In a few studies (Chavan and Talange, 2017; Fouquet et al., 2006; Kumar et al., 2017; Moreira and Da-Silva, 2009), a voltage model takes temperature as input along with PEMFC input Hydrogen (fuel) pressure and load current. This temperature is measured using sensors connected in a PEMFC stack. Temperature models have been developed to eliminate temperature sensors in voltage modeling (Ay, Midilli and Dincer, 2006; Del-Real, Arce and Bordons 2007; Jee-Hoon, Ahmed and Enjeti, 2011; Hyun-Il Kim et al., 2010; Martín, Ursúa, and Sanchis, 2014; Moore et al., 2018; Salim et al., 2015). These models use modeled output voltage and the temperature of a PEMFC stack simultaneously by utilizing a feedback loop to model a complete PEMFC system.

In recent years, numerous researchers have aimed to simplify PEMFC (thermal) temperature models based on output load current and ambient temperature. The artificial intelligence techniques utilized in such model development include fuzzy logic (Qun et al., 2014), artificial neural networks, and predictive control methods (Belmokhtar, Doumbia and Agboussou, 2014; Panos et al., 2012; Tao et al., 2005). The main limitations of these models are the requirement of large training data and expert knowledge prior to the development of the models. To overcome these limitations, a first-order polynomial temperature model has been introduced for the NEXA 1.2 kW PEMFC system using current and ambient temperature as inputs (Restrepo et al., 2015; Soltani and Bathaee, 2008). This model fits the experimental system temperature for linear and abrupt changes in load. Conversely, another model (Soltani and Bathaee, 2008) uses a first-order equation in which the initial value is set as ambient temperature. In addition, the final value of temperature and the time constant are current-dependent polynomials of degree one and degree two, respectively. However, temperature variation is as abrupt as current changes but with relatively fewer spikes. Noting the above limitation, an electrical analogous model has been introduced (Restrepo et al., 2015), where the source EMF and time constant of an RC circuit are represented as sinusoidal functions of PEMFC current. This implementation reduces the effect of large changes in current on temperature. To make the model more realistic, the cooling effect has been discussed as a current source, this cooling effect depends on the rate of change in the temperature of PEMFCs. Nonetheless, this technique does not provide accurate results in cases where abrupt large changes in load are observed. It is needed to develop a model which incorporates simple first-order equation using load current and incorporates elapsed time along-

with ambient temperature, the model will be applicable to all PEMFC systems which consist of same cooling auxiliary.

2.6.1 Current polynomial temperature model

This model is proposed by (Soltani and Bathaee, 2008; Wu et al., 2006) to represent the dynamic temperature variation of the PEMFC module. It uses an exponential function where the state variables are the initial and final value of stack temperature, and a time constant as shown in equation (2.1).

$$T(t) = T_{amb,c} + (T_{final} - T_{amb,c}) \times \left(1 - e^{\frac{-t}{\tau}}\right) \qquad (2.1)$$

The time constant (τ) and the final value (T_{final}) of stack temperature used in the above equation are entirely depended on the two polynomial functions where the dependent variable is the stack current. Equations (2.2) and (2.3) represent the required expressions for the time constant (τ) and the final value (T_{final}) respectively.

$$\tau = p_1 \times I^2 + p_2 \times I + p_3 \qquad (2.2)$$

$$T_{final} = p_4 \times I + p_5 \qquad (2.3)$$

The empirical constants p_1 to p_5 in Equations (2.2) and (2.3) for tested NEXA 1.2 kW system are obtained by using curve fitting method. The obtained values mentioned in (Soltani and Bathaee, 2008) are depicted in Table 2.

Table 2: Current polynomial temperature model parameter values

Empirical constants	Values
p_1	-0.03802
p_2	0.5095
p_3	172.6
p_4	1.1
p_5	27.56

Although the model is simple, it does not provide any information about the effect of the cooling mechanism on stack temperature. Therefore, a model that incorporates a cooling system is discussed below.

2.6.2 RC equivalent circuit model

This model uses the analogy between electrical and thermal variables. The heat flow is represented in the form of current while the temperature is considered analogous of electrical voltage (Restrepo et al., 2015). The initial RC electrical circuit model (without cooling effect) representing system temperature is shown in Figure 7.
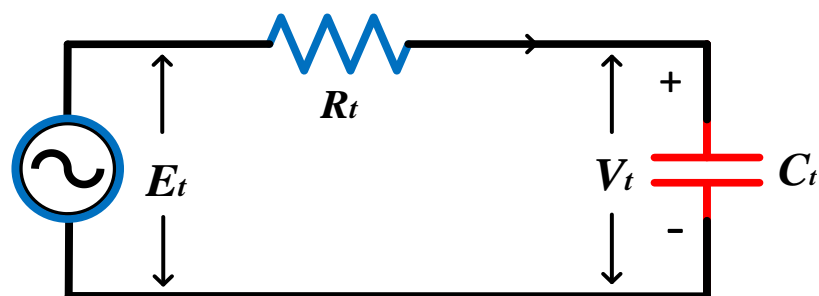
Figure 7: RC equivalent circuit temperature model

The voltage across the capacitor (V_t) representing the temperature of the PEMFC stack system can be obtained as:

$$V_t(I) = E_t \times \left(1 - e^{\frac{-t}{\tau(I)}}\right) + T_{amb,c} \qquad (2.4)$$

In the above equation, τ represents the time constant which is the product of current dependent resistance of the circuit R_t and capacitance C_t. This C_t is the heat capacity (C_{fc}) of the PEMFC system for the NEXA system and the value is 282.8416 J/mol. K.

$$\tau = R_t \times C_t \qquad (2.5)$$

τ can also be obtained as a time-varying sinusoidal function of PEMFC current I given as:

$$\tau = a_3 \times \sin(b_3.I + c_3) + a_4 \times \sin(b_4 I + c_4) \qquad (2.6)$$

Similarly, the source voltage can also be expressed as:

$$E_t = a_1 \times \sin(b_1.I + c_1) + a_2 \times \sin(b_2 I + c_2) \qquad (2.7)$$

The empirical constants a_i and b_i in the above expressions are optimized by using the evolutionary algorithm and optimized values are given in (Restrepo et al., 2015) are duplicated in Table 3.

Table 3: RC equivalent circuit model parameters

Parameters	Values	Parameters	Values	Parameters	Values
a_1	2399	b_1	0.0004962	c_1	0.0005747
a_2	0.8628	b_2	0.2776	c_2	-2.251
a_3	3291	b_3	0.03089	c_3	2.199
a_4	2818	b_4	0.03619	c_4	5.253

It should be noted the effect of the cooling system is not considered in the above model. Therefore, in order to in cooperate cooling system (a fan in the case of NEXA 1.2 kW PEMFC stack system), an additional current source (I_{fan}) included. Figure 8 shows the final temperature model of the NEXA 1.2 kW PEMFC system with an additional current source.
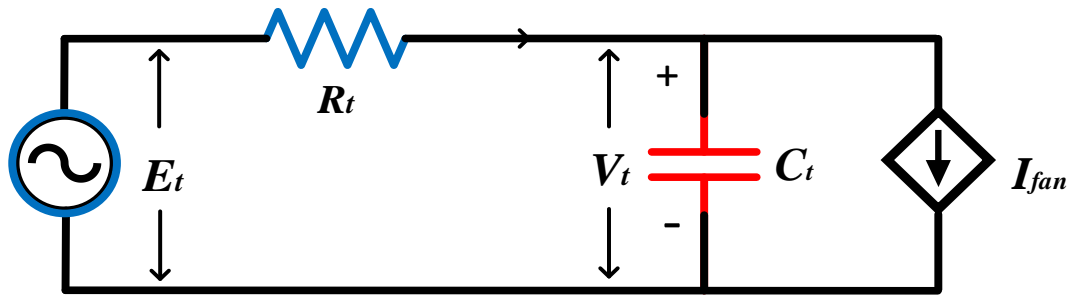
Figure 8: Final RC equivalent circuit temperature model with cooling system

The cooling system current source (I_{fan}) model varies depending upon temperature ranges (T_1, T_2, T_3) of PEMFC as shown below:

$$I_{fan}(T) = \begin{cases} E_1 - \tau_1 \frac{dT}{dt} & if\ T \leq T_1 \\ (E_1 + E_2 - (\tau_1 + \tau_2)\frac{dT}{dt} & if\ T_1 < T < T_2 \\ I_t - \frac{T_t}{R_t} & if\ T \geq T_2 \end{cases} \tag{2.8}$$

Based on the parameters defined in the Equation (2.8), the suggested fan model parameters such as E_1, E_2, T_1, T_2, τ_1 and τ_2 are listed in Table 4 (Restrepo et al., 2015). Here I_t is the equivalent circuit current which was given in Figure 9.

Table 4: Parameter values for fan model

Parameter	Values	Parameter	Values	Parameter	Values
E_1	4.151	τ_1	1000	T_1	65.11
E_2	1.68	τ_2	1000	T_2	69.77

Note that all the said temperature models require experimentation prior to the development of the model.

2.7 Chapter summary

The literature discussed in this chapter enlightens the importance of PEMFC models. Different modelling techniques of PEMFC have been discussed along-with water balance in the PEMFC system and also the possible situations of drying and flooding faults. It is concluded that the semi-empirical modelling technique has the advantage to incorporate ambient conditions and also it has added quality to diagnose water management faults in the PEMFC system.

Chapter 3: Voltage modelling of PEMFC

3.1 Introduction

This research introduces a novel dynamic semi-empirical model for the proton exchange membrane fuel cell (PEMFC). The proposed model not only considers the stack output voltage but also provides valid waveforms of component voltages, such as the no-load, activation, ohmic and concentration voltages of the PEMFC stack system. Experiments under no load, ramping load and dynamic load conditions are performed to obtain various voltage components. According to experimental results, model parameters are optimized using the quantum lightning search algorithm (QLSA) by providing valid theoretical ranges of parameters to the QLSA code. In addition, the correlation between the vapour and water pressures of the PEMFC is obtained to model the component voltages. Finally, all component voltages and the stack output voltage are validated by using the experimental/theoretical waveforms mentioned in previous research. The proposed model output voltage and component voltage drops are also compared with a recently developed semi-empirical model of PEMFC through particle swarm optimization. The proposed dynamic model may be used for in-depth studies on PEMFC behaviour and in dynamic applications for health monitoring and fault diagnosis.

3.2 Basic model of PEMFC stack

The general PEMFC output voltage V_{out} , which is the function of time and other voltages mentioned below, is modelled on the basis of the following mathematical expression:

$$V_{out} = E_{stack} - V_{act} - V_{ohm} - V_{con} \qquad (3.1)$$

Where V_{act} is the activation voltage, V_{ohm} is the ohmic voltage, V_{con} is the concentration voltage and E_{stack} is the internal generated voltage by the stack. The PEMFC characteristic curve showing voltage variations versus current with different component voltages at different stages of current is already depicted and explained in Figure 4.

E_{stack} is the emf of the stack. The emf voltage of a single cell is commonly assumed as added to form the emf of the stack. The emf of a single PEMFC, which is also the internal potential of PEMFC, is expressed as follows (Larminie and Dicks, 2003):

$$E_{cell} = E_{0,cell} + \frac{RT}{2F} ln \left(\frac{P_{H2} P_{O2}^{0.5}}{P_{H2O}} \right) \qquad (3.2)$$

where

$E_{0,cell}$ is the reference potential, which is expressed as follows:

$$E_{0,cell} = 1.229 - 8.5 \times 10^{-4}(T - 298) \qquad (3.3)$$

where T is the fuel cell (FC) temperature (K), which is the function of time.

R is the gas constant (8.3143 J/mol K), F is the Faraday constant (96,487 C/mol), P_{O2} is the pressure of Oxygen (atm), P_{H2} is the pressure of Hydrogen (atm) and P_{H2O} is the pressure of water (atm).

When E_{cell} is determined, the stack emf (E_{stack}) can be obtained by multiplying the number of cells (N) with E_{cell} as follows:

$$E_{stack} = N \times E_{cell} \qquad (3.4)$$

Ideally, the no-load voltage of the PEMFC is equal to E_{stack}. Nevertheless, this finding is inapplicable in practical models because fuel cells (FCs) contain internal currents due to fuel crossover. The FC membrane is porous, which allows fuel gases to diffuse through the membrane. Consequently, free electrons are produced, and an internal current is generated. The effect of the internal current i_{int} is considered in the voltage expression in (3.1). The typical value of i_{int} is in milliampere (mA) for a single PEMFC; this value commonly remains constant for normal operation in healthy PEMFC (Larminie and Dicks, 2003). Hence, the voltage losses created by i_{int} are constant for single PEMFC.

The activation voltage component is distinct to PEMFCs. This voltage drop is dominant at low currents, i.e. when the current exceeds the exchange current density i_o. The exchange current density i_o is the limit of output current. Afterward, the activation voltage effect becomes dominant. This current limit usually depends on the temperature of the PEMFC, and its typical value is also in mA range for PEMFC (Larminie and Dicks, 2003). The following equation depicts the activation voltage for a single cell (Larminie and Dicks, 2003):

$$V_{act} = \frac{NRT}{2\alpha F} ln\left(\frac{I+i_{int}}{i_o}\right) = \frac{RT}{2\frac{\alpha}{N}F} ln(\frac{I+i_{int}}{i_o}) \ if \ (I > i_o) \qquad (3.5)$$

Where factor α is called the charge transfer coefficient, and its value varies from 0 to 1 (Larminie and Dicks, 2003).

Unlike the activation voltage, the ohmic voltage is the linear voltage drop that is dominant in output voltage at the middle ranges of current. This result is due to the internal resistance of the PEMFC. The internal resistance R_{int} is the combination of ionic resistance R_{ionic} and the electronic resistance R_e of the PEMFC. The former

resistance is offered to ions, whereas the latter is presented to electrons. R_{ionic} mainly depends on temperature, current and membrane humidity level, and R_e mainly depends on membrane thickness and its electronic conductivity (Moreira and Da-Silva, 2009; Živko and Bilas, 2006). The ohmic voltage drop is given as follows:

$$V_{ohm} = (I + i_{in}) \times N \times (R_{ionic} + R_e) \qquad (3.6)$$

The final voltage component is the concentration voltage, which is due to the concentration of gases in the PEMFC. This change in concentration provides a voltage drop in the PEMFC output voltage given in (3.1). The change in concentration voltage mainly depends on the current drawn from PEMFC. The concentration voltage (V_{con}) is given as follows (Salim et al., 2015):

$$V_{con} = \frac{-NRT}{2F} ln(1 - \frac{I}{I_{lim}}) \qquad (3.7)$$

Where I_{lim} is the maximum current that can be drawn from the PEMFC system. The internal current i_{int} is absent in the concentration voltage drop in (3.7) as mentioned in (Atifi, Mounir and El-Marjani, 2014).

3.3 Proposed PEMFC model

The proposed model aims to accurately extract component voltages, namely, the no-load voltage of PEMFC $V_{no-load}$, the activation voltage V_{act}, the ohmic voltage V_{ohm} and the concentration voltage V_{con}, as explained in the general modelling of PEMFC.

3.3.1 No-load voltage model

To obtain the PEMFC no-load voltage, the modified PEMFC stack voltage $E_{stack,m}$ is extracted from (3.4), which is rewritten as (3.8). Given that the water pressure is unknown, the voltage drops due to water pressure (V_{H2O}) and internal currents (V_{int}) are separated in modelling the no-load voltage of PMFC. Furthermore, to avoid the complexity of the design, V_{int} can be taken as constant. With these considerations, $V_{no-load}$ can be represented as in (3.9):

$$E_{stack,m} = N \times \left(E_{0,cell} + \frac{RT}{2F} ln\left(P_{H_2} P_{O_2}^{0.5}\right)\right) \quad\quad\quad (3.8)$$

When the temperature is less than 373 K (100°C), the P_{H2O} is neglected, i.e. its value is close to unity (Motapon, Tremblay and Dessaint, 2012). Consequently, V_{H2O} will be considered small.

$$V_{no-load} = E_{stack,m} - N \times \left(V_{int} + V_{H_2O}\right) \qu\quad\quad\quad (3.9)$$

The term ($V_{int} + V_{H2O}$) is required to obtain the no-load voltage. Therefore, a few experiments are essential, as discussed in the later chapter.

3.3.2 Activation voltage model

The activation voltage used in this design is same as that in previous basic model. However, the effects of internal currents are neglected because they are already considered in the no-load voltage. The equation for the modified activation voltage $V_{act,m}$ can be represented as follows (Larminie and Dicks, 2003):

$$V_{act,m} = \frac{NRT}{2\alpha F} ln\left(\frac{I}{i_o}\right) = \frac{RT}{2\frac{\alpha}{N}F} ln\left(\frac{I}{i_o}\right) \ if(I > i_o) \quad\quad\quad (3.10)$$

Where the exchange current density i_o is given as follows (Živko and Bilas, 2006):

$$i_o = B_1 \times F \times exp\left(\frac{-1.229 \times B_2 \times F}{RT}\right) \qquad (3.11)$$

To decrease the complexity of the model, constants B_1 and B_2 are used. These constants are symmetrical factors of PEMFC. Hence, i_o becomes the only temperature-dependent variable. The typical value of i_o is in a few mA (Larminie and Dicks, 2003). Parameters B_1, B_2, and α will again be extracted in later stages when all the component voltages are combined as the overall PEMFC model using optimization techniques. The charge transfer coefficient α in (3.10) can be taken as constant; nevertheless, α displays a complex temperature/humidity dependency (Giner-Sanz, Ortega and Pérez-Herranz, 2015). Moreover, α is a measure of the fuel cell (FC) reaction (Larminie and Dicks, 2003).

3.3.3 Ohmic voltage model

The ohmic voltage V_{ohm} is difficult to calculate because R_{ionic} is also difficult to estimate. As previously mentioned, R_{ionic} depends on membrane humidity. The first step in calculating the membrane humidity level is to compute the relative humidity φ of the PEMFC system, which is expressed as follows (Zhang et al., 2008; Živko and Bilas, 2006):

$$\varphi = \frac{P_{H_2O}}{P_{vap}} \qquad (3.12)$$

Where P_{vap} is the vapour pressure. This parameter can be calculated as a function of the PEMFC temperature T from the formula given in (Moreira and Da-Silva 2009; Zhang et al., 2008), which is taken as the general equation for PEMFC stack.

$$\log_{10}\left[P_{\text{vap}}(T)\right] = 6.02724 \times 10^{-3} + 4.38484 \times 10^{-4}(T - 273.15) +$$

$$1.39844 \times 10^{-5}(T - 273.15)^2 + 2.71166 \times 10^{-7}(T - 273.15)^3 + 2.57731 \times$$

$$10^{-9}(T - 273.15)^4 + 2.82254 \times 10^{-11}(T - 273.15)^5 \quad (3.13)$$

To determine the water pressure, V_{H2O} can be calculated from (3.14) when N ($V_{H2O} + V_{int}$) is already known. V_{int} is a small constant because the internal current presents a considerably low value (Larminie and Dicks, 2003) and requires extraction using optimization techniques. Finally, if V_{H2O} can be calculated, then the water pressure P_{H2O} can be easily obtained, as shown in Equation (3.15).

$$N \times V_{\text{H}_2\text{O}} = N \times (V_{\text{H}_2\text{O}} + V_{\text{int}}) - N \times V_{\text{int}} = N \times A_{\text{H}_2\text{O}} \times T \times \log\left(P_{\text{H}_2\text{O}}\right)$$

$$(3.14)$$

$$P_{\text{H2O}} = \exp\left(\frac{N \times V_{\text{H}_2\text{O}}}{N \times T \times A_{\text{H}_2\text{O}}}\right) \quad (3.15)$$

Where A_{H2O} and V_{int} are unknown constants, and N is the number of PEMFCs in a stack, which will be extracted after experimentation with gradual incremental load with the help of optimization.

The membrane water content λ is dependent on relative humidity φ, which is given as follows (Zhang et al., 2008; Živko and Bilas, 2006):

$$\lambda = 0.043 + 17.81\varphi - 39.85\varphi^2 + 36\varphi^3 \quad (3.16)$$

The ionic resistance of PEMFC is highly dependent on membrane water content λ, stack temperature T, current I and membrane thickness l_m. The ionic resistance R_{ionic} can be expressed as follows (Moreira and Da-Silva, 2009; Živko and Bilas, 2006):

$$R_{ionic} = l_m \frac{181.6N\left[1+0.03I+0.062\left(\frac{T}{303}\right)^2 I^{2.5}\right]}{(\lambda-0.634-3I)\,exp\left[4.18\left(\frac{T-303}{T}\right)\right]} \qquad (3.17)$$

Where the factor $181.6Nl_m$ is taken as an unknown constant in this design, which is $0.0022C_1$. The remaining unknown factors can be calculated from the preceding equations provided. The electronic resistance R_e formula is remarkably simple and given by the following equation (Moreira and Da-Silva, 2009; Živko and Bilas, 2006):

$$R_e = \frac{2 \times N \times l_m}{\sigma_e} \qquad (3.18)$$

The electronic conductivity of the membrane σ_e and its thickness are commonly considered constant to avoid complexity in design. Hence, their ratio, i.e. R_e, is taken as constant in the static model. This electronic resistance may vary by changing the number of fuel cells in the stack.

Finally, V_{ohm} after neglecting the effect of the internal current is given as follows:

$$V_{ohm} = I \times (R_{ionic} + R_e) \qquad (3.19)$$

The ohmic voltage characteristic is partly linear with the increase in current, as previously mentioned in Figure 4. R_e is related to membrane electronic conductivity σ_e, which is dependent on the temperature of PEMFC with complex equations given in (Du et al., 2004). This parameter can be taken as constant to reduce design complexity. However, R_e may vary in the dynamic model.

3.3.4 Final semi-empirical proposed model

After combining Equations (3.9), (3.10),(3.19) and (3.7), the final PEMFC model output voltage equation is given as follows:

$$V_{out} = E_{stack,m} - N \times (V_{int} + V_{H2O}) - \frac{NRT}{2\alpha F} ln\left(\frac{I}{i_o}\right) - (I) \times (R_{ionic} + R_e) -$$

$$\frac{-NRT}{2F} ln\left(1 - \frac{I}{I_{lim}}\right) \tag{3.20}$$

The parameters will be optimized using quantum lightening search algorithm (QLSA) , the details of QLSA are given in Chapter 4. The parameters which will be optimized are given in Table 5;

Table 5: PEMFC proposed model parameters and their ranges based on the literature given above

Parameter	Lower range	Upper range
Charge transfer coefficient (α/N)	1×10^{-6}	0.0213
Exchange current density coefficient (B_1)	1×10^{-6}	20
Exchange current density coefficient (B_2)	1×10^{-6}	20
Voltage drop due to internal current (V_{int})	1×10^{-6}	0.1
Pressure of water constant (A_{H2O})	1×10^{-6}	0.1
Ionic resistance constant (C_1)	1×10^{-6}	1.5
Electronic resistance (R_e)	1×10^{-6}	2

These parameters need to be optimized with the help of QLSA. Some parameters may change with the number of fuel cells in the stack and also they may change with ambient conditions. In order to make the model more generic the detailed analysis of variations in parameters is required at varying ambient conditions for different PEMFC systems with the help of optimization. Statistical regression analysis and some additional factors (based on the number of fuel cells) can be very helpful in making this semi-empirical voltage more generic. When this model becomes generic,

the model can be used for fault diagnosis for flooding and drying faults using membrane water content λ calculated from Equation (3.16). The threshold limits of membrane water content need to be set where the PEMFC can run without going through flooding and drying faults. Equation (3.21) explains the membrane water content threshold limits.

$$\lambda = \left\{ \begin{array}{ll} < \lambda_{lower-threshold} & Drying\ fault \\ > \lambda_{upper-threshold} & Flooding\ fault \end{array} \right\} \qquad (3.21)$$

The $\lambda_{lower-threshold}$ is the lower limit of membrane water content λ, if λ decreased below this limit the PEMFC undergoes drying fault. $\lambda_{upper-threshold}$ is the higher limit of membrane water content λ, if λ increased above this limit the PEMFC undergoes flooding fault. The detailed analysis including final results is given in Chapter 5.

3.4 Empirical model for PEMFC voltage change for varying ambient conditions

In this research, after presenting an overview of PEMFC models discussed in (Salim et al., 2015) , here it is called as PSO (Particle swarm optimization) model as it uses PSO technique for optimization, along with its drawbacks and limitations, in order to remove the shortcomings and drawbacks of the previously mentioned model, a novel model is proposed. The proposed model uses the advantages of the complex semi-empirical model of PEMFC suggested in (Salim et al., 2015) with some modifications to consider the effect of ambient conditions, such as ambient temperature in Kelvin scale denoted by T_{amb}, and uses Oxygen/Hydrogen pressure as input, which can be easily extracted from the air pressure P_{air} and humidity of PEMFC. The proposed model is further simplified to develop another model by considering the PEMFC model discussed in (Salim et al., 2015). Models in (Salim et al., 2015) uses the PEMFC type of 1.2kW Nexa PEMFC with 47 cells in the stack, for their

experimental validity. The main contribution in the proposed model is the introduction

of a voltage source that depends on R_c (output/load resistance), T_{amb}, and P_{air} . The

given parameters are all external and independent of the PEMFC type. The proposed

model can be very helpful for further studies on designing enhanced PEMFC

especially for aircraft applications and unusual ambient temperature conditions.

The PSO model used in (Salim et al., 2015) is the semi-empirical model that

predicts the internal potential E_{stack}, ohmic voltage drop V_{ohm}, activation voltage drop

V_{act}, and concentration voltage drop V_{conc} based on the experimental waveform. The

general model in the form of an equation for PEMFC V_{out} is interpreted in Equation

(3.22) as follows:

$$V_{out} = E_{stack} - V_{act} - V_{ohm} - V_{conc} \qquad (3.22)$$

Where E_{stack} is the stack emf, V_{act} is the activation voltage drop, V_{ohm} is the

ohmic voltage drop in the PEMFC stack, and V_{conc} is the concentration voltage drop in

the PEMFC.

The E_{stack} is related to the partial pressure of fuels, that is, the pressure of

Oxygen P_{O_2} and P_{H_2} along with the effect of stack temperature. Equation (3.23)

represents the E_{stack}, where n is the number of cells in the stack. R, F, and k_e are

constants with values 8.3143 J/mole·K, 96,487 C/mol, 8.5×10^{-4} V/K, respectively as

mentioned earlier.

$$E_{stack} = N \times \left(1.229 - k_e(T - 298) + \frac{RT \times \log(P_{H_2} P_{O_2}^{0.5})}{2F} \right) \qquad (3.23)$$

V_{act} is represented in Equation (3.24) and depends on the current and

temperature of the PEMFC.

$$V_{act} = n_o + (T - 298) \times a + (R_{act}) \times I \tag{3.24}$$

Where R_{act} is the temperature and current dependent polynomial. V_{ohm} is given in Equation (3.25), and the ohmic resistance also depends on the current and temperature of the PEMFC.

$$V_{ohm} = (R_{ohm}) \times I \tag{3.25}$$

The concentration voltage is given in Equation (3.26) as follows:

$$V_{conc} = \frac{-NRT}{2F} \ln\left(1 - \frac{I}{I_{lim}}\right) \tag{3.26}$$

Where I_{lim} is the PEMFC stack current limit. The temperature model is also mentioned in (Salim et al., 2015), in which the stack temperature T is extracted using T_{amb}, voltage, and current. Several other parameters from the PEMFC are required and can be extracted from the data sheet of NEXA 1.2 kW PEMFC.

$$T = \int \frac{q_{net}}{M_{FC}C_{FC}} dt \tag{3.27}$$

Where M_{FC} (kg) is the mass of the PEMFC stack, and C_{FC} is the overall specific heat capacity of the stack (J/mol K). q_{net} is the net heat produced in the fuel cell which is given as follows:

$$q_{net} = q_{chem} - q_{elec} - q_{sens+latent} - q_{loss} \tag{3.28}$$

q_{chem} is the heat energy produced for the chemical reaction during the PEMFC operation which can be obtained as follows:

$$q_{chem} = -\frac{I}{2F} \times N \times 237153.66 \tag{3.29}$$

Meanwhile, q_{elec} is the electrical power, that is, the heat produced by electrical power, which can be obtained as follows:

$$q_{\text{elec}} = V \times I \tag{3.30}$$

Moreover, $q_{sens+latent}$ is the sensible and latent heat given as follows:

$$q_{\text{sens+latent}} = (K_1 + K_2)(T - T_{\text{amb}}) + K_3 I \tag{3.31}$$

In addition, q_{loss} is the heat loss and expressed as follows:

$$q_{\text{loss}} = h_{\text{cell}}(T - T_{\text{amb}}) \times N \times A_{\text{cell}} \tag{3.32}$$

In Equations (3.31) and (3.32), K_1, K_2, and K_3 are constants, A_{cell} is the area of the cell, and h_{cell} is the convective heat transfer coefficient. The constants in above equations are listed in Table 6. Using Equations (3.27)–(3.32), the PEMFC operating temperature can be extracted with V_{out} as feedback, while the current and T_{amb} as input. The validity of this temperature has already been experimentally proven in (Salim et al., 2015).

Table 6: Parameter values for PSO model optimized through particle swarm optimization (PSO)

Parameter	Values
n_o	26.5230 V
A	-8.9224 x10^{-2} V/K
R_{act}	-1.0526+6.945×10^{-11}(I^6)-1.7272×10^{-8}(I^5)+1.7772×10^{-6}(I^4)-9.8133×10^{-5}(I^3)+3.143×10^{-3}(I^2)-3.532×10^{-2}(I)+1.3899×10^{-3}(T-298)
R_{ohm}	1.7941-2.3081×10^{-2} (I)-2.0060×10^{-3} (T-298)
A_{cell}	1.2×10^{-2} m^2
M_{FC}	13 Kg
C_{FC}	282.8416 J/mol.K
h_{cell}	19.6434 W/m^{2}K
K_1	10.3597 J/K
K_2	0.3259 J/A.K
K_3	4.7337 J/A

3.4.1 Drawbacks of the PSO model

The PSO model (Salim et al., 2015) has several drawbacks. First, the current is considered as input. This condition indicates that an experiment on the PEMFC system is first needed to record the values of the current and input into the model to obtain the PEMFC temperature and V_{out}. Moreover, P_{H_2} and P_{O_2} are directly considered by the model to be inside the PEMFC. However, P_{H_2} at the anode is not easy to estimate. Estimating this parameter requires several sensors the in PEMFC system, or several equations should be used to calculate the vapor pressure. The external applied pressure P_{H_2} can be calculated. If the R_c is to be encoded in the PEMFC model and current as of the feedback, the model will become very complex and will require a considerable amount of time to simulate. Thus, this model cannot be used as a convenient model for estimating PEMFC performance, because it is time-consuming and needs significant modifications.

3.4.2 Proposed modifications in PSO model

The model in Salim et al., (2015) has deficiencies that can be easily corrected with few modifications. In (Salim et al., 2015), P_{O_2} and P_{H_2} are considered as constant. However, these conditions are not true when T_{amb} and P_{air} vary. P_{O_2} and P_{H_2} depend on the PEMFC water vapor content and operating conditions, such as current and PEMFC temperature. The equations for calculating P_{H_2} and P_{O_2} according to (Moreira and Da-Silva, 2009) can be expressed as follows:

$$P_{O_2} = \left(\frac{1}{1+\beta_{no}}\right) \times \left(P_{air} - P_{vap}\right) \tag{3.33}$$

$$\beta_{no} = \frac{x_{N_2}}{x_{O_2}} \tag{3.34}$$

$$P_{H_2} = P_{an} - 0.5 P_{vap} \tag{3.35}$$

$$\log_{10}\left[P_{vap}(T)\right] = 6.02724 \times 10^{-3} + 4.38484 \times 10^{-4}(T - 273.15) +$$
$$1.39844 \times 10^{-5} (T - 273.15)^2 + 2.71166 \times 10^{-7} (T - 273.15)^3 + 2.57731 \times$$
$$10^{-9} (T - 273.15)^4 + 2.82254 \times 10^{-11} (T - 273.15)^5 \tag{3.36}$$

Where x_{N_2} and x_{O_2} are the concentrations of Nitrogen and Oxygen in the air, respectively. P_{an} is the applied Hydrogen pressure which depends on air/fuel stoichiometry. This parameter is usually 600 mbar for NEXA 1.2kW PEMFC system.

Thus, when T_{amb} and P_{air} changes, the effect on PEMFC performance is evident from Equations (3.31), (3.32), and (3.33).

Moreover, instead of using the current obtained from the experiments, R_c can be used and set at different values using Ohm's Law. Consequently, the model will

only require R_c, T_{amb}, and P_{air} as input along with applied anode P_{an}. The rest can be calculated with the procedure given in Figure 9 and Equations (3.22) – (3.36) with T (stack temperature) and V_{out} as feedback. The Matlab model of the PEMFC is shown in Figure 10.
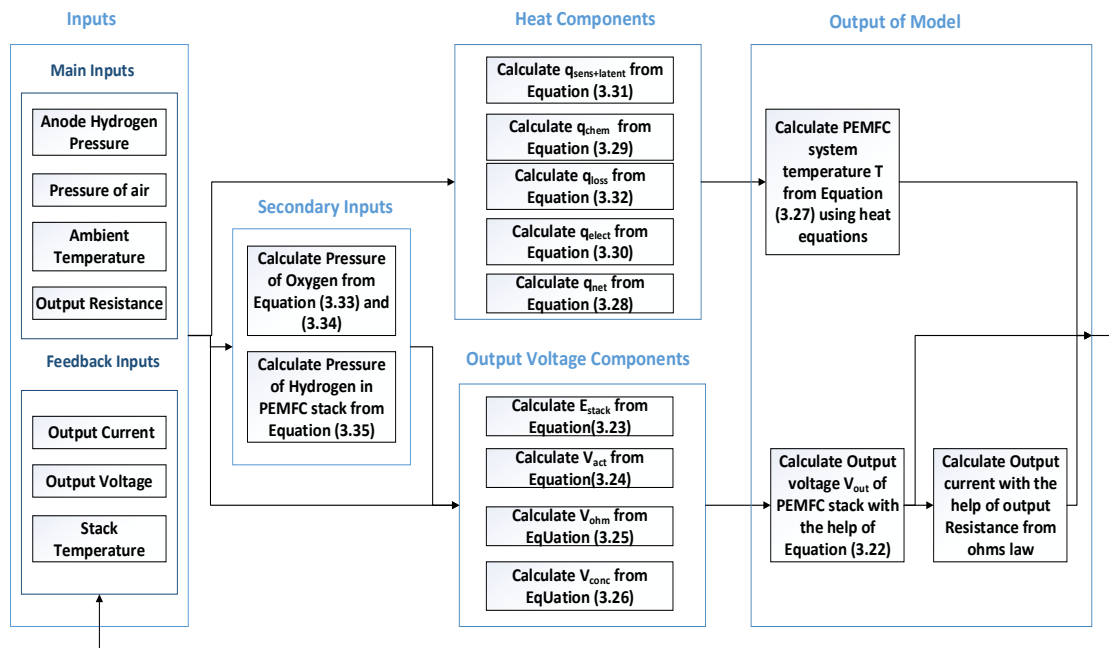
Figure 9: Procedure for calculating output voltage by varying ambient temperature and pressure through PSO model
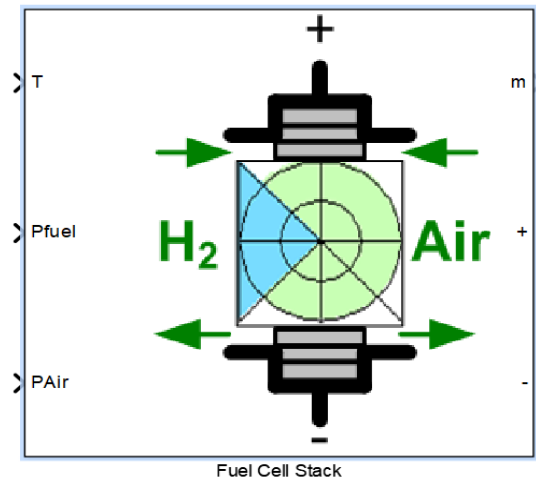
Figure 10: Matlab PEMFC Model

3.4.3 Proposed empirical model

The PSO model is a complete model, but it uses the complex equations as explained earlier. The model considers T_{amb}, P_{air}, R_c, and P_{an} as inputs and calculates V_{out} with current as feedback. Thus, V_{out} is determined. Variation in the PEMFC voltage caused by a change in ambient conditions can be depicted simply by a voltage source V_{amb} which depends on T_{amb}, R_c, and P_{air}. A linear model may not be an option, because the equations in the PSO model are complex and have various interactions among parameters. V_{amb} can be defined as follows:

$$V_{amb} = V_{nor} - V_{var} = f(T_{amb}, P_{air}, R_c) \qquad (3.37)$$

Where V_{nor} is the voltage of the PEMFC at different loading conditions (R_c) at T_{amb} of 298 K and P_{air} of 1 atm, while V_{var} is the voltage at different T_{amb} and P_{air} values apart from normal (298K, 1 atm). This V_{amb} depends on T_{amb} and P_{air} and a function of input variables R_c, T_{amb}, and P_{air}.

T_{amb} and P_{air} have high and low limits. The high limit (or state 1) for T_{amb} is considered as 323 K (50°C), which is the maximum T_{amb} in hot climates (Al-Zeyoudi, Sasmito and Shamim, 2015), while the lowest T_{amb} (state −1) is considered at as low as 273 K (0°C), which is observed at high altitude in aircraft applications (Pratt, Brouwer and Samuelsen, 2007). The mean temperature (state 0) is at 298 K.

Similarly, P_{air} is maximum at sea level (state 1) and the pressure at sea level is 1 atm, while P_{air} can be as low (state −1) as 0.6 atm in aircraft applications (Werner et al., 2015). The mean pressure (state 0) in this work is considered as 0.8 atm.

To obtain V_{amb}, the regression model is suggested to consider the nonlinear effects using central composite surface statistical design (Montgomery, 2013).

3.4.4 Central composite surface design for V_{amb} calculations

Central composite design (CCD) is most frequently used to fit second-order model designs. This design consists of 2^k factorial (or fractional factorial of resolution V) with the cube, center, and axial points as described in Figure 11. Points (1, 1), (−1, 1), (−1, −1), and (1, −1) are cube points, while (0, 0) is the center point. Any points that involve α_i are axial points.
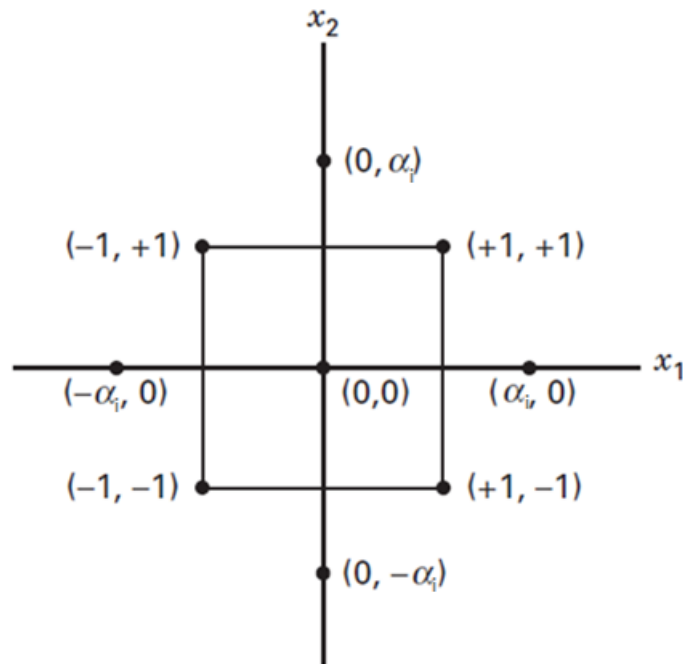
Figure 11: Central Composite design considering two input factors

To determine the second-order V_{amb} model in Equation (3.38), two variables are used when $R_c > R_{th} = 1\ \Omega$. R_{th} is obtained from the results obtained from the proposed Model 1.

$$V_{amb} = A_o + A_1 T_{amb} + A_2 P_{air} + A_3 T_{amb} P_{air} + A_4 T_{amb}^2 + A_5 P_{air}^2 \qquad (3.38)$$

Where A_i ($i = 0$ to 5) are the coefficients which can be extracted using Minitab statistical software with V_{amb} for given T_{amb} and P_{amb} from the proposed Model 1. For the two-variable model, R_c is a constant, because the impact of R_c on V_{amb} is negligible when R_c varies from $1\ \Omega$ to $39.75\ \Omega$ as depicted in the results from the proposed model in Figures 9 and 10. Thus, R_{th} of $1\ \Omega$ is considered after several simulations. The CCD for extracting V_{amb} regression model in Equation (3.38) is given in Table 7.

Table 7: Central composite design (CCD) parameters for V_{amb} when $R_c > R_{th}$

Central Composite Design	
Two-level factorial: Full factorial	
Factors	2
Replicates	1
Base runs	9
Total runs	9
Base Blocks	1
Total Blocks	1
Cube points	4
Centre points in cube	1
Axial points	4
Centre points in axial	0
Note ; $\alpha_i = 1$	

For resistance with $R_c \leq R_{th} = 1\ \Omega$, R_c should be considered as the third factor in the design and only one replicate is used in the CCD. The resultant equation for V_{amb} using R_c as an additional factor is as follows:

$$V_{amb} = A_6 + A_7 T_{amb} + A_8 P_{air} + A_9 T_{amb} P_{air} + A_{10} T_{amb}^2 + A_{11} P_{air}^2 + A_{12} R_c +$$

$$A_{13} R_c^2 + A_{14} T_{amb} R_c + A_{15} P_{air} R_c + A_{16} P_{air} T_{amb} R_c. \tag{3.39}$$

For this additional variable, the state 1 is observed when $R_c = 1\ \Omega$, state 0 at 0.75 Ω, and state -1 at 0.5 Ω. In Equation (3.39), A_i (i = 6 to 16) are the coefficients which can be extracted using the Minitab ® statistical software using V_{amb} for a given T_{amb} and P_{amb} from the proposed Model 1. The CCD for extracting the regression model in Equation (3.39) is listed in Table 8.

Table 8: CCD parameters for V_{amb} when $R_c \leq R_{th}$

Central Composite Design	
Two-level factorial: Full factorial	
Factors	3
Replicates	1
Base runs	15
Total runs	15
Base Blocks	1
Total Blocks	1
Cube points	8
Centre points in cube	1
Axial points	6
Centre points in axial	0
Note ; $\alpha_i = 1$	

The CCD does not only provide the regression model but also indicates the significance of the terms used in the design and may also rule out insignificant terms. All terms, except for the ones which are really insignificant, are included. The significance of the terms is given in the form of p-values depicting the probability of terms. The significance of the regression model given in Equations (3.38) and (3.39) is based on 95% confidence probability.

This variation in voltage V_{amb} has been appended with the electrical equivalent model in (Aglzim et al., 2014) as a voltage source, the complete details of the proposed electrical equivalent model have been shared after V_{amb} coefficients have been finalized in Chapter 5.

3.5 Experiments required

The experiments are required to validate the semi-empirical model where current is changed linearly and abruptly. To enhance the semi-empirical voltage model

to fit in varying ambient conditions, some experiments are also needed where dry, humid and normal conditions are tested. Statistical analysis may be used to modify the semi-empirical voltage model parameters. In addition to that, the experiments are needed to perform on at least two different PEMFC systems with different number of fuel cells in the stack, in order to make the model applicable to various types of PEMFC systems where fuel cells in a stack are different. The complete details of experiments are given in Chapter 5.

3.6 Chapter summary

This chapter introduces the concept of voltage modelling of PEMFC, the voltage model depends upon the emf of stack and voltage drops. These voltage drop equations are close to theoretical equations but they are not very complex. Also the no-load voltage of PEMFC has been addressed as per theoretical explanation. These equations will also satisfy theoretical pattern of voltage drop waveform which will be shown later. Also the empirical model has been proposed that tracks the voltage variation with the change in ambient conditions by using the previously validated semi-empirical model of PEMFC.

Chapter 4: Temperature modelling of PEMFC

4.1 Introduction

This chapter presents a dynamic temperature model for a proton exchange membrane fuel cell (PEMFC) system. The proposed model overcomes the complexity of conventional models using first-order expressions consisting of load current and ambient temperature.

The temperature of PEMFC is very important to predict, since the voltage model uses temperature of PEMFC, this temperature can also be measured with the help of sensors inside stack but not all commercial PEMFCs are equipped with internal sensors because it increases the cost of PEMFC system. Thus it is needed to predict the temperature of PEMFC based on load current and ambient temperature. The proposed temperature model also incorporates a PEMFC cooling system, which depends upon the temperature difference between events. A dynamic algorithm is developed to detect load changing events and calculate instantaneous PEMFC temperature variations. The parameters of the model are extracted by employing the quantum lightning search algorithm (QLSA). The temperature characteristics of the NEXA 1.2 kW PEMFC system are experimentally studied to validate model performance. The proposed model must have the tendency to give accurate results for both linear and abrupt changes in load current. The model is not only helpful for simulations but also suitable for dynamic real-time controllers and emulators.

4.2 Basic temperature model

The basic PEMFC temperature model relies on the heat produced in the PEMFC stack. The heat is generated owing to the chemical reaction in the PEMFC system. The PEMFC thermodynamic energy balance can be represented as (Salim et al., 2015):

$$q_{net} = q_{chem} - q_{elec} - q_{sens+latent} - q_{loss} \qquad (4.1)$$

Where the basic equations for q_{chem}, q_{elec}, $q_{sens+latent}$ and q_{loss} are given below, these equations are basic theoretical equations so they differ from the equations given in the PSO model in Chapter 3.

The chemical energy (q_{chem}) produced by PEMFCs depends on the rate of consumption of Hydrogen fuel (N_{H_2}), the number of cells (N), and the Gibbs free energy constant (ΔG), as shown:

$$q_{chem} = N_{H_2} \times \Delta G \times N \qquad (4.2)$$

Electrical energy (q_{elec}) is simply the product of the voltage (*V*) and current (*I*) of the PEMFC stack in unit time (t).

$$q_{elec} = V \times I \times t \qquad (4.3)$$

Sensible and latent heat ($q_{sens+latent}$) not only depends upon the consumption of Hydrogen but also upon the rate of consumption of Oxygen (N_{O_2}), PEMFC temperature (T), ambient temperature (T_{amb}), the rate of production of water and vapors and their specific heat capacities (C_{H_2}, C_{H_2O}, C_{O_2}), and the vaporization heat of water (H_v), as expressed in (4.4).

$$q_{sens+latent} = N_{H_2}(T - T_{amb})C_{H2} + N_{O_2}(T - T_{amb})C_{O_2} + N_{H_2O}(T - T_{amb})C_{H_2O} +$$

$$N_{H_2O}H_V \tag{4.4}$$

Finally, heat loss (q_{loss}) depends upon the cooling system of the PEMFC stack, which is related to the convective heat transfer coefficient (h_{cell}) in W/m^{2}K, the number of fuel cells, and the area of fuel cells (A_{cell}), as expressed below.

$$q_{loss} = h_{cell}(T - T_{amb})N \times A_{cell} \tag{4.5}$$

In the NEXA 1.2 kW PEMFC system, cooling is performed by cooling fans.

By determining the net heat produced (q_{net}), PEMFC temperature can be obtained as:

$$T = \int \frac{q_{net}}{M_{fc}C_{fc}} dt \tag{4.6}$$

where M_{fc} and C_{fc} are the mass and overall specific heat capacity of the PEMFC stack, respectively.

As seen in the above model, considerable information is required, such as the consumption of Hydrogen and Oxygen, the production of water, the area of PEMFCs, and several thermodynamic parameters. Moreover, the model requires PEMFC output voltage and current. This model is clearly complex, and thus, a simplified PEMFC temperature model that depends only on current and ambient air pressure and temperature is required. Figure 12 reveals the basic temperature model of PEMFC.
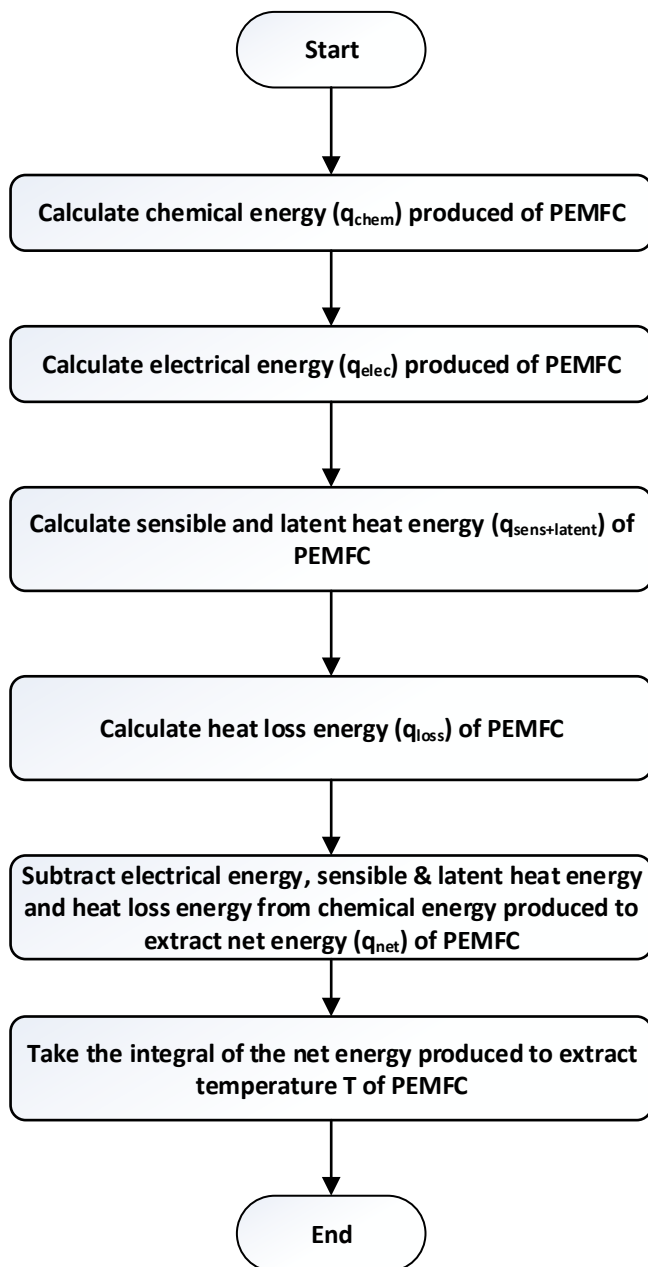
Figure 12: Basic temperature model of PEMFC

4.3 Proposed PEMFC temperature model

The aim of the proposed PEMFC temperature model is to reduce the complexity and limitations of the various PEMFC temperature models proposed in the literature. The proposed model is developed based on the first-order discrete equation given by (4.7).

$$T_{mod}(t) = L_1 I_t + L_2(I_q - I_t)e^{-L_3(t-q)} + T_{amb,c}(t) - L_4 \qquad (4.7)$$

Where I_q is the value of current for time q which is the time sample just before a significant change in current occurs and I_t is the present value of current for time t. L_1 and L_2 are scaling constants, which convert current values into temperature, L_3 is the time constant of the first-order model, and L_4 is a constant that takes the unit of temperature. $T_{amb,c}$ is the ambient temperature in the Celsius scale.

Two equations are developed to represent the effect of the cooling system. These equations depend upon the difference between the modeled temperatures calculated from (4.7) for time t and q. Equations (4.8) and (4.9) help in deriving the final value of modeled temperature, i.e., T_{mod2} (t).

$$T_{mod1}(t) = T_{mod}(t) - L_5 \frac{\{T_{mod}(t) - T_{mod}(q)\}}{(t-q)} \qquad (4.8)$$

Note that in the above expression, $\Delta T_{mod_{t-q}} = \{T_{mod}(t) - T_{mod}(q)\}$ is used to account for the cooling system in the PEMFC system using fan with constant speed. However, instead of utilizing the change in time (Δt), time difference (t-q) is used, which is dynamic and varies with time. Therefore, the sampling rate does not affect the model. The temperature of the PEMFCs used in this study is typically less than 65 °C at room temperature (less than 28°C), no additional modeling for cooling is

required, as given in previous model mentioned in (Restrepo et al., 2015). Here $T_{amb,c}$

and $T_{mod,2}$ are in the Celsius scale.

$$T_{mod2}(t) = T_{mod1}(t) + L_6\{T_{mod1}(t) - T_{mod1}(q)\} \qquad (4.9)$$

The final temperature $T_{mod,2}$ must be added with 273.15 constant in order to

convert the temperature from Celsius to Kelvin scale for its implementation in voltage

model. In the above equations, L_i (i = 1 to 6) denotes constant parameters that are

calculated using optimization techniques. In this study, the QLSA (Ali, Hannan, and

Mohamed 2015) is used as an optimization tool. The pseudo-code for implementing

the proposed model is shown in Table 9.

Table 9: Pseudo-code for temperature model of PEMFC

Data: Experimental measurements of T_{amb} , current I and PEMFC temperature T_{exp}   Output: Modelled temperature T_{mod} T_{mod} **(initial value)** $\rightarrow T_{amb,c}$; *Set initial Modelled temperature equal to ambient temperature at start* $j \rightarrow t$; *set j equal to present value of sample time*   **While (j>1)**   **If abs($I_t - I_j$) > 1** *check for sufficient deviation in current i.e above 1.5% of rated current* $I_q \rightarrow I_j$; *Save previous value of current before sufficient deviation* $q \rightarrow j$; *time sample value for last significant deviation of current*   **end;** *end if* $j \rightarrow j\text{-}1$; *move back to previous time sample*   **end;** *end while loop*   **Calculate $T_{mod,2}(t)$ from Equations (4.7) to (4.9) while using q, t, I_t, and I_q from the above algorithm**

The Table 10 will give the parameters and their proposed limits for temperature model

of PEMFC.

Table 10: PEMFC temperature model parameters limit

Parameter	Ranges		Parameter	Ranges	
	Min	Max		Min	Max
L_1	1×10^{-6}	5	L_4	-400	400
L_2	1×10^{-6}	5	L_5	-200	200
L_3	1×10^{-6}	5	L_6	-200	200

4.4 Quantum lightening search algorithm (QLSA)

For the voltage and temperature model the parameters given must be optimized using optimization technique. In this research the optimization technique that has been used is Quantum Lightening Search Algorithm (QLSA).

Lightening Search Algorithm (LSA) is an optimization technique which was inspired from the natural phenomena of lightening flash which was set by the propagation of negative charged particles in space. The idea was first introduced in (Shareef, Ibrahim and Mutlag, 2015) as Lightening Search Algorithm (LSA) and then it is extended in (Ali, Hannan and Mohamed, 2015) as Quantum LSA (QLSA). Lightening search process is not continuous but through a regular discrete steps using a concept called step leader propagation. Projectiles model the progression of step leaders. The three projectiles that are presented in (Ali, Hannan and Mohamed, 2015) are (i) transition projectiles which are the step leader of the main population (ii) space projectiles which strive for the best position as leader (iii) and the lead projectiles which holds the best position among the whole population. In the standard LSA algorithm, the search processes for these three projectiles are based on exponential, uniform and normal probability density functions. But in QLSA quantum physics analogy is used along-with special quantum physics equations to improve search

ability. The algorithm is fast and reliable and it has been proven in (Ali, Hannan and Mohamed, 2015) that this algorithm works better than Lightening search algorithm (LSA), Particle swarm optimization (PSO), Backtracking search algorithm (BSA) and Genetic search algorithm (GSA).

The QLSA search the new position for its population in order to get the best step leader position. At start QLSA develops a memory which stores the best positions for step leaders, these step leaders are called global step leaders $Gsl_{i,j}{}^{t}$ .These global step leaders are obtain with the help of objective function evaluation. In this case it is the root mean square error.

$$RMSE = \sqrt{\frac{\sum Value_{modelled} - Value_{experimental})^2}{Total\ number\ of\ samples}} \qquad (4.10)$$

In QLSA each step leader attains the best position with the help of stochastic attractor which is expressed as:

$$p_{i,j}^{t} = \frac{a_{i,j}^{t} P_{i,j,best}^{t} + b_{i,j}^{t} Gsl_{i,j}^{t}}{F \times c_{i,j}^{t}} \qquad (4.11)$$

Here i varies from 1 to population size (N_P), j varies from 1 to problem dimension (D) and t varies from 1 to maximum number of iterations (Z). The constants a,b and c in the Equation (4.11) are random numbers (uniformly distributed) from 0 to 1. $P_{i,j,best}$ is the best step leader for every individual population. F is the scale factor, the typical value of this factor is 10.

QLSA makes the LSA to follow a quantum physics analogy where each step leader displays the behavior of quantum with the help of quantum wave equation. For extracting the time and space dependency for the probabilistic model of step leaders

to guide their correct movement, quantum physics equations are used with probability density and distribution functions. These equations are explicitly given in (Ali, Hannan and Mohamed, 2015).

In general, QLSA started with initialization of population with N×D number of step leaders (P). Then the standard deviation $L_{i,j}$ which is dependent upon mean best position of step leaders is extracted by using Equation (4.12):

$$L_{i,j} = 2\beta |Mbest_j - P_{i,j}| \tag{4.12}$$

Here expansion/contraction coefficient β which controls the speed of algorithm.

In the above expression, $MBest_j$ is termed as mean best position (depending upon the objective function) for the step leaders and it is basically the mean value of $P_{i,j}$ positions of all step leaders. The formula to calculate $Mbest_j$ is:

$$MBest_j = \frac{1}{N}\sum_{i=1}^{N} P_{i,j} \tag{4.13}$$

The coefficient β usually controls the speed of convergence of QLSA. The equation to obtaining the β coefficient is given as:

$$\beta = \beta_o + \frac{(Z-t)\times(\beta_1-\beta_o)}{t} \tag{4.14}$$

Here β_1 and β_o are the final and initial values of coefficient which are generally set as 1.2 and 0.6 respectively, t is the present iteration. Finally the position of step leaders is updated with the help of Equation (4.15):

$$P_{i,j,new} = p_{i,j,old} \pm \beta |Mbest_j - P_{i,j,old}| ln\left(\frac{1}{u_{i,j,new}}\right) \tag{4.15}$$

where $u_{i,j}$ is the random number (uniformly-distributed) between 0 and 1. The

basic implementation steps of the QLSA are shown in Figure 13.
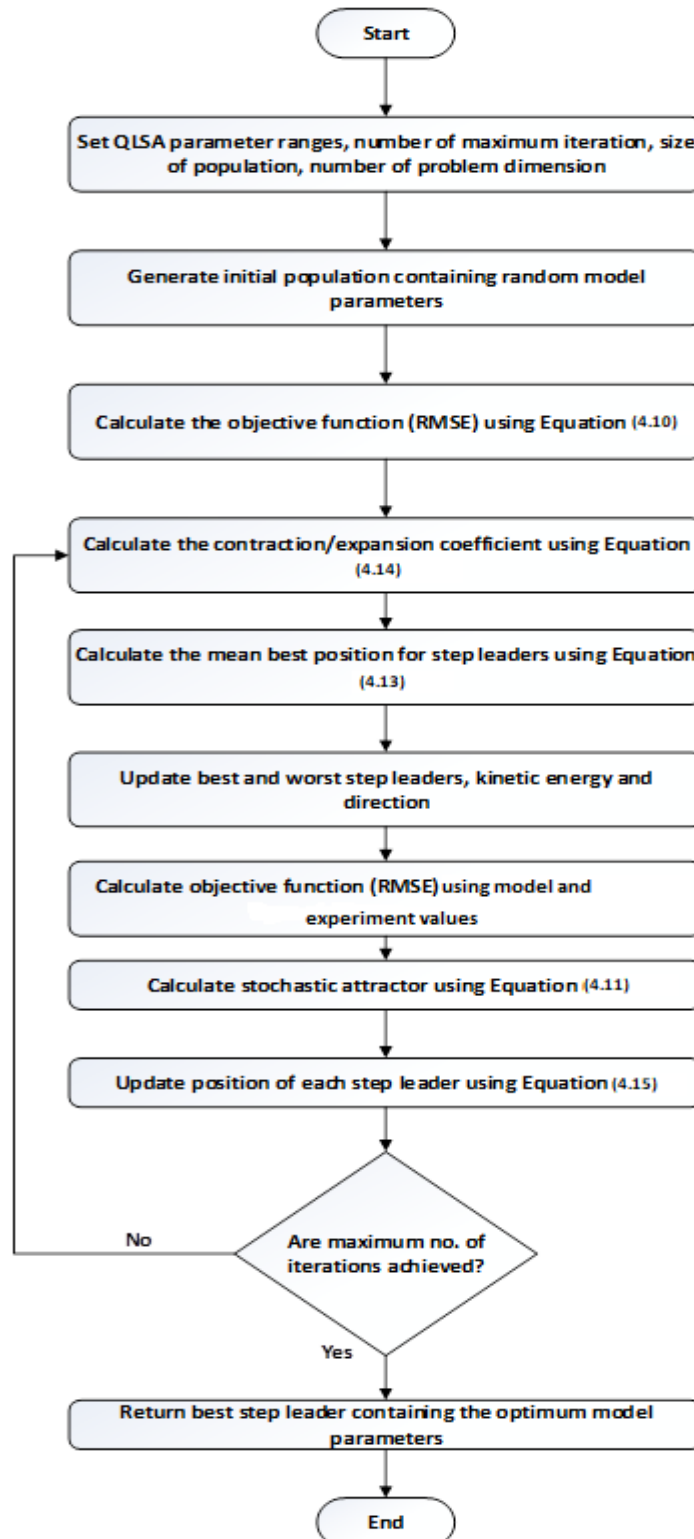
Figure 13: QLSA implementation schematics

4.5 Chapter summary

This chapter explains the temperature modelling of PEMFC. The modelling equations are simple, however a memory has been used for the temperature modelling algorithm which tracks the time and load current values. This memory feature though adds another memory device for modelling but it reduces the complexity of model equations. Also this temperature model can be applicable to all PEMFC system with simple fan cooling system at constant speed. At the end, this chapter briefly explains the working of quantum lightening search algorithm (QLSA) which optimizes the parameters of an objective function. This algorithm uses the natural phenomena of lightening and it has been fast, modern and reliable than other known optimization algorithm.

Chapter 5: Results and discussion

5.1 Experiments and results for PEMFC voltage and temperature models

The major part for the extracting results of the voltage and temperature models is extracting parameters with the help of QLSA but before extracting the parameters the laboratory experiments are required for no-load, smooth and dynamic variations of load.

5.2 Laboratory tests required to extract unknown parameters

Three different experiments are essential to determine the unknown parameters involved with no load, activation and ohmic voltage models. With consideration of 1.2 kW Nexa PEMFC system as the subject, these experiments are explained in detail in the following sections.

5.2.1 Experiment 1: Variation in ambient parameters under no-load condition

The experimental setup of the PEMFC 1.2 kW Nexa System is shown in Figure 14. In this experiment, the parameters, such as temperature T of the PEMFC stack and Hydrogen pressure P_{H_2} at different ambient/experimental conditions, are varied under no-load condition. The experimental waveforms are given in Figure 15, where the variation in PEMFC voltage is shown with the variation in Hydrogen pressure and PEMFC temperature. Notably, the current is zero because no-load is connected across the PEMFC.

Figure 14: NEXA 1.2kW setup in UAE University
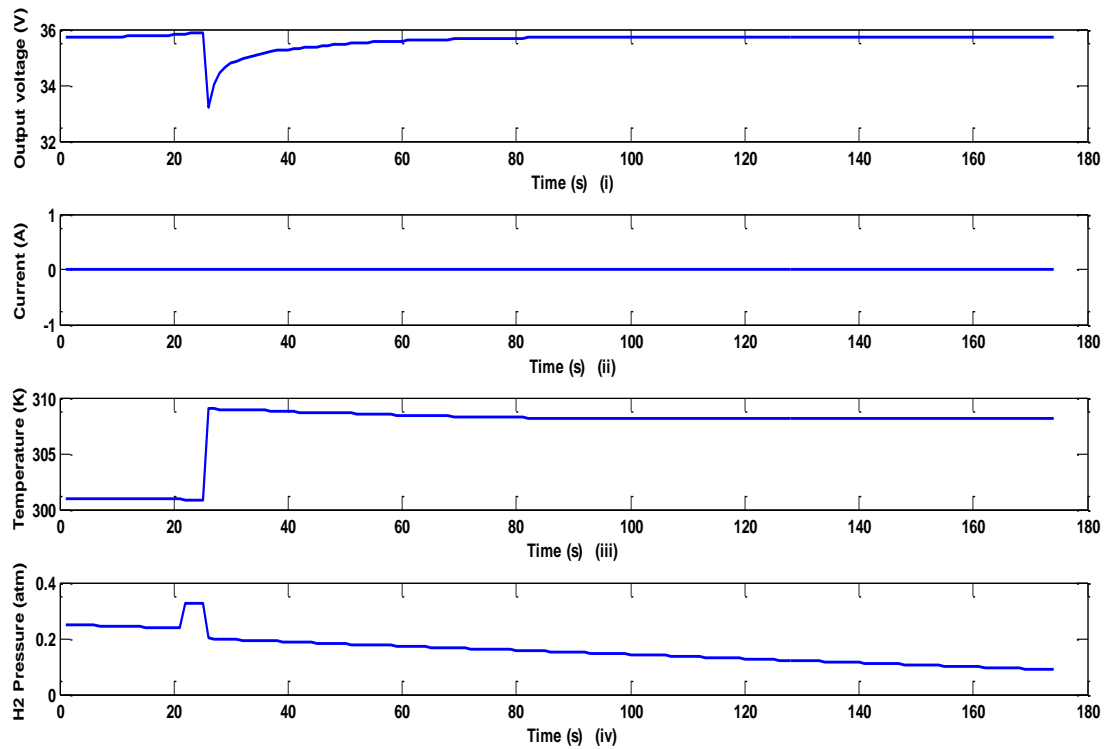
Figure 15: Experimental results for no-load conditions of PEMFC (i) output voltage

at no-load (V), (ii) current (A), (iii) temperature (K) and (iv) Hydrogen pressure

(atm)

According to this experiment, $N(V_{int} + V_{H_2O})$ can be extracted using previous

Equations (3.8), (3.9) and Equation (7.1), and the no-load voltage is as follows:

$$N \times (V_{int} + V_{H_2O}) = E_{stack,m} - V_{no-load_{expertiment}} \qquad (7.1)$$

To express the above voltage component, the general linear regression model

can be used when the effects of two parameters interact as follows:

$$N \times (V_{int} + V_{H_2O}) = NA_1 \times T \times P_{H_2} + NA_2, \qquad (7.2)$$

where NA_1–NA_2 are constants.

The required parameters NA$_1$ and NA$_2$ of the polynomial function in Equation (7.2) can be easily extracted using the MATLAB curve fitting toolbox. The extracted parameter values of NA$_1$ and NA$_2$ are 0.0219 and 18.8223, respectively. Thus, Equation (7.2) is transformed as follows:

$$N \times (V_{int} + V_{H2O}) = 0.0219 \times T \times P_{H2} + 18.8223. \qquad (7.3)$$

The no-load voltage model is the key voltage because it provides the basis for all component voltages. Experiment 1 supports the no-load estimate of the model voltage. Figure 16 shows the no-load voltage output of the model. The no-load voltage model is compared with the experimental no-load voltage. The performance of the no-load voltage model, which follows the pattern of the experimental values, is appropriate.
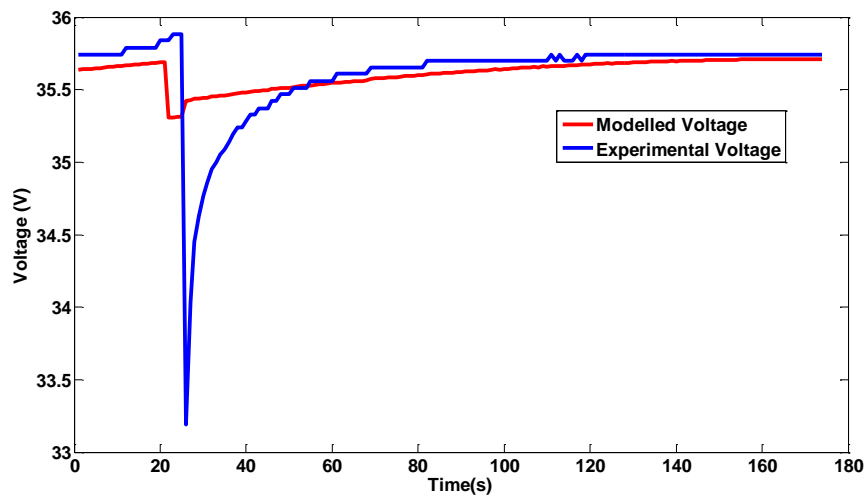

Figure 16: Comparison of experimental voltage versus modelled no-load voltage

5.2.2 Experiment 2: Variation in ambient parameters under gradual loading

The concentration and ohmic voltage are considerably important under loading condition because their complex equations complicate the PEMFC design. Previous researchers exerted efforts to plot these parameters as a function of current. Nevertheless, the model parameters used are largely complex, and they require a considerable amount of internal details about PEMFC. These types of details and complexity are excluded in this paper. The only required factors are fuel pressure, temperature, voltage and current to save complexity. The waveforms of the ohmic and activation voltages must be plotted with current, where current linearly increases with time. Hence, experiment 2 is essential for PEMFC modelling.

In this experiment, the current is increased from 0 A to 61 A with a constant slope to determine the waveform validity of V_{act}, V_{ohm}, V_{con}, water and vapour pressures according to the theoretical waveforms or valid experimental waveforms provided in previous research. The experimental data are presented in Figure 17. The experimental stack voltage decreases with increased current I and temperature T. A slight increase in Hydrogen pressure is also shown in Figure 17.
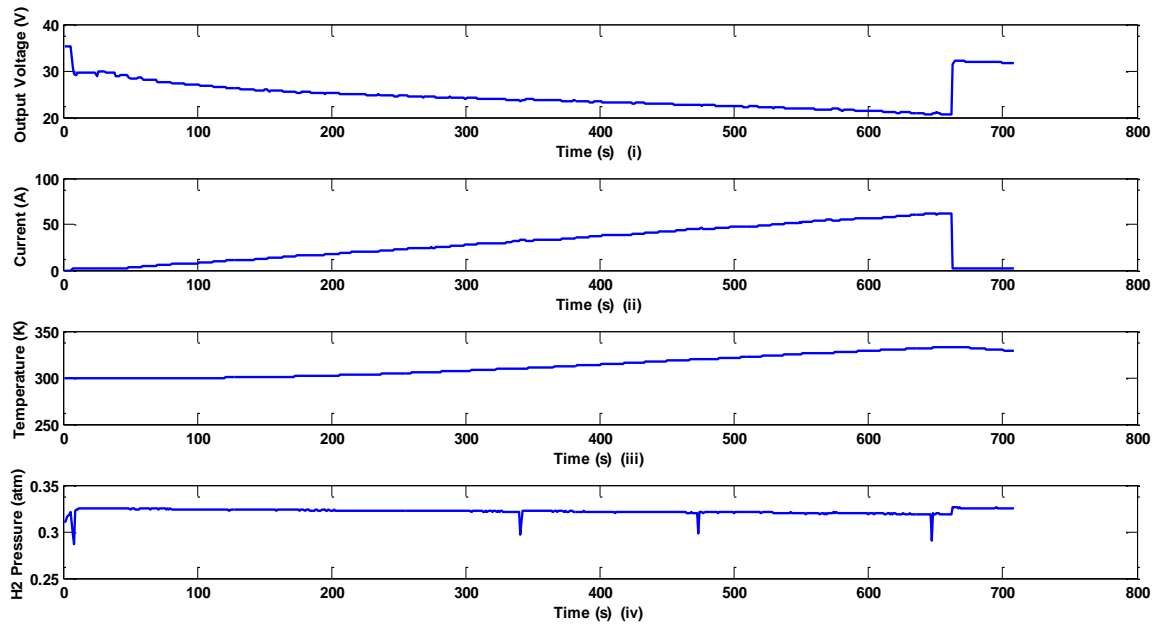
Figure 17: Experimental results under gradual load increments (i) output voltage (V),

(ii) current (A), (iii) temperature (K) and (iv) Hydrogen pressure (atm)

This experiment helps in extracting parameters from Table 5 using an optimization technique, such as QLSA, and providing the ohmic, activation voltage waveforms and the final model output voltage.

Figure 17 displays the effects of load current increase with constant slope and the sudden turn-off condition of PEMFC load. The voltage decreases with the increase in current, until it suddenly becomes zero, i.e. off-load condition. Nevertheless, when the current suddenly decreases to zero after the load shutdown, the voltage starts to increase rapidly. The designed PEMFC model follows the voltage decrease and the sudden increase in voltage after the load shutdown. When the output voltage is obtained using QLSA, the parameters, such as B_1, B_2, α, V_{int}, C_1 and R_e, are obtained. The voltage output of the model and the QLSA convergence characteristics and optimization parameters are presented in Figure 18 and Table 11, respectively.
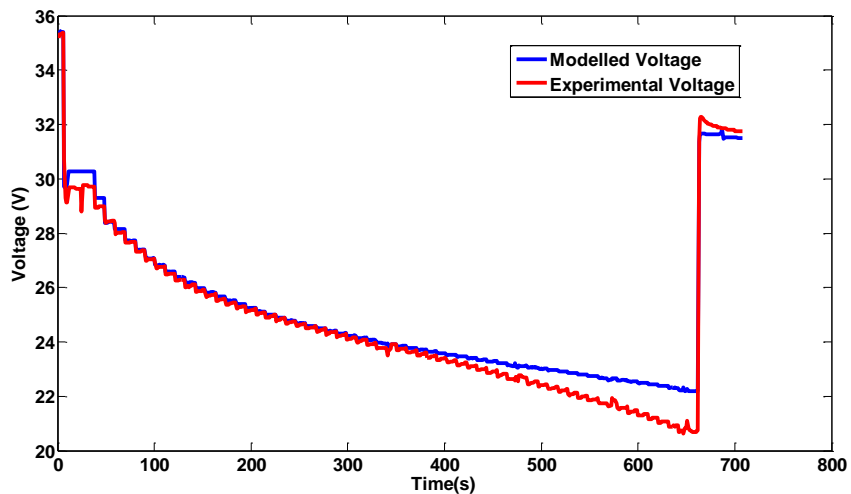
(i)
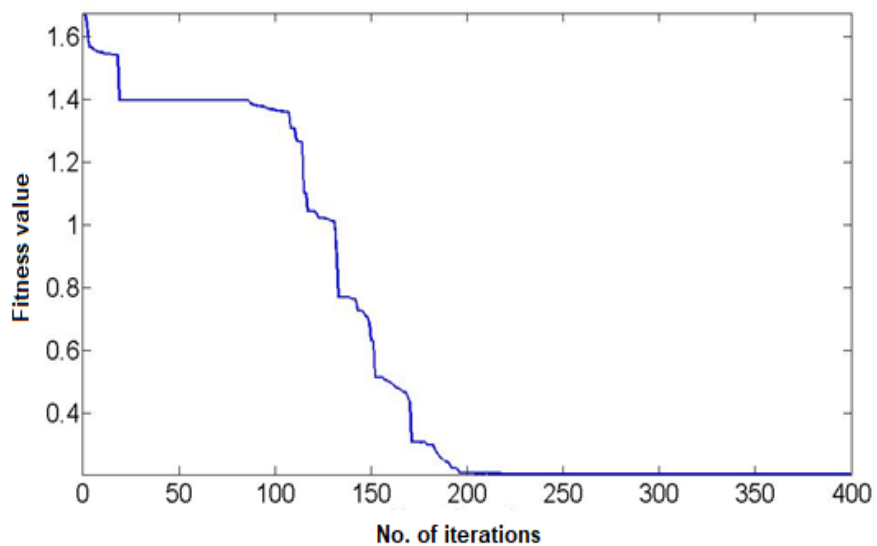
(ii)

Figure 18: Comparison of output voltage using QLSA (i) with experimental output

voltage (ii) QLSA convergence characteristics

Table 11: Parameters extracted using QLSA from the data obtained in experiment 2

Parameter	Lower range	Upper range	Extracted values
Charge transfer coefficient (α/N)	1×10^{-6}	0.0213	0.00683
Exchange current density coefficient (B_1)	1×10^{-6}	20	20
Exchange current density coefficient (B_2)	1×10^{-6}	20	0.3508
Voltage drop for internal current (V_{int})	1×10^{-6}	0.1	0.099
Pressure of water constant (A_{H2O})	1×10^{-6}	0.1	0.1
Ionic resistance (R_{ionic}) constant (C_1)	1×10^{-6}	1.5	1
Electronic resistance (R_e)	1×10^{-6}	2	0.02637
Maximum iterations for QLSA code	400		
Elapsed time by QLSA	60 s		

The parameters shown in Table 11 are appropriate for the plotting of waveforms of the no load, ohmic and activation voltages with increased current and the verification of waveform patterns. The final parameters will be different from the preceding parameters, but slight changes in these parameters may exert no effect on waveform patterns.

5.2.3 Experiment 3: Variation in ambient parameters under dynamic loading

Experiment 3 is necessary to extract the required parameters for abrupt/real current changes, which will be finalized parameters. All parameters, except for R_e and α, are not expected to change considerably. The change in R_e is assumed as more than $\pm 100\%$ and that in α must be within $\pm 50\%$ based on the complexity of their equations. Given that experiment 2 presents a small number of samples and a constant change in load, this condition cannot estimate the dynamics of PEMFC reaction and its conductivity with high precision. This experiment helps re-optimize R_e and α to cater

for dynamic conditions. Experimental data from experiment 3 are illustrated in Figure 19.

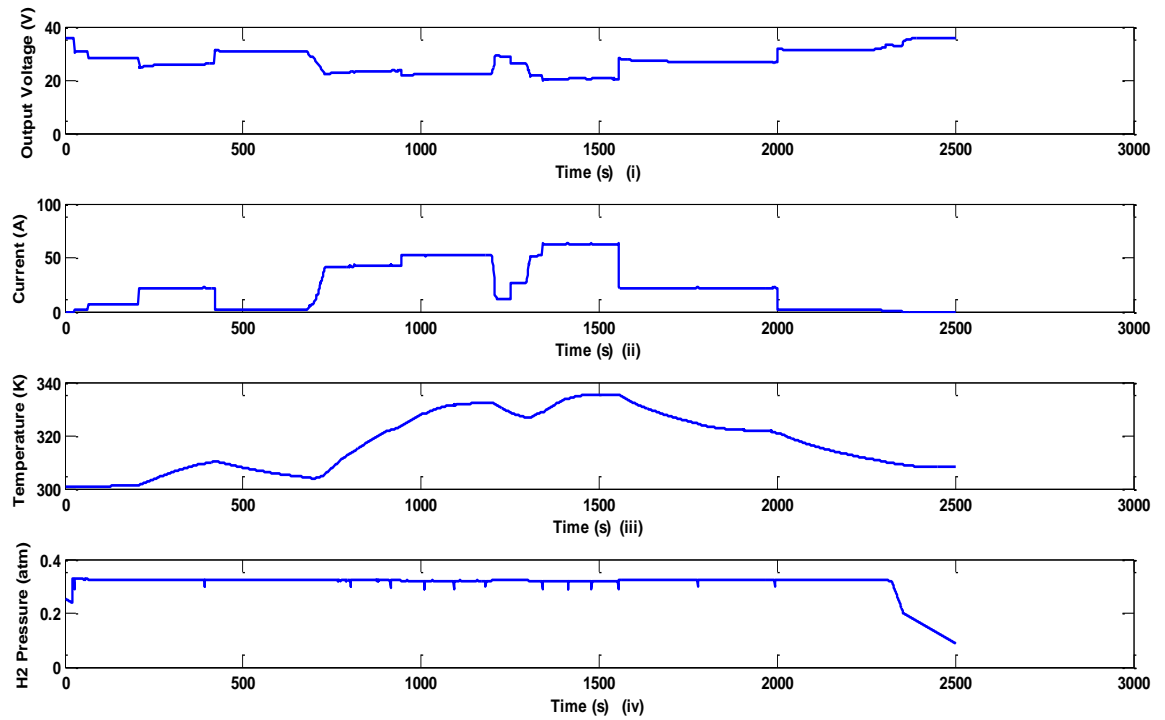Figure 19: Experimental results of abrupt changes in load condition (i) output voltage (V), (ii) current (A), (iii) temperature (K) and (iv) Hydrogen pressure (atm)

The performance of the proposed model due to the dynamic variation of current, i.e. step change in a haphazard manner with the parameters given in Table 11 is depicted in Figure 20. Output voltages obtained from the proposed models is inaccurate at medium currents.
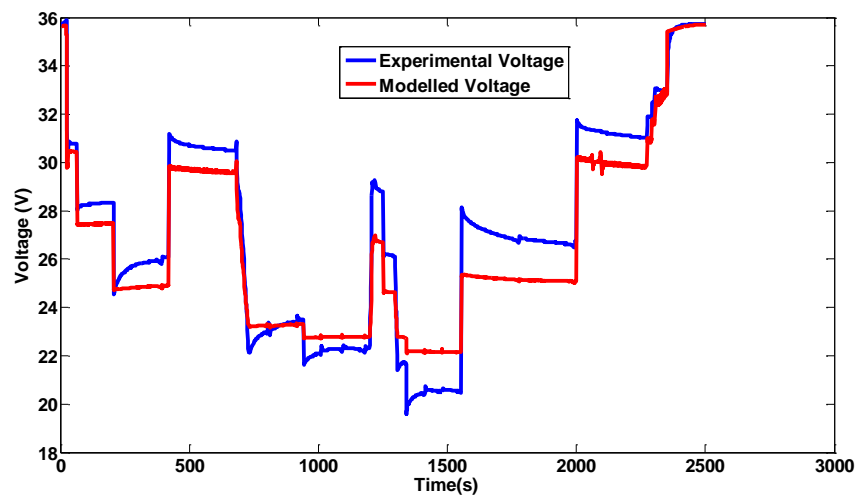
Figure 20: Comparison of proposed model voltage with experimental voltage for

abrupt changes of load

Therefore, parameters, namely, α and R_e, should be re-optimized using the output voltage data obtained from experiment 3. Both of these parameters are carefully optimized at high number of samples and for the real changes in current. Given that PEMFC electronic conductivity and its reaction dynamics cannot be estimated with low number of samples and with linear change in load, these parameter values are final; they can also be used for the PEMFC system for dynamic analysis under real loading conditions where load change is nonlinear. Figure 21 and Table 12 show the QLSA convergence characteristics and calculated output voltage after re-optimization. In Figure 21 the comparison of proposed model output voltage not only compared with experimental output voltage but also it has been compared with PSO model, as mentioned in Chapter 3 without modifications. The proposed model output is now very close to experimental voltage but also it is better than PSO model output. PSO model gives huge error when the current is very low as shown in the Figure 21, which clearly states that the no-load voltage model is very poor in the modelling. The obtained

voltage in this case is appropriate. Additionally, the variation in parameters matches the anticipated variation.
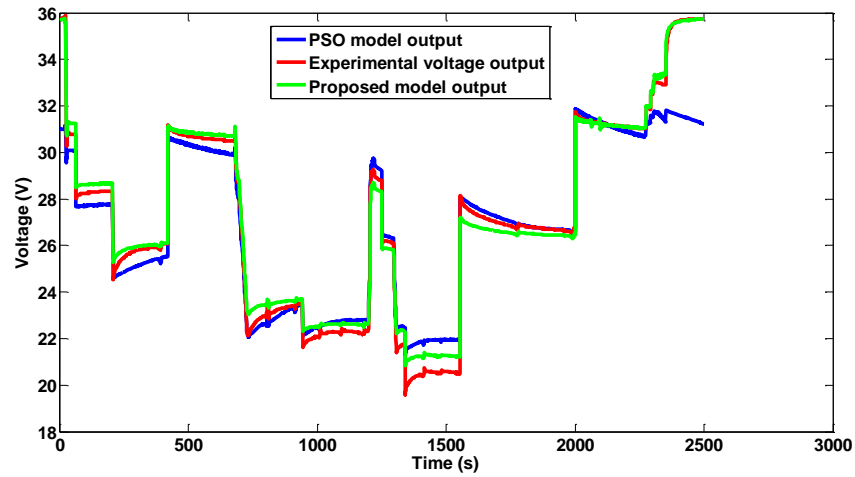
(i)
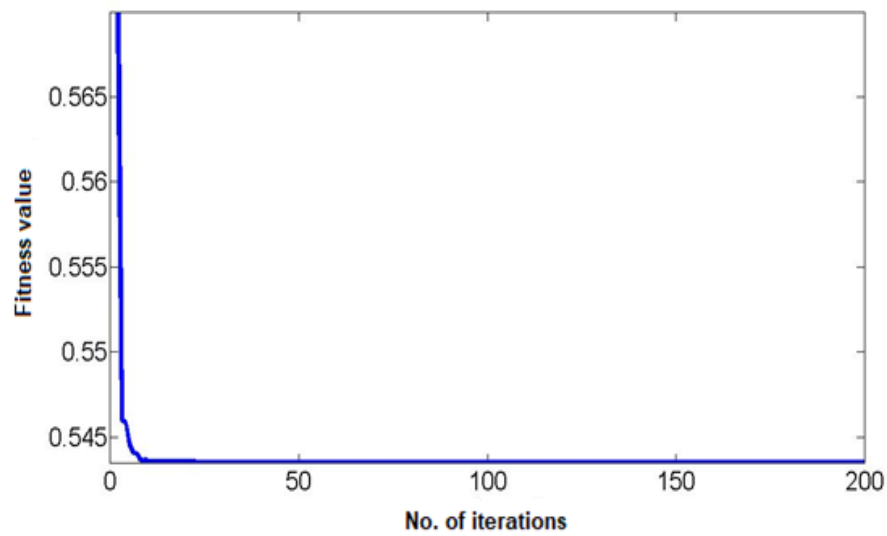
(ii)

Figure 21: Final output voltage after extracting finalized parameters (i) comparison of experimental voltage versus the proposed PEMFC and PSO model (ii) QLSA convergence characteristics for re-optimization

Table 12: Re-optimized parameters using QLSA from the data obtained in experiment 3

Parameter description	Lower range	Upper range	Obtained values		Relative percentage error compared with experiment 2
			Experiment 2 data	Experiment 3 data	
Charge transfer coefficient (α/N)	0.003416	0.0102466	0.00683	0.008094	18.5%
Exchange current density coefficient (B_1)	19.5	20.5	20	19.999	0.00
Exchange current density coefficient (B_2)	0.34207	0.3596193	0.3508	0.3432	2.1647%
Voltage drop due to internal current (V_{int})	0.0975	0.1025	0.0999	0.0999	0.0%
Pressure of water constant (A_{H_2O})	0.0975	0.1025	0.1	0.0999	0.00%
Ionic resistance R_{ionic} constant (C_1)	0.5	1.5	1	1	0%
Electronic resistance R_e	2.6×10^{-5}	0.0791034	0.02636	0.0626	137.43%
Maximum iterations for QLSA code for experiment 3, 200					
Elapsed time by QLSA for experiment 3, 74 s					

The parameters extracted from experiment 3 can also fit the output voltage from experiment 2. Figure 22 shows that the output voltage fit of experiment 2 using finalized parameters with RMSE is less than the acceptable limits.
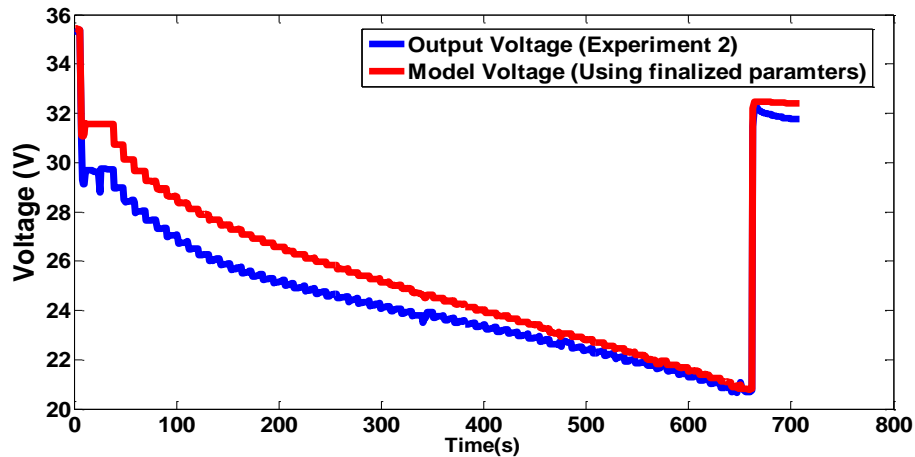
Figure 22: Comparison of output voltage obtained from the proposed PEMFC model using finalized parameters for experiment 2 output voltage

5.3 Temperature model validation

The temperature model mentioned above can be validated by using the temperature waveform in experiment 2 and experiment 3. The ambient temperature is needed in the temperature model, the average ambient temperature $T_{amb,c}$ (subscript c is for Celsius) during experiment 2 is 23°C and air relative humidity RH_{air} is 31%. For experiment 3 the ambient temperature $T_{amb,c}$ and RH_{air} are 28°C and 29% respectively. Both $T_{amb,c}$ and RH_{air} remains almost constant during experiment 2 and experiment 3

This section initially describes the results of the optimal model parameters obtained for the proposed temperature model using QLSA. Unitizing the optimized parameters, a comparative study is then performed to validate the accuracy of the proposed model.

To determine the final model, it is necessary to determine the optimal parameters (L_1 to L_6) of the proposed temperature model. Test results acquired from experiment 3 and the boundary limits for L_1 to L_6 depicted in Table 10 are used in implementing QLSA described before. In addition, the program code developed in Table 9 also required to objective function presented in Equation (4.10).

Figure 23 shows convergence characteristics of QLSA during model parameter optimization. As seen from the figure that the RMSE value reduces to 0.9 in 200 iteration. The optimized parameters after the optimization are listed in the Table 13.
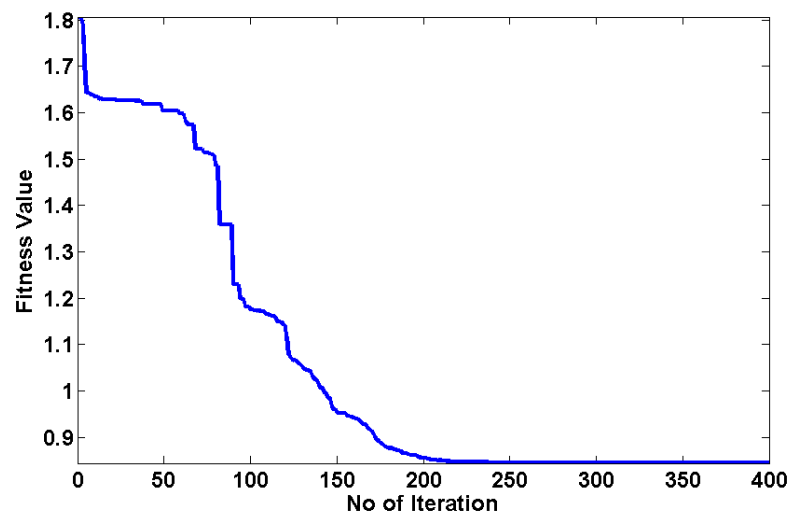
Figure 23: Convergence characteristics of QLSA

Table 13: Optimized proposed temperature model parameters

Parameter	Values	Parameter	Values
L_1	2.62783	L_4	-4.2895
L_2	2.78253	L_5	13.0207
L_3	0.01122	L_6	-0.36143

After knowing all the necessary model parameters and variable the accuracy of the proposed PEMFC temperature model is verified by comparing the experimental results obtained from experiments 2 and 3. In addition, PEMFC temperatures acquired from current polynomial and RC equivalent circuit models are generated for comparison. Figure 24 shows the comparison of PEMFC temperatures obtained from the proposed model (T_{mod2}) and the temperature recorded during Experiment 3 (T_{exp}). From Figure 24 it is evident that the proposed model is reasonable and follows the PEMFC temperature obtained from the experiment.
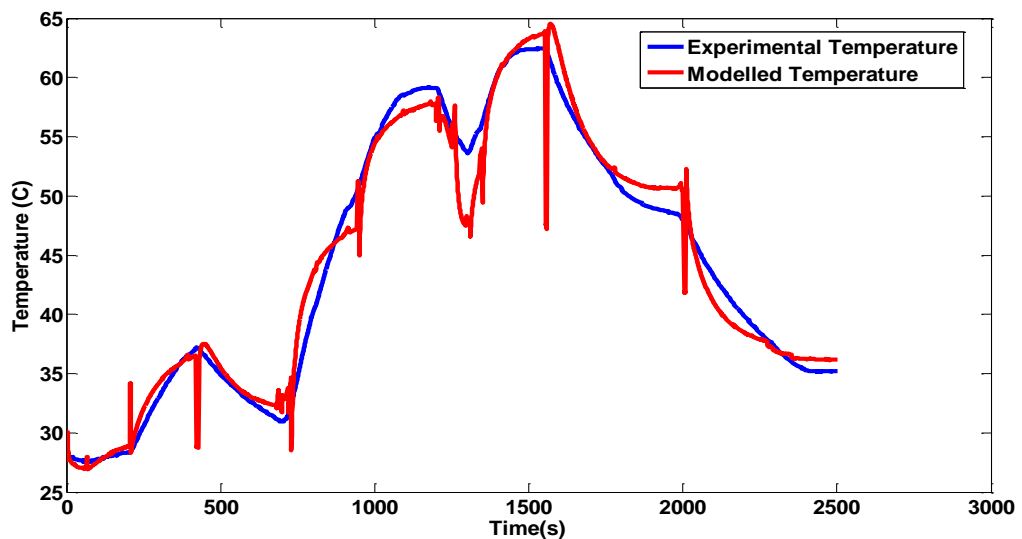
Figure 24: Comparison of proposed model temperature with experiment 3 temperature data

Note that, there are still some deficiency in the proposed model due to temperature spikes arise abrupt changes in output current. This problem is resolved by observing the actual system (experimental) temperature does not change sharply in short interval of time.

It is observed that in 10 samples the temperature variation is less than 1°C. This implies that it is appropriate to apply simple filter such as a median filter to improve model performance (Junyan and Shudan, 2015). Using such type of filter, the values of T_{mod2} can be re-adjusted as shown in Figure 25. The Figure 25 also reveals the output of other temperature models (current polynomial model and RC equivalent model) mentioned in Chapter 2 and shows how they are not satisfactory as this model for abrupt changes of load.
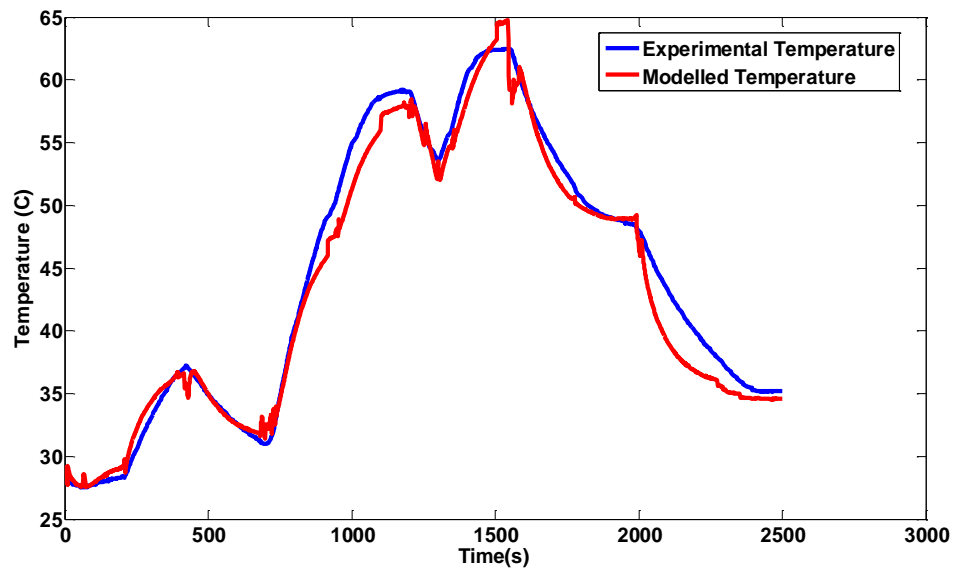
(i)
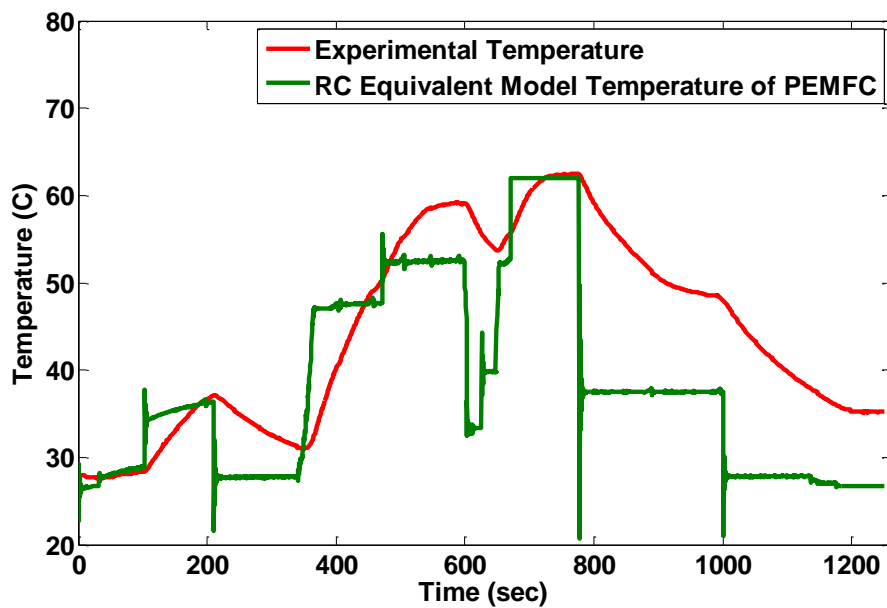
(ii)
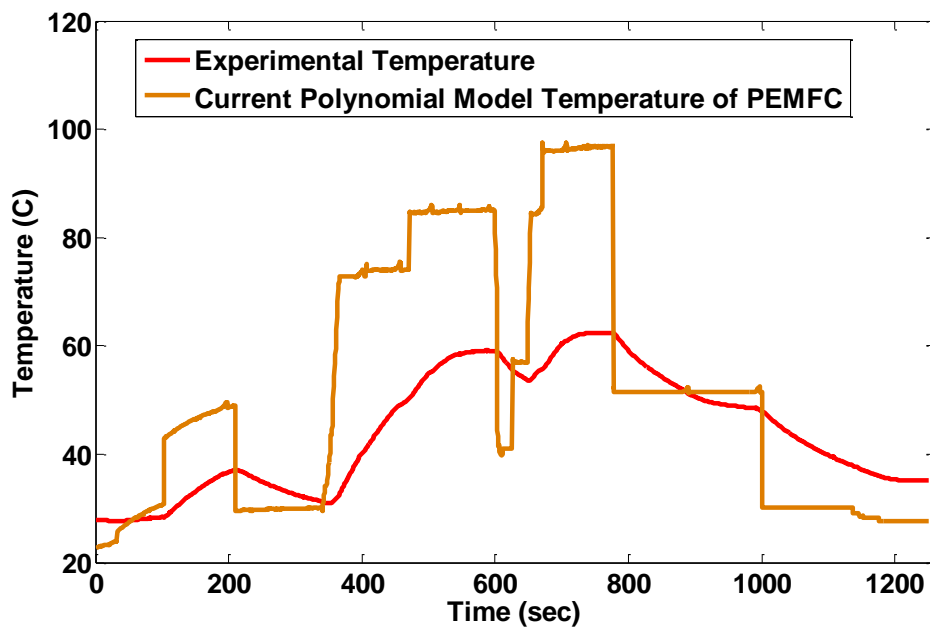
(iii)

Figure 25: Comparison of temperature model after filtering with experiment -3 temperature data (i) for the proposed temperature model (ii) for RC- equivalent temperature model (iii) for current polynomial temperature model

The performance of proposed model with the filter implementation is also tested using the data collected in Experiment 2. As mentioned earlier, Experiment 2 is conducted to observe the variation of PEMFC temperature due to linear variation of load current. Figure 26 clearly demonstrate the adequacy of the proposed model in the context of linear load charges. The proposed model also works well for smooth changes of load.
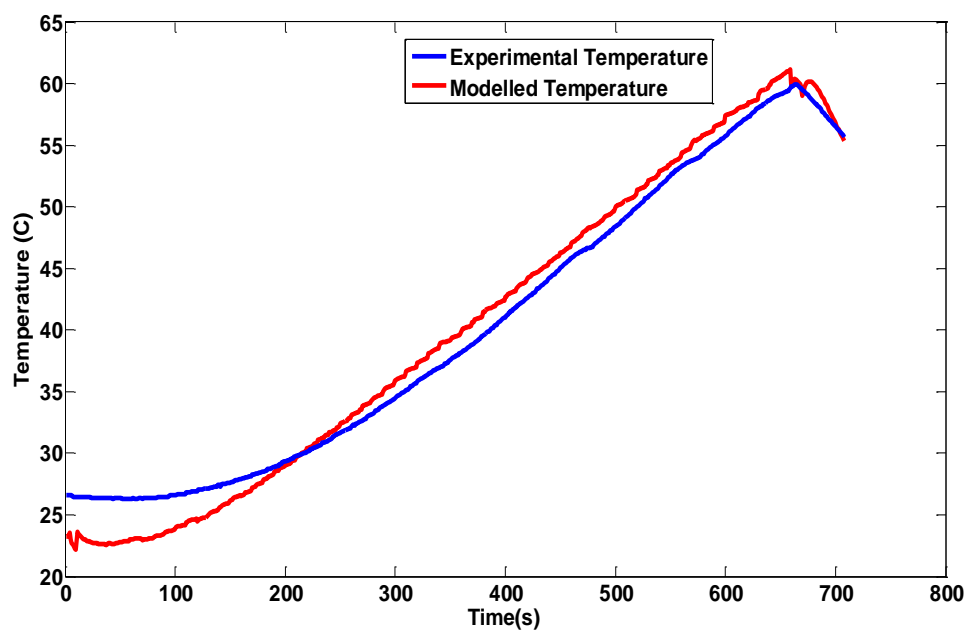
Figure 26: Comparison of Proposed model with experimental temperature for

experiment -2 (after filter)

5.4 Modifications in the proposed voltage model

The voltage model mentioned above still cannot be considered as generalized model for two reasons (i) the model is only tested for one type of PEMFC system with 47 number of fuel cells (ii) the model has not been tested at different ambient temperature and relative humidity. Considering these two reasons now another type of

PEMFC has been selected with different number of PEMFC in the stack also that PEMFC system isn't as sophisticated system like NEXA 1.2 kW system, that way the new PEMFC system will be more prone to ambient condition changes.

From the above stated reason Horizon 300 W PEMFC system has been selected. The PEMFC system is ordinary system with similar fan cooling system. This system is more prone to ambient changes and it has 72 number of fuel cells with rated 7 A current. Figure 27 shows the Horizon 300 W PEMFC system in UAEU renewable energy lab.
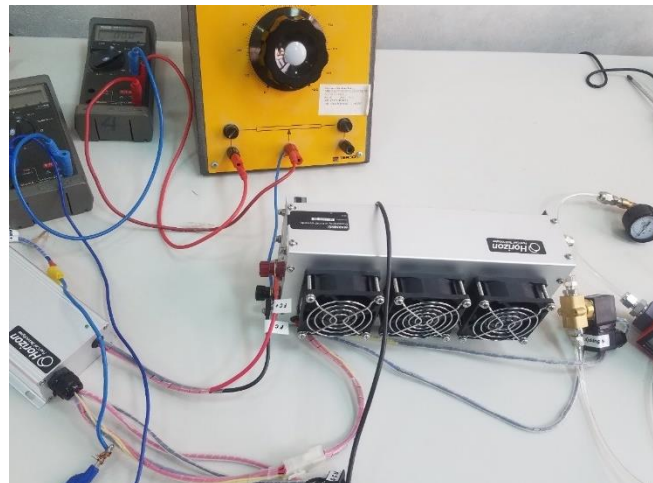
Figure 27: PEMFC Horizon 300 W setup in UAE University renewable energy lab

Three experiments are performed on Horizon 300 W PEMFC system, the first experiment performed at normal conditions, second experiment is performed for humid conditions while the third is performed for relatively dry conditions.

5.4.1 Experiment 4

The experiment 4 is performed with average ambient temperature $T_{amb,c}$ 28.32 °C and average relative humidity RH_{air} is 27.02%. The PEMFC load is varied and the

corresponding the voltage of PEMFC is recorded. Figure 28 reveals the variation of voltage, $T_{amb,c}$ and RH_{air} with respect to current respectively. Normal room temperature with appropriate air conditioning system is selected for this experiment where both $T_{amb,c}$ and RH_{air} ranges between 28 to 28.8°C and 25 to 29% respectively.
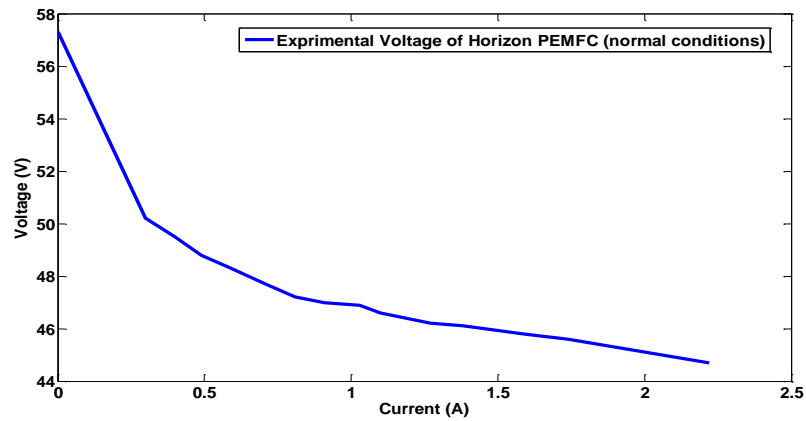
(i)
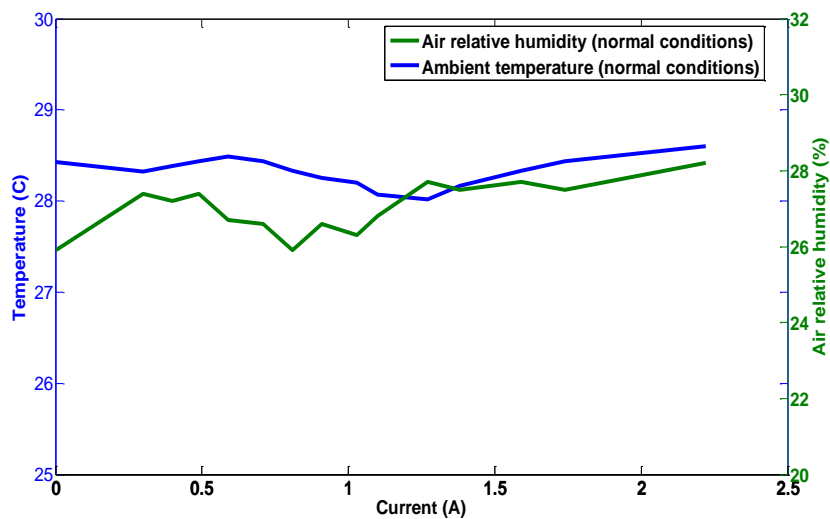
(ii)

Figure 28: PEMFC performance for normal indoor conditions (i) voltage of PEMFC (ii) ambient temperature of PEMFC and percentage relative air humidity of PEMFC.

5.4.2 Experiment 5

The fifth experiment is performed for a more humid conditions where average $T_{amb,c}$ is set to 27.35°C and average RH_{air} is set to 43%. Figure 29 depicts the variations of PEMFC voltage, $T_{amb,c}$ and RH_{air} with respect to current respectively. This experiment has been done by incorporating special air humidifiers in the small closed room where RH_{air} ranges between 40% to 48% but the temperature lies in normal range i.e from 25.5 to 30°C.
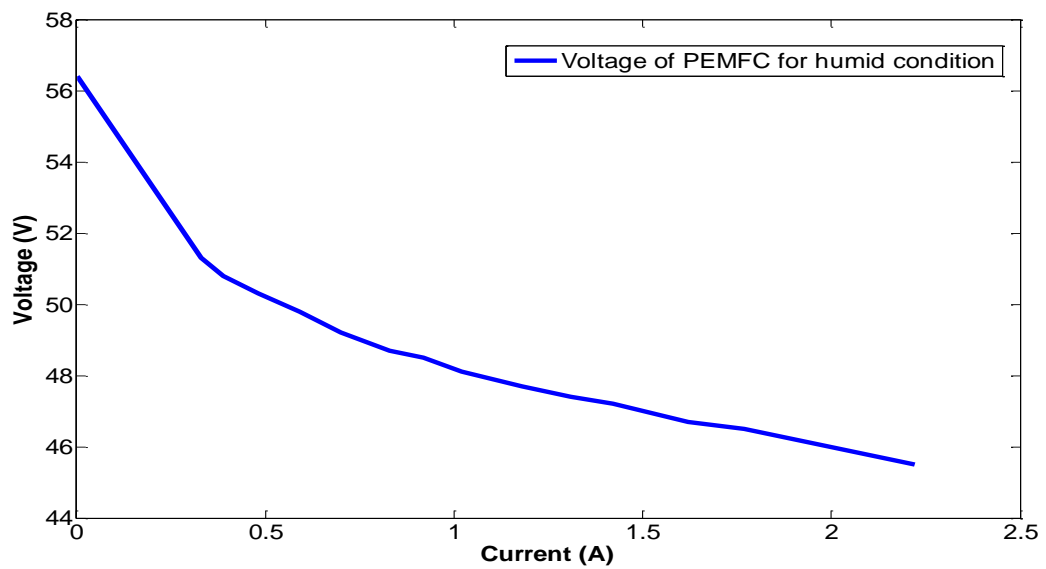
(i)
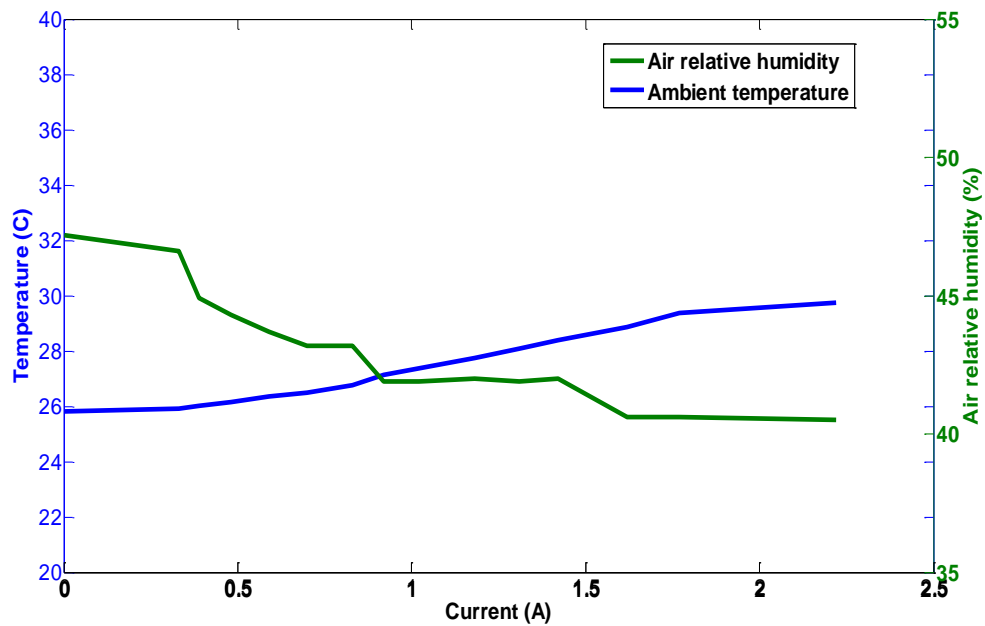
(ii)

Figure 29: PEMFC performance for humid indoor conditions (i) voltage of PEMFC (ii) ambient temperature of PEMFC and percentage relative air humidity of PEMFC

5.4.3 Experiment 6

The sixth experiment is performed for relatively high temperature and dry conditions where average $T_{amb,c}$ is found to be 35.8°C and average RH_{air} is found to be at 19.8%. Figure 30 shows the variations of PEMFC voltage, $T_{amb,c}$ and RH_{air} with respect to current respectively. This experiment is done by turning off the air conditioning system since UAE has hot weather the temperature rises to 40°C but due to air ventilation system the range of $T_{amb,c}$ lies between 34 to 40°C approx. The air relative humidity ranges from 18 % to 21%.
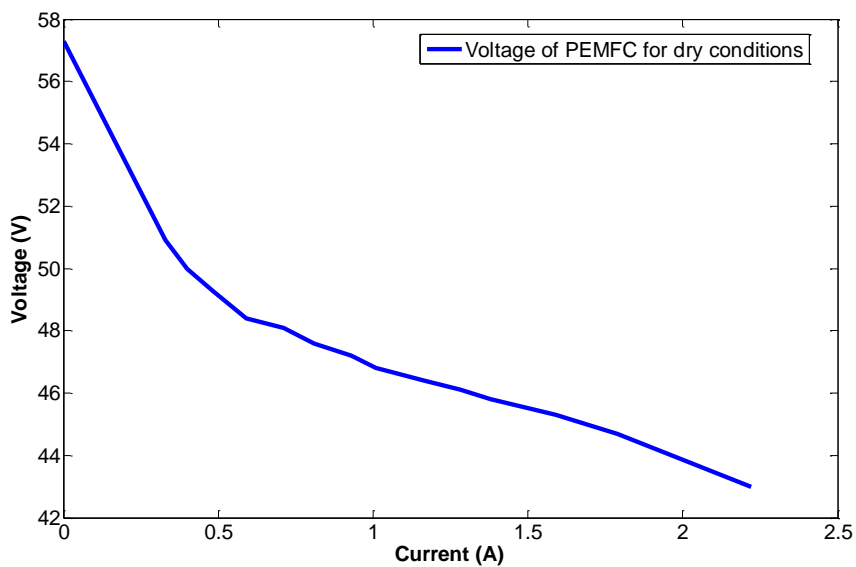
(i)
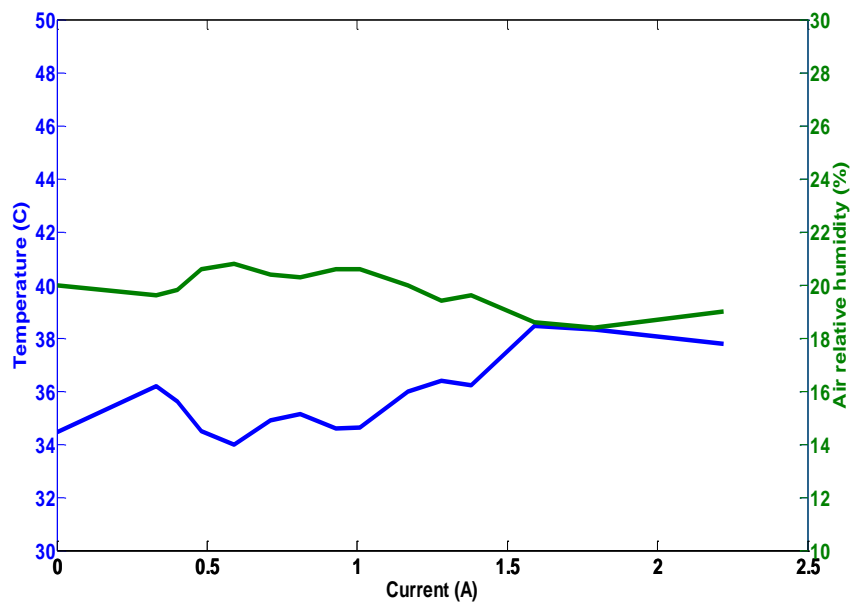
(ii)

Figure 30: PEMFC performance for dry indoor conditions (i) voltage of PEMFC (ii)

ambient temperature of PEMFC and percentage relative air humidity of PEMFC

5.4.4 Parameter optimization results for semi-empirical voltage model

The final voltage model parameters obtained for Horizon 300 W system at normal conditions are listed in Table 14. For the purpose of comparison, the relative error between model parameters of Horizon 300W and NEXA 1.2 kW system is also presented in Table 14.

It can noted that almost all the parameter values vary widely with more than 15% except parameter B_2. The parameters which are decreasing compared to the NEXA 1.2 kW model parameters are α, B_1, (NA_1) while other parameters have a higher value compared to NEXA 1.2 kW model parameters. Therefore, it cannot be considered as a general model and further modifications are required. It should be noted that both the system have the different number of fuel cells and therefore the first attempt to generalize the model is to use a compensation factor (C_f =72/47) corresponding to the number of cells in the stack. After using this compensation factor, new parameter values for the Horizon system are given in column 5 of Table 14 where α/N , B_1, and NA_1 of NEXA parameters are divided by C_f while V_{int} , R_e , A_{H2O} , C_1, and NA_2 of NEXA parameters are multiplied by C_f. The compensated parameters for the Horizon system have similar parameter values to that of extracted horizon parameters (given in column 5 of Table 14) with reduced relative error (less than 15% approximately for all parameters).

Table 14: NEXA and Horizon PEMFC parameters with relative error along-with modifications using compensation factor

Parameters	For NEXA	For Horizon (Normal Condition)	Relative error of parameters for Horizon (%) w.r.t NEXA system	Compensated parameters for Horizon using (C_f = 72/47)	Relative error (%) of compensated parameters w.r.t NEXA system
Charge transfer coefficient (α/N)	0.0081	0.0048	40.7	0.0053	-10.417
Exchange current density coefficient (B_1)	20	12.0283	39.9	13.0556	-8.541
Exchange current density coefficient (B_2)	0.3433	0.3827	-11.5	N/A	N/A
Voltage drop due to internal current (V_{int})	0.1	0.1375	-37.5	0.1532	-11.418
Electronic resistance (R_e)	0.0626	0.0876	-40	0.0959	-9.475
Pressure of water constant (A_{H2O})	0.1	0.1396	-39.6	0.1532	-9.742
Ionic resistance (R_{ionic}) constant (C_1)	1	1.3971	-39.7	1.5319	-9.649
NA_1	0.0219	0.0169	22.9	0.0143	15.385
NA_2	18.8223	26.3512	-40	28.8342	-9.423

Using compensation factor C_f, the model becomes more general and parameter values for different PEMFCs with the different number of cells can be easily estimated. The error (within 15%) could be due to a change in the area of fuel cell membrane thickness and variation in other shape factors.

Figure 31 reveals the model output voltage of Horizon with experimental voltage for normal, dry and humid conditions with parameters listed in Table 15.
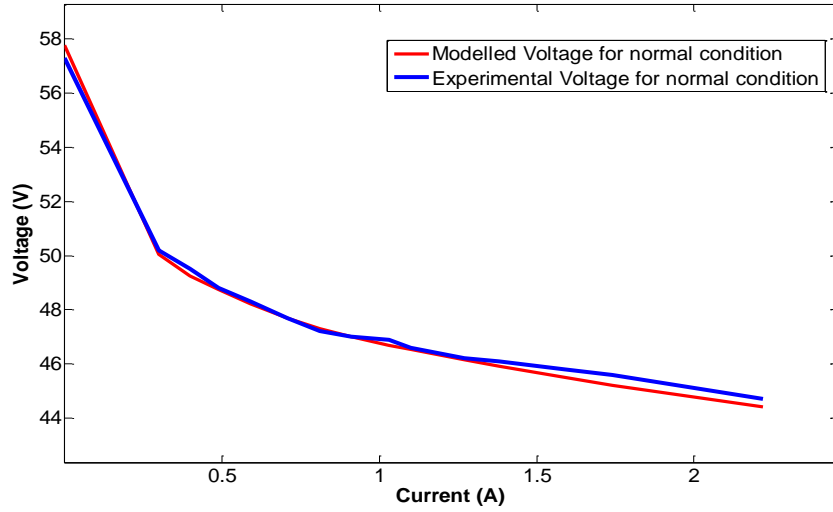
(i)
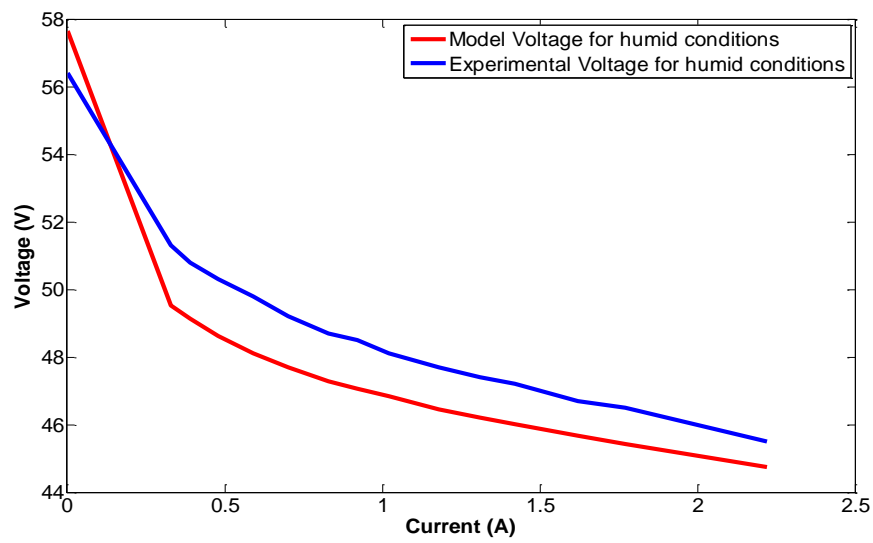
(ii)
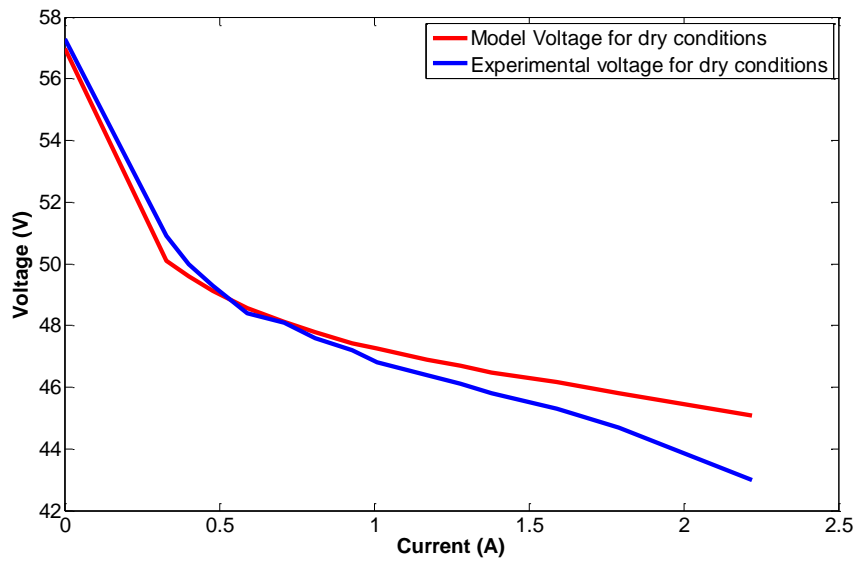
(iii)

Figure 31: Horizon PEMFC model voltage in comparison with experimental voltage
for Horizon parameters (i) normal condition (ii) humid condition (iii) dry condition

The RMSE in the case of the Horizon PEMFC system for the normal condition is less than 0.5 but for the dry and humid condition, it is more than 0.5. As seen from the figures and RMSE value, the ambient conditions affect the PEMFC voltage model performance. Therefore, to identify which model parameters are affecting the performance, the parameters for dry and humid conditions are again optimized. Table 15 shows the data analysis. Note that, the coefficients which are changing more than 15% are α/N, NA_1, and V_{int}. But relative absolute error for A_{H2O} is also more than 15% due to significant changes from humid to dry condition. This is a clear indication that these four parameters are dependent upon $T_{amb,c}$ and RH_{air}. As a final attempt to generalize the model, the identified model parameters required to be $T_{amb,c}$ and RH_{air} dependent. For this purpose and obtain a suitable equation for the identified parameters, statistical regression analysis is conducted.

Table 15: Horizon PEMFC parameters for variations in ambient conditions

Parameter	For Horizon (N=72) average T_{amb} = 28.3 °C, RH = 27.02% (Normal)	For Horizon (N=72) average T_{amb} = 27.6 °C, RH = 43.98% (Humid)	Relative (%) error of Horizon (humid) w.r.t Horizon (Normal)	For Horizon (N=72) average T_{amb} = 36.3 °C, RH = 19.65% (Dry)	Relative error (%) of Horizon (dry) w.r.t Horizon (Normal)
Charge transfer coefficient (α/N)	0.0048	0.0047	3.1	0.00409	15
Exchange current density coefficient (B_1)	12.0283	13.5888	-13.0	13.0337	-8.4
Exchange current density coefficient (B_2)	0.3827	0.3601	5.9	0.3739	2.3
Voltage drop due to internal current (V_{int})	0.1375	0.1119	18.6	0.1199	12.8
Electronic resistance (R_e)	0.0876	0.0939	-7.1	0.0939	-7.1
Pressure of water constant (A_{H_2O})	0.1396	0.1234	11.6	0.1498	-7.4
Ionic resistance R_{ionic} constant (C_1)	1.3971	1.4268	-2.1	1.4985	-7.3
NA_1	0.0169	0.0082	51.4	0.0022	87.0
NA_2	26.3512	28.8982	-9.7	28.3165	-7.5

5.4.5 Statistical regression analysis for voltage model parameters

Basic regression analysis is conducted for all parameters separately using experiment 1 to experiment 3. Here, in this case, the temperature $T_{amb,c}$ and humidity

RH$_{air}$ (%) dependent empirical models of α/N, NA$_1$, A$_{H2O}$, and V$_{int}$ are to be extracted using regression analysis.

The parameter α/N depicts the reaction speed of PEMFC, this parameter is affected in dry conditions. For humid conditions, it does not change significantly. This means that dry conditions affect the reaction speed more than any other condition. This agrees with the theoretical analysis given in the review (Ji and Wei, 2009). The regression analysis is given in Table 16.

Table 16: α/N regression analysis based on ambient temperature and ambient relative humidity

Source	DF	Adj SS	Adj MS	F-Value	P-Value
Regression	2	0.000004	0.000002	182.77	0.000
T$_{amb,c}$	1	0.000003	0.000003	272.01	0.000
T$_{amb,c}$ × RH$_{air}$	1	0.000000	0.000000	9.97	0.003
Error	42	0.000000	0.000000		
Total	44	0.000004			
Model Summary					
S	R^2	R^2 (adjusted)	R^2 (predicted)		
0.0001027	89.69%	89.20%	87.97%		

The regression Equation (5.1) highlighted from the model in Table 17 has the term T$_{amb,c}$ × RH$_{air}$ that has almost zero coefficient and thus it can be neglected. The other coefficients are also very small but this is because of the low value of α/N. so α/N is totally depending upon T$_{amb,c}$ and RH$_{air}$, T$_{amb,c}^2$, and RH$_{air}^2$ have also been applied in the design but they come out to be insignificant in the design. The final Equation of α/N is given in Equation (5.1).

$$\frac{\alpha}{N} = 0.007354 - 0.000084 \times T_{amb,c} \qquad\qquad (5.1)$$

The normality test of residuals shown in Figure 32 reveals that the p-value is more than 0.05 so the residuals of the design are normal.
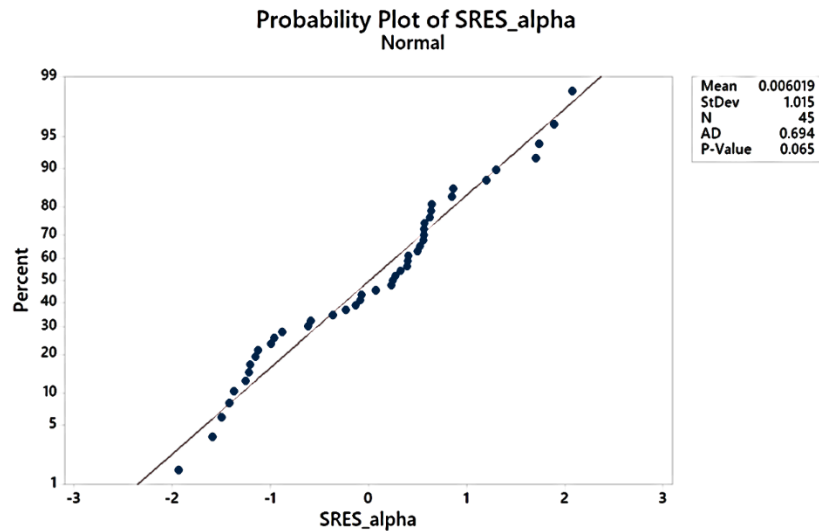
Figure 32: Residual normality plot and analysis for α/N

The second parameter to be modeled is V_{int} which is the average internal voltage for a cell. This internal voltage drop is due to internal currents that produce the non-linear internal voltage drop. This internal voltage drop is also affected by the change in ambient conditions. For humid conditions, it has the least value which means voltage drop improves with humid conditions which are in agreement with the analysis given in (Ji and Wei, 2009). The regression analysis for extracting the regression equation for V_{int} is given in Table 17.

Table 17: Regression analysis of V_{int} with respect $T_{amb,c}$ and RH_{air}

Source	DF	Adj SS	Adj MS	F-Value	P-Value
Regression	2	0.004655	0.002327	199.22	0.000
$T_{amb,c}$	1	0.002418	0.002418	206.99	0.000
$T_{amb,c} \times RH_{air}$	1	0.004600	0.004600	393.77	0.000
Error	42	0.000491	0.000012		
Total	44	0.005146			
Model Summary					
S	R^2	R^2 (adjusted)	R^2 (predicted)		
0.0034180	90.46%	90.01%	88.93%		

In the regression Equation (5.2) from the analysis in Table 17, the $T_{amb,c} \times RH_{air}$ term is significant and this implies that this interaction cannot be ignored. Thus, V_{int} is totally depending upon $T_{amb,c}$ and $T_{amb,c} \times RH_{air}$. RH_{air} , $T_{amb,c}^2$ and RH_{air}^2 have also been applied in the design but they come out to be insignificant in the design. The final Equation of V_{int} is given in Equation (5.2).

$$V_{int} = 0.25333 - 0.002430\, T_{amb,c} - 0.000064\, T_{amb,c}\, RH_{air} \quad (5.2)$$

The normality test of residuals shown in Figure 33 reveals that the p-value is more than 0.05 so the residuals of the design are normal.

Figure 33: Residuals of regression analysis of V_{int} for variables $T_{amb,c}$ and RH_{air}

The third parameter to be considered is the A_{H2O} which measures the pressure of water in Equation (5.3). This parameter decreases with pressure of water in PEMFC. So for dry condition it must the highest as pressure of water drops and for humid conditions it is vice versa. The regression analysis is given in Table 18.

Table 18: Regression analysis of A_{H2O} with respect $T_{amb,c}$ and RH_{air}

Source	DF	Adj SS	Adj MS	F-Value	P-Value
Regression	2	0.005251	0.002626	1678.09	0.000
$T_{amb,c}$	1	0.000386	0.000386	246.84	0.000
$T_{amb,c} \times RH_{air}$	1	0.001674	0.001674	1069.62	0.000
Error	42	0.000066	0.000002		
Total	44	0.005317			
Model Summary					
S	R^2	R^2 (adjusted)	R^2 (predicted)		
0.0012509	98.76%	98.71%	98.56%		

The term in the $T_{amb,c} \times RH_{air}$ regression Equation (5.4) from that regression analysis in Table 18 implies its interaction and significance. V_{int} is totally depending

upon $T_{amb,c}$ and $T_{amb,c} \times RH_{air}$. RH_{air}, $T_{amb,c}^2$ and RH_{air}^2 have also been applied in the design but they come as insignificant in the design. The final Equation of A_{H2O} is given in Equation (5.4).

$$A_{H_2O} = 0.25333 - 0.002430T_{amb} - 0.000064T_{amb}RH_{air} \qquad (5.4)$$

The normality test of residuals shown in Figure 34 reveals that the p-value is more than 0.05 so the residuals of the design are normal.
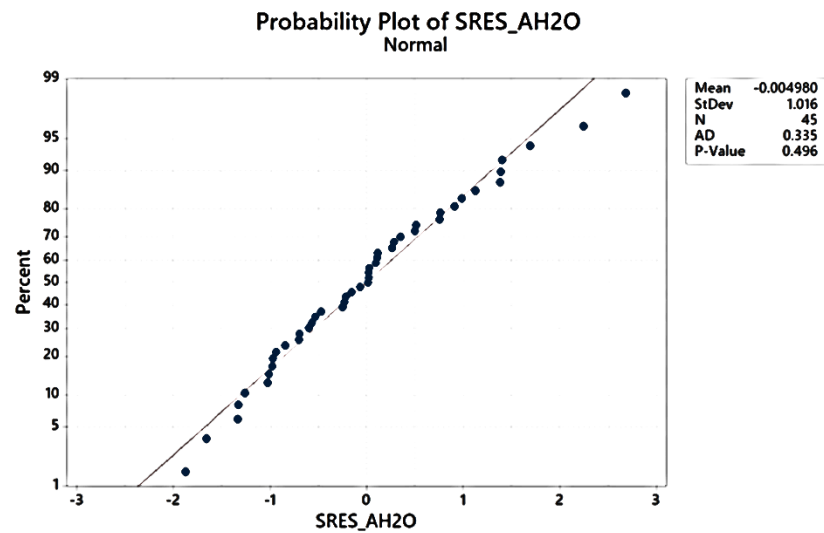
Figure 34: Residuals of regression analysis of A_{H2O} for variables $T_{amb,c}$ and RH_{air}

The fourth parameter is (NA_1) which depends upon the combination of (V_{int} and V_{H2O}). This parameter also varies from humid to dry conditions. The regression analysis for extracting the regression equation for (NA_1) is given in Table 19.

Table 19: Regression analysis of NA_1 with respect $T_{amb,c}$ and RH_{air}

Source	DF	Adj SS	Adj MS	F-Value	P-Value
Regression	2	0.001403	0.000702	124.97	0.000
$T_{amb,c}$	1	0.001403	0.001403	249.94	0.000
$T_{amb,c} \times RH_{air}$	1	0.000570	0.000570	101.51	0.000
Error	42	0.000236	0.000006		
Total	44	0.001639			
Model Summary					
S	R^2	R^2 (adjusted)	R^2 (predicted)		
0.0023693	85.61%	84.93%	83.25%		

The regression equation term mentioned in Equation (5.5) based on analysis given in Table 19 has the term $T_{amb,c} \times RH_{air}$ which means the interaction is significant. V_{int} is totally depending upon $T_{amb,c}$ and $T_{amb,c}$ x RH_{air}. RH_{air} , $T_{amb,c}^2$ and RH_{air}^2 have also been applied in the design but they come as insignificant in the design. The final equation of NA_1 is given in Equation (5.5).

$$NA_1 = 0.08529 - 0.001851\, T_{amb,c} - 0.000022 T_{amb,c}\, RH_{air} \quad (5.5)$$

The normality test of residuals in Figure 35 reveals that p-value is more than 0.05 so the residuals of the design are normal.

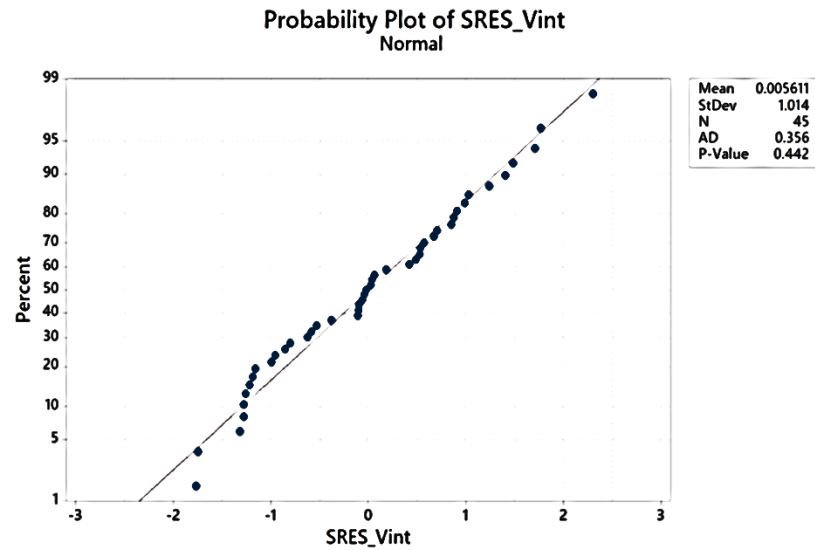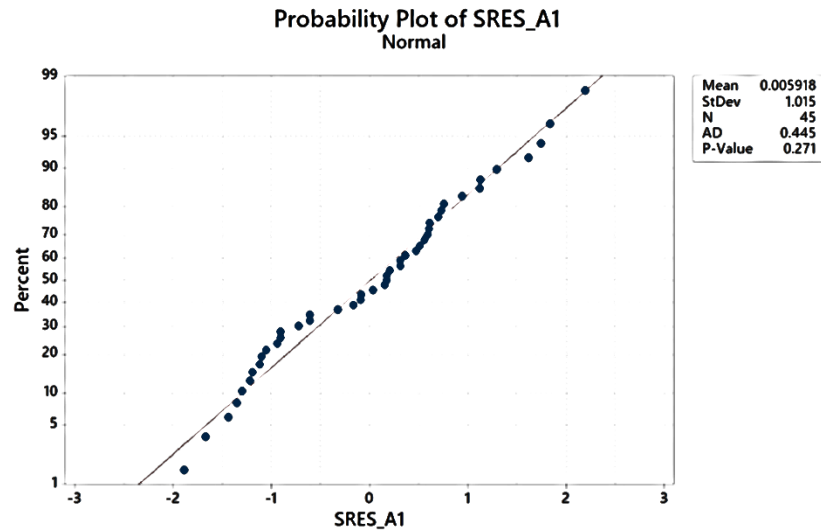Figure 35: Residuals of regression analysis of NA_1 for variables T_{amb} and RH_{air}

From the above analysis, the regression equations for parameters α/N , V_{int}, A_{H2O} and NA_1 is finally extracted. These equation accounts for the change in the parameters with respect to ambient condition changes. The modified voltage model for normal, humid and dry conditions now fits the experimental voltage with RMSE less than 0.5. Figure 36 reveals the final model voltage with respect to experimental voltage for normal, humid and dry conditions.
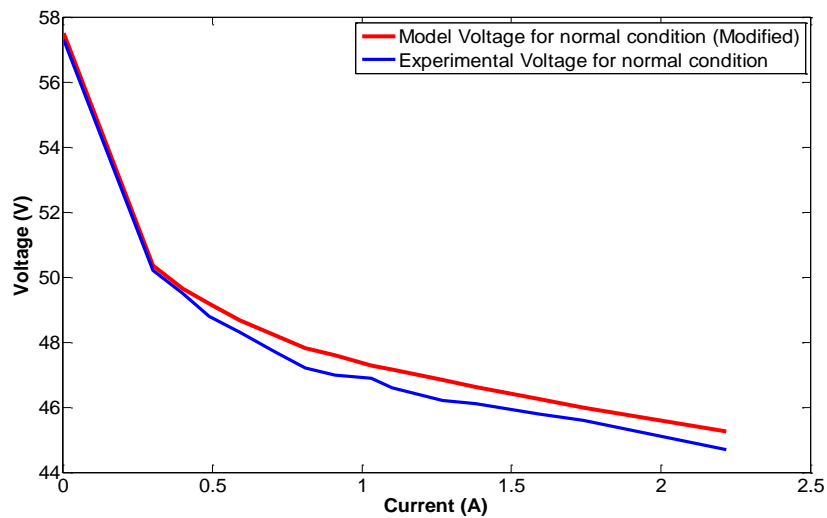
(i)
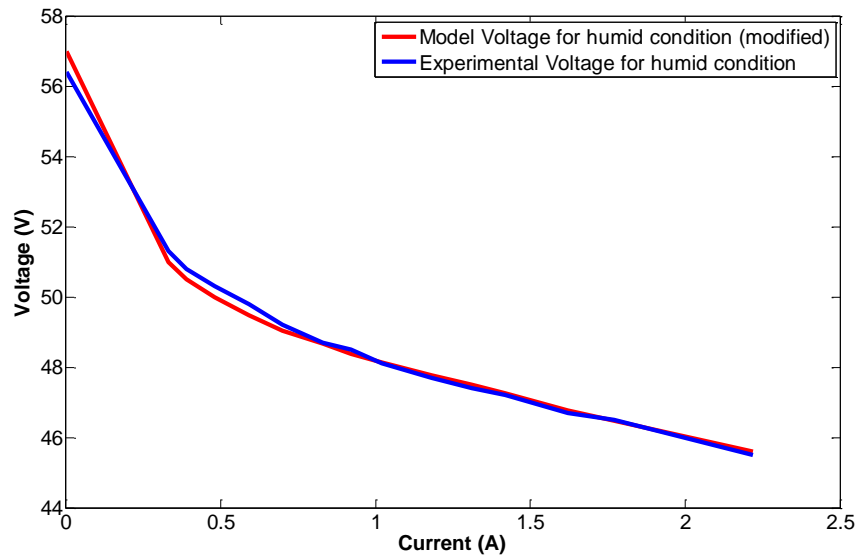
(ii)
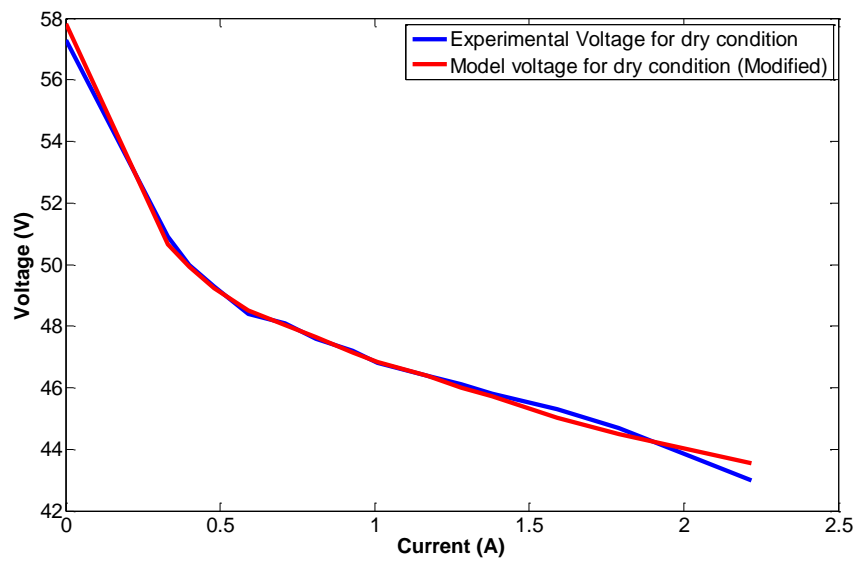
(iii)

Figure 36: Horizon PEMFC modified model voltage in comparison to experimental

voltage (i) normal condition (ii) humid condition (iii) dry condition

The modified model voltage on NEXA 1.2 kW system can also be extracted

by using compensation factor C_f and the modified equations for parameters including

ambient conditions mentioned above for experiment 2 and experiment 3. Figure 37

shows the model PEMFC voltage for NEXA system in comparison with experimental

PEMFC voltage.
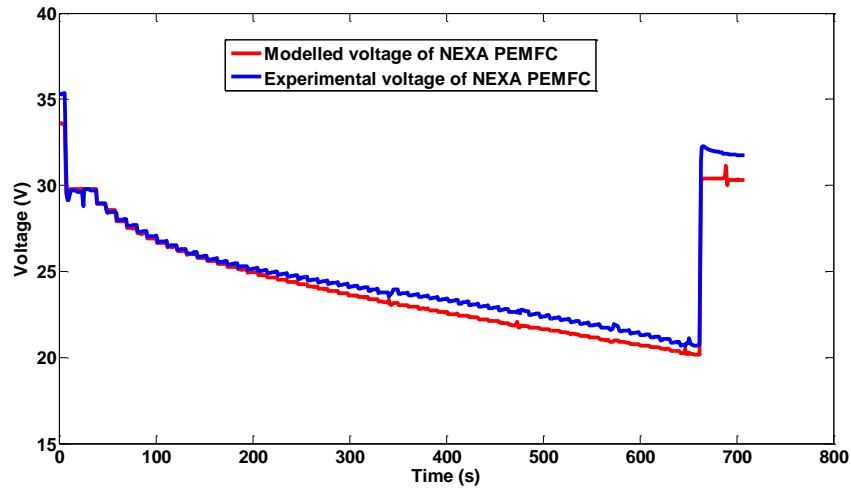
(i)
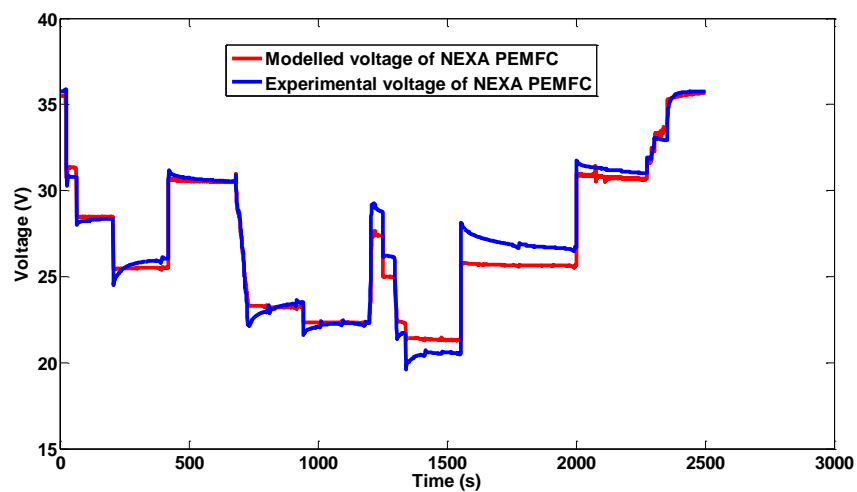
(ii)

Figure 37: Model voltage for NEXA PEMFC system in comparison to experimental

voltage for modified PEMFC voltage model parameters incorporating ambient

conditions (i) experiment-2 (where average $T_{amb,c} = 23°C$ and $RH_{air} = 31\%$) (ii)

experiment-3 (where average $T_{amb,c} = 28°C$ and $RH_{air} = 29\%$)

The results for both PEMFC system (NEXA and Horizon) shows that the model voltage has improved. The RMSE for NEXA system is also less than 0.5. Not only the modified model is good for both PEMFC system i.e NEXA and Horizon at different ambient conditions, but also the waveforms of activation, ohmic and concentration voltage drops follow the theoretical pattern as given in (Larminie and Dicks, 2003). The waveforms of these three voltage with respect to current for NEXA PEMFC system are presented in Figure 38 and the comparison with PSO model has also been made. PSO model voltage waveforms fail to follow the theoretical pattern.
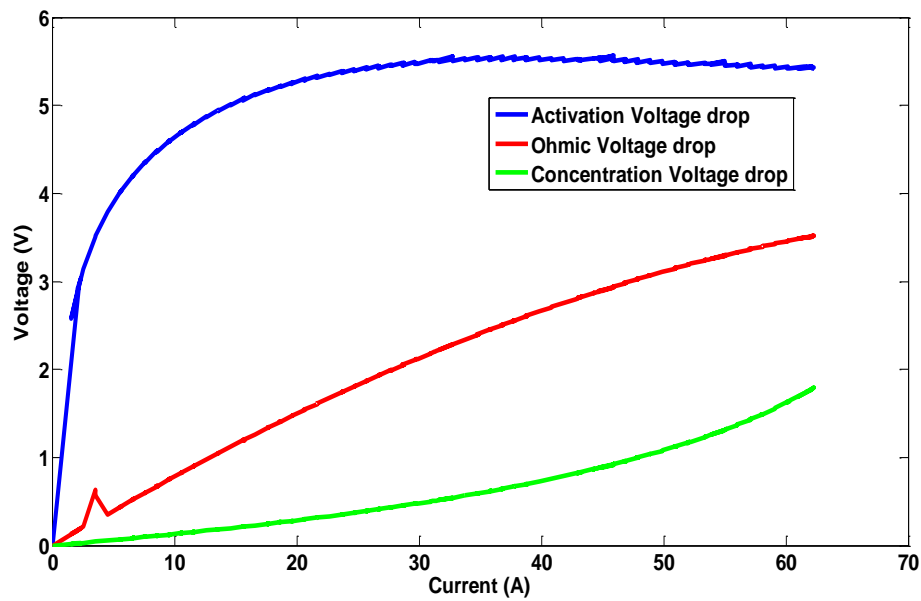
(i)
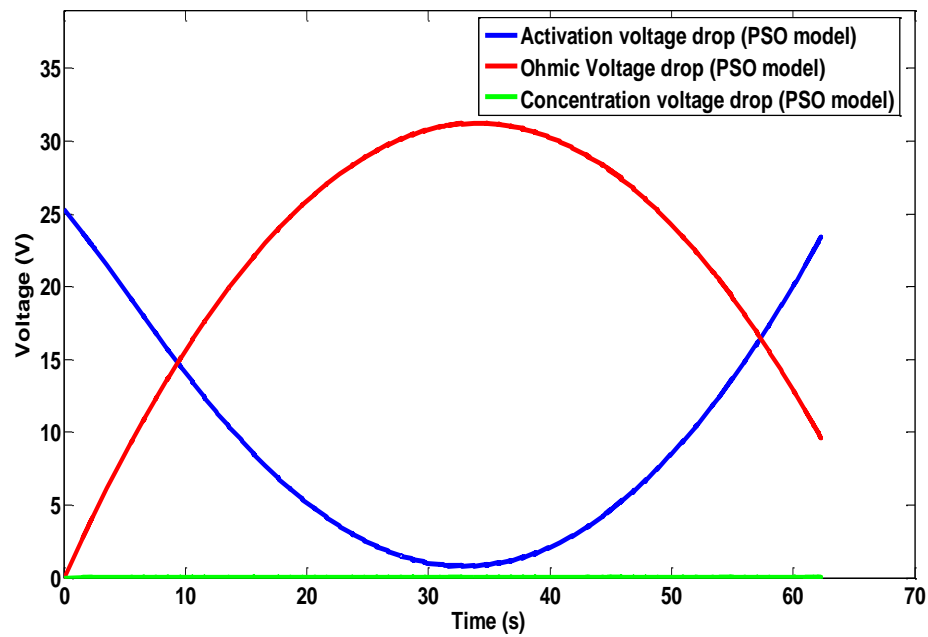
(ii)

Figure 38: Activation, ohmic and concentration voltage drop waveforms (i) calculated from the modified proposed voltage model of the NEXA PEMFC system for experiment-2 (ii) calculated from PSO model equations

5.5 Membrane water content and fault diagnosis system

The pressure of water P_{H2O} and membrane water content λ are the key factors in the voltage model of PEMFC. These two factors can easily determine the PEMFC system hydration state and also gives the prior indication about flooding and drying faults.

The validation of these two factors can be confirmed by analyzing the plot of P_{H2O} and λ for Horizon system in normal, humid and dry conditions. Figures 39 and 40 shows the membrane water content λ and pressure of water P_{H2O} against current.
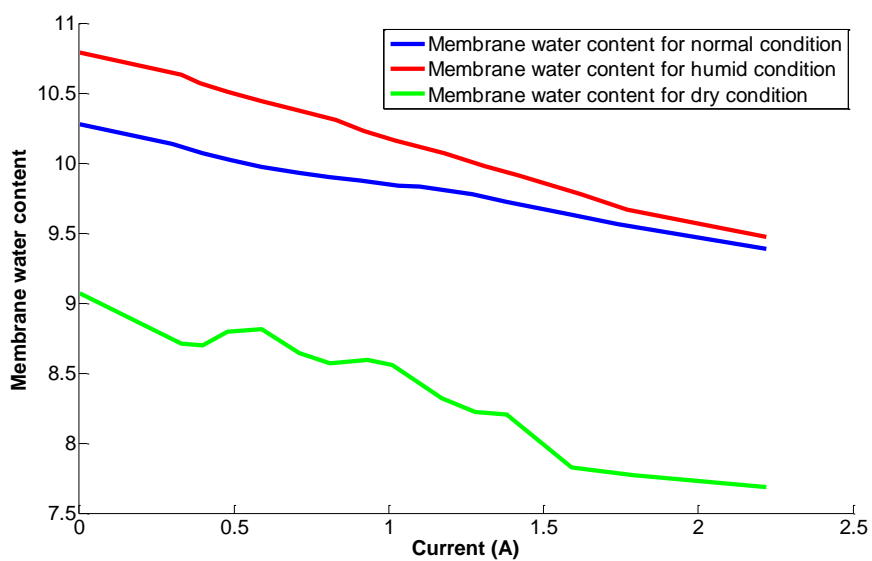
Figure 39: Membrane water content for Horizon PEMFC in different ambient
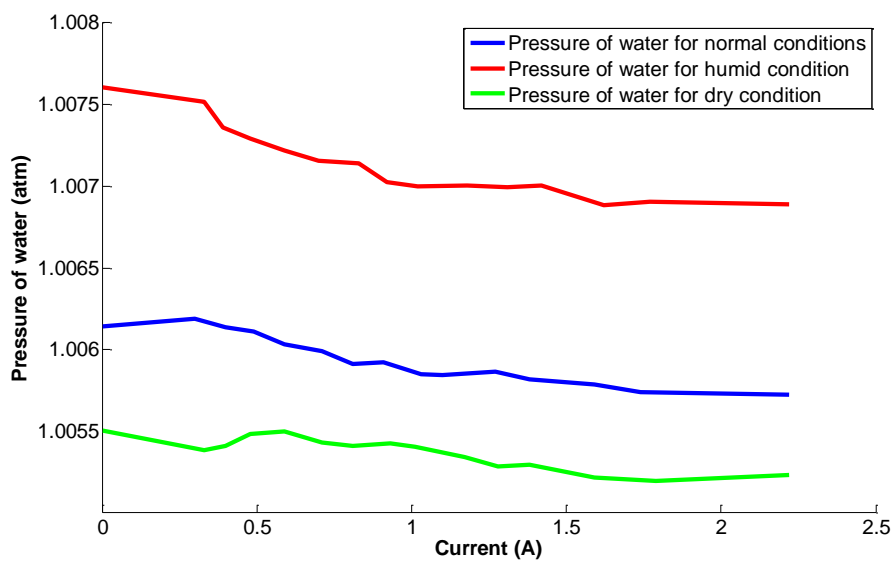
conditions

Figure 40: Pressure of water for Horizon PEMFC in different ambient conditions

The pressure of water P_{H_2O} (atm) remains close to 1 for all ambient conditions,

which also proves that for PEMFC temperature less than 100°C (373 K) stays close to

1 as mentioned earlier (Motapon, Tremblay and Dessaint, 2012). The membrane water content also shows clear variation with ambient condition.

The pressure of water and membrane water content λ for experiment-3 using NEXA PEMFC system has also been revealed in Figures 41 and 42 respectively. The pressure of water again remains close to 1 and membrane water content λ variations don't exceed 11 and also it varies with changing load conditions which is according to the study presented in (Ji and Wei, 2009).
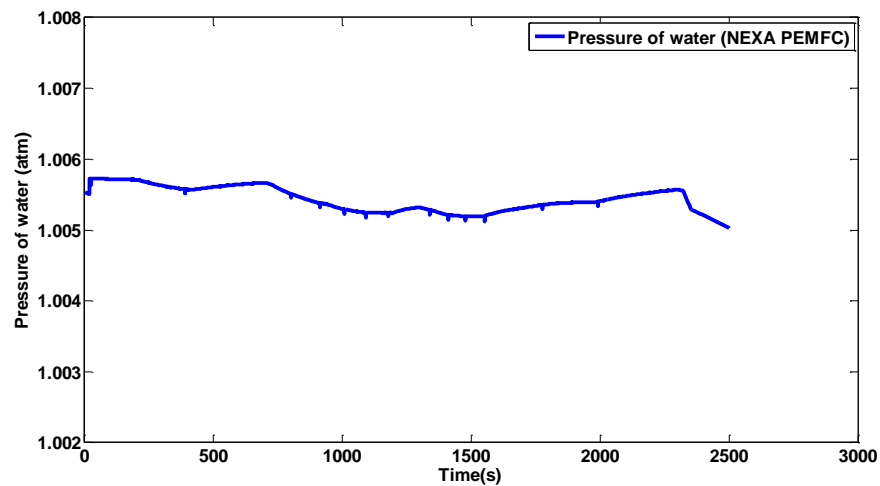
Figure 41: Pressure of water calculated via modified model using NEXA PEMFC system from experiment-3
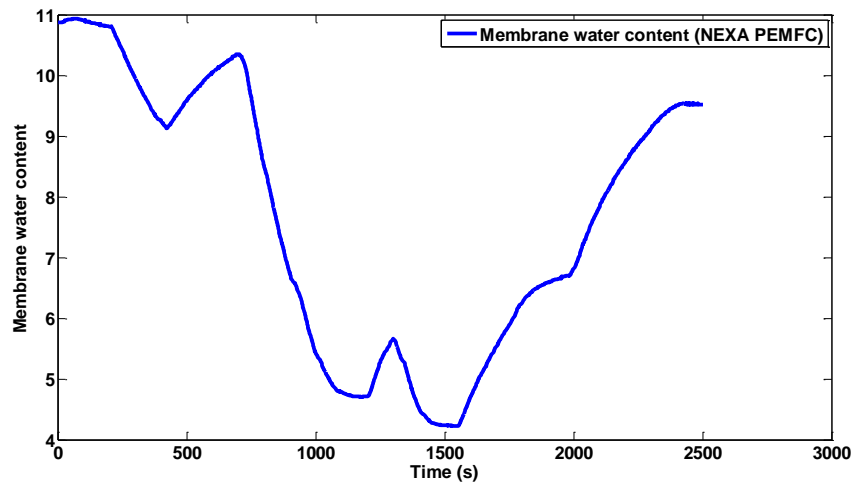
Figure 42: Membrane water content calculated via modified model using NEXA

PEMFC system from experiment-3

For the NEXA PEMFC system the membrane water content ranges between 11 to 4 with current changes from 0 to 50 A, for the average $T_{amb,c}$ and RH_{air} values are 28°C and 29% respectively. The values of membrane water content may vary from one PEMFC system to another PEMFC system. For the Horizon, the value of membrane water content ranges from 10.5 to 9.5 with current changes from 0 to 2.5 A, for the average $T_{amb,c}$ and RH_{air} values are 28.32°C and 27.03% respectively. These values of membrane water content for stack may depend upon the number of fuel cells and power ratings of the stack i.e. more current it draws from the PEMFC the more drop in membrane water content has been witnessed. Further analysis of membrane water content versus the change in ambient conditions has been done on the Horizon PEMFC system. As compared to the NEXA PEMFC system the Horizon system is more prone to vary its membrane water content for ambient condition changes.

5.6 Membrane water content analysis for possible faults via simulation

There is no proper measuring device or an indicator that can exactly tell whether the drying/ flooding faults occur or not. Thermal imaging and X-rays technique has been used to observe water content in the membrane as mentioned in (Ji and Wei, 2009; Um, Wang and Chen, 2000). But this is not possible for all commercial PEMFC systems, as these technologies and associated equipment can be very costly. On a normal PEMFC system, if flooding/drying faults can be persisted for a long time, it can surely damage the PEMFC system (Ji and Wei, 2009). So with the help of simulation, it is desired to make a case where possible flooding and drying faults may occur. Since flooding and drying faults can produce permanent damage therefore it is not advisable to run PEMFC system for adverse cases. The modified model does fit the experimental results clearly stated in the comparison figures above. Now if the $T_{amb,c}$ and RH_{air} in this modified model have been varied to introduce the severe hot and dry conditions (high $T_{amb,c}$ and low RH_{air}) , similarly cold and humid conditions (low $T_{amb,c}$ and high RH_{air}) can also be adopted. Then adverse drying and flooding conditions will occur in PEMFC through the above-mentioned variation of ambient conditions via simulation in the next sub-section.

5.7 Drying fault in horizon PEMFC via simulation

At very high ambient temperature and very low air relative humidity, the drying fault can occur if this condition persisted for the long-term. Consider a case with Horizon PEMFC system where $T_{amb,c}$ is as high as 40°C and RH_{air} is as low as 12%. This may possibly produce the drying fault in the PEMFC system. Figure 43 reveals the PEMFC model voltage and membrane water content at hot and dry ambient conditions.
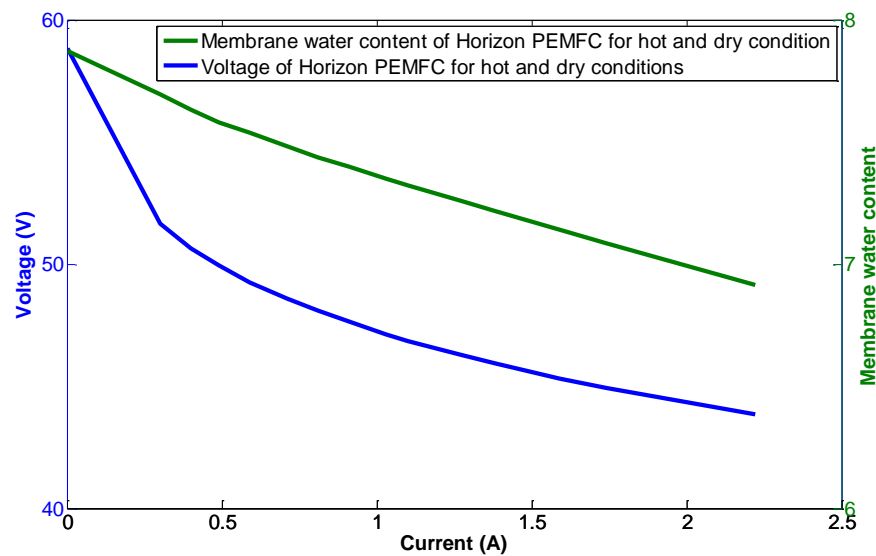
Figure 43: Voltage and membrane water content of Horizon PEMFC for hot and dry

conditions with $T_{amb,c} = 40°C$ and $RH_{air} = 12\%$

The membrane water content is less than 8 and drops below 7 which may be

an indicator of drying faults in the PEMFC system. So membrane water content less

than 6.5 in the Horizon PEMFC system can suggest the occurrence of drying fault.

5.8 Flooding fault in horizon PEMFC via simulation

At very low temperatures and high relative humidity, the flooding fault can

occur, but on the contrary, too low temperature may also cause freezing conditions

which have adverse effects on PEMFC as explained in (Kandlikar and Lu, 2009). Now

consider a case with Horizon PEMFC system where T_{amb} is as low as 15°C and RH_{air}

is as high as 65%. This is possible based on the study given in (Hannan, 2015) for

UAE indoor conditions with an air conditioning system. This may possibly produce

the flooding conditions in the PEMFC system. Figure 44 reveals the PEMFC model

voltage and membrane water content at cold and humid ambient conditions. Here the

voltage graph shows stable voltage with cold and humid conditions with increasing

current and the membrane water content starts from just below 12.5 and decreases to

value just above 11.5 with increase in current. This may be an indicator to flooding

fault as values above 12.5 may point to flooding faults in Horizon PEMFC system.
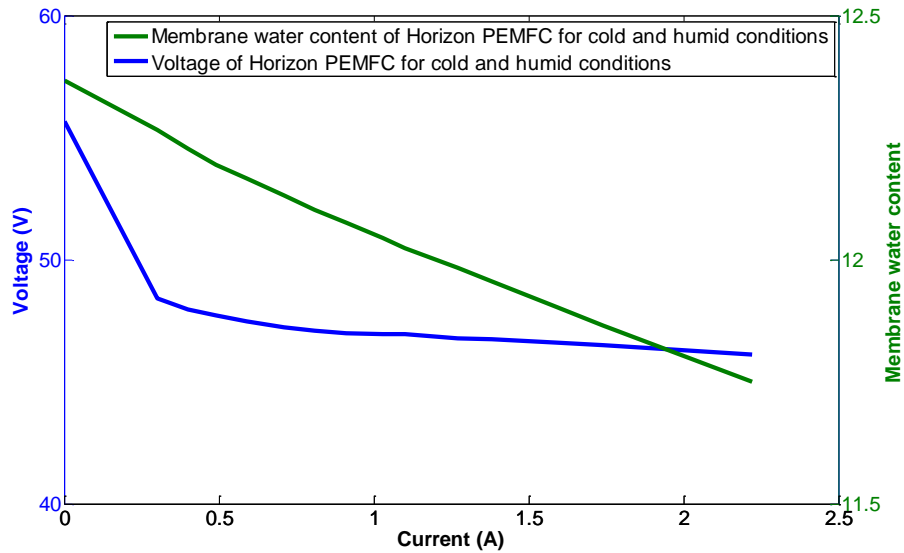
Figure 44: Voltage and membrane water content of Horizon PEMFC for cold and

humid conditions with $T_{amb,c} = 15°C$ and $RH_{air} = 65\%$

The final fault diagnosis procedure is given in Figure 45 in an organized diagram.
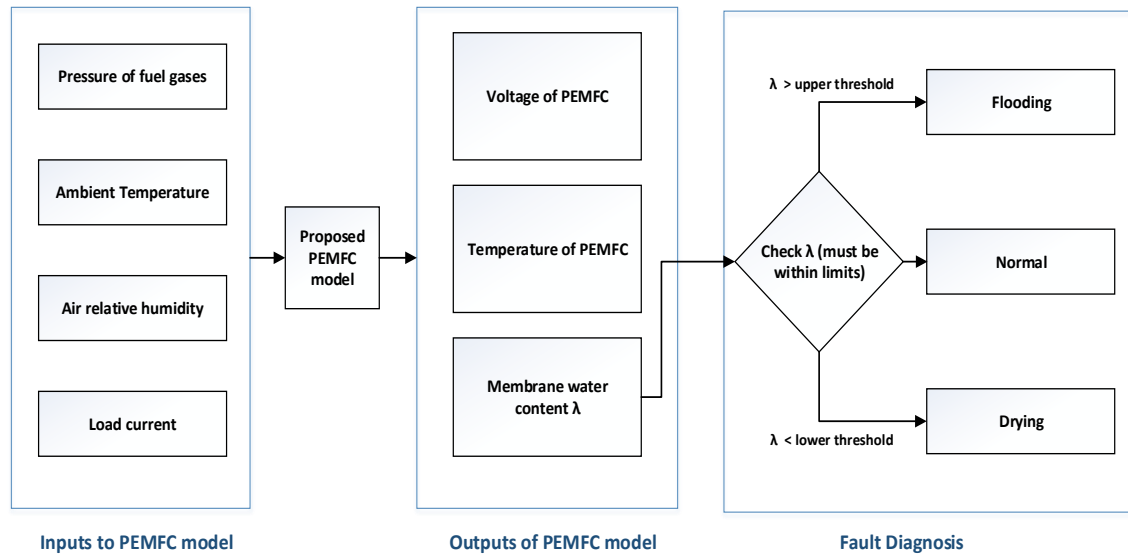
Figure 45 Schematic diagram for fault diagnosis by using membrane water content

5.9 Proposed empirical models results

The empirical models discussed above have the potential to calculate voltage variations due to the change in ambient temperature and pressure. The proposed model is entirely based upon the model given in (Salim et al., 2015) but the model equations are simplified and only the variation of voltage with respect to ambient conditions has been estimated.

5.9.1 Results of PSO model

The change in T_{amb} from 273 K to 323 K at different values of Rc from 0.5 Ω to 39.75 Ω is shown in Figure 46. The graph indicates that when the resistance greater than or equal to 3.43 Ω, variations in V_{amb} for T_{amb} are relatively the same. This variation becomes dominant when $R_c \leq 1$ Ω. When $T_{amb} < 298K$, V_{amb} is negative, which indicates that the voltage of PEMFC becomes higher than that at normal T_{amb} temperature and P_{air}. R_c does not have much impact at lower temperatures, which

agrees with experimental results in (Hottinen et al., 2003). However, R_c values have higher impact on V_{amb} when $T_{amb} > 298$ K. This impact of R_c becomes more prominent when $R_c < 1$ Ω, and this result is also consistent with experimental results presented in (Hottinen et al., 2003).
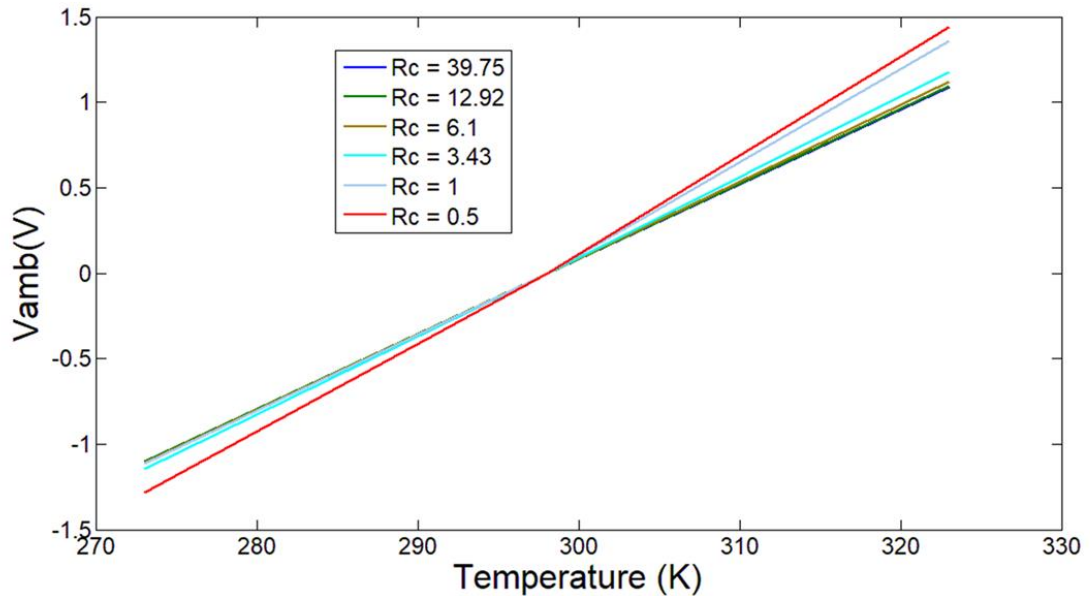
Figure 46: PEMFC voltage (V_{amb}) variation with T_{amb} when $P_{air} = 1$ atm

The V_{amb} with variations in P_{air} from 0.6 atm to 1 atm is shown in Figure 47. V_{amb} increases with a decrease in pressure which indicates that the voltage of PEMFC declines as pressure decreases. This impact is more prominent at high loads (low R_c values) and agrees with the experimental waveforms given in (Pratt, Brouwer and Samuelsen, 2007; Werner et al., 2015) .The effect of R_c becomes more obvious at $R_c \leq 1$ Ω.
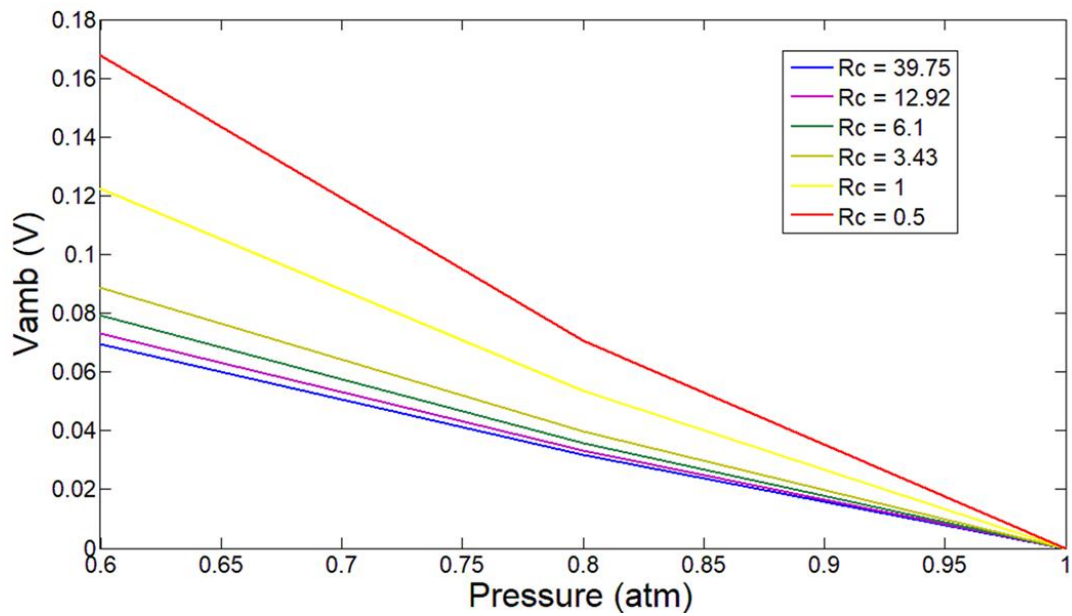
Figure 47: Voltage (V_{amb}) variation with ambient pressure when $T_{amb} = 298$ K

5.9.2 Statistical analysis results of proposed empirical model

The desired set of input states with responses (output) are given in Table 20 with $R_c > R_{th}$. The response voltage V_{res} is considered as $V_{amb}+2$ V. The extra 2 V is only added to make V_{amb} positive for all values, because negative values cannot be transformed in Box-Cox, especially logarithm transformation.

Table 20: Statistical design input and output for V_{amb} when $R_c > R_{th}$

Ambient Temperature -1 =273K 0 = 298 K 1 = 323 K	Ambient Pressure -1 = 0.6 atm 0 = 0.8 atm 1 = 1 atm	R_c = 6 ohms Response	
T_{amb}	P_{air}	V_{amb}	V_{res}
-1	1	-1.40049	0.59951
0	-1	0.036768	2.03677
0	0	0.017358	2.01736
-1	0	-1.38908	0.61092
1	0	1.446677	3.44668
0	1	0	2
1	-1	1.475345	3.47534
1	1	1.422026	3.42203
-1	-1	-1.37674	0.62326

The design results obtained from Minitab statistical software are listed in Table 21. The model has a p-value lower than 0.05, which indicates the significance of the model. All factors and their combinations, including quadratic terms, are significant because the p values are lower than 0.05, except P_{air}^2, which has no significant effect (p=0.126). The Box-Cox transformation shows that λ_b =1, which suggests that no transformation of V_{res} is required.

Table 21: Statistical design analysis for V_{amb} when $R_c > R_{th}$

Box-Cox transformation

Rounded $\lambda_b = 1$

Estimated $\lambda_b = 0.920539$

95% CI for $\lambda_b = (0.715039, 1.15104)$

Analysis of Variance

Source	DF	Seq SS	Contribution	Adj SS	Adj MS	F-Value	P-Value
Model	5	12.07	100.00%	12.0737	2.4147	3931374	0
Linear	2	12.07	100.00%	12.0732	6.0366	9828037	0
T_{amb}	1	12.07	99.98%	12.071	12.071	19652558	0
P_{air}	1	0.002	0.02%	0.0022	0.0022	3515.9	0
Square	2	3×10^{-04}	0.00%	0.0003	0.0001	220.53	0.001
T_{amb}^2	1	3×10^{-04}	0.00%	0.0003	0.0003	436.64	0
P_{air}^2	1	0	0.00%	0	0	4.42	0.126
Two-way interaction	1	2×10^{-04}	0.00%	0.0002	0.0002	355.65	0
$T_{amb} \times P_{air}$	1	2×10^{-04}	0.00%	0.0002	0.0002	355.65	0
Error	3	0	0.00%	0	0		
Total	**8**	**12.07**	**100.00%**				

After neglecting the quadratic term P_{air}^2, the new model is purely linear, and the regression equation for V_{res} is given in Equation (5.6). The residuals for this linear model are satisfactory, indicating good model probabilistic normality.

$$V_{res} = V_{amb} + 2 = 2.01804 + 1.41839T_{amb,1} + 0.01158T_{amb,1}^2 -$$

$$0.007390T_{amb,1}P_{air,1} - 0.018972P_{air,1}, \qquad\qquad (5.6)$$

where $T_{amb,1} = \dfrac{T_{amb} - \frac{273+323}{2}}{\frac{323-273}{2}}$ and $P_{air,1} = \dfrac{P_{air} - \frac{0.6+1}{2}}{\frac{1-0.6}{2}}$.

The final equation of V_{amb} for $R_c > R_{th}$ is given in Equation (5.7) with real factors T_{amb} and P_{air}. The resultant equation is fully quadratic, based on T_{amb} and P_{air} factors. The effect of T_{amb} is more prominent than P_{air} as proven experimentally in (Hottinen et al., 2003; Werner et al., 2010; Pratt, Brouwer and Samuelsen, 2007) .

$$V_{amb} = 0.01804 + 1.41839 \frac{(T_{amb} - 298)}{25}) - 0.0189 \frac{(P_{air} - 0.8)}{0.2}) -$$

$$0.00739 \frac{(T_{amb} - 298)}{25}) \frac{(P_{air} - 0.8)}{0.2}), + 0.01158 \frac{(T_{amb} - 298)}{25})^2 = -15.52 + 0.04688 T_{amb} +$$

$$0.3451 P_{air} + 1.853 \times 10^{-5} T_{amb}^2 - 1.478 \times 10^{-3} T_{amb} P_{air}, \qquad (5.7)$$

where $R_c > R_{th}$.

To find the regression model for the case $R_c < R_{th}$, a similar procedure given above is adopted, except that R_c is considered as the third factor. The desired set of input states with responses are given in Table 22.

Table 22: Statistical design input and output for V_{amb} when $R_c \leq R_{th}$

Ambient Temperature -1 =273K 0 = 298 K 1 = 323 K	Ambient Pressure -1 = 0.6 atm 0 = 0.8 atm 1 = 1 atm	Resistance Load -1 = 0.5 ohm 0 = 0.75 ohm 1 = 1 ohm	Response Factors	
T_{amb}	P_{air}	R_c	V_{amb}	V_{res}
-1	-1	-1	-1.60824	0.39176
1	-1	-1	2.19034	4.19034
-1	1	-1	-1.71712	0.28288
1	1	-1	2.06811	4.06811
-1	-1	1	-1.67100	0.32900
1	-1	1	2.01542	4.01542
-1	1	1	-1.74789	0.25211
1	1	1	1.91832	3.91832
-1	0	0	-1.74407	0.25593
1	0	0	2.07253	4.07253
0	-1	0	0.10241	2.10241
0	1	0	0.00000	2.00000
0	0	-1	0.05075	2.05075
0	0	1	0.03941	2.03941
0	0	0	0.04524	2.04524

The design results are given in Table 23. The p value of the model is less than 0.05, which implies that the model is significant. Table 23 shows that R_c has a significant effect because the p-value is less than 0.05. Thus, the assumption of R_{th} has been proven. T_{amb}, P_{air}, and T_{amb}^2 are also significant. The other factors, such as $T_{amb} \times P_{air}$, R_c^2, and P_{air}^2, have no significant effect ($p>0.05$). The Box-Cox transformation shows that $\lambda_b=1$, indicating that the transformation of V_{res} is not required.

Table 23: Statistical design analysis for V_{amb} when $R_c \leq R_{th}$

Box-Cox transformation							
Rounded $\lambda_b = 1$							
Estimated $\lambda_b = 0.920539$							
95% CI for $\lambda_b = (0.715039, 1.15104)$							
Analysis of Variance							
Source	**DF**	**Seq SS**	**Contribution**	**Adj SS**	**Adj MS**	**F-Value**	**P-Value**
Model	9	35.276	99.98%	35.276	3.9196	3147.95	0
Linear	3	35.211	99.80%	35.2119	11.7373	9426.68	0
T_{amb}	1	35.167	99.68%	35.1677	35.1677	28244.52	0
P_{air}	1	0.0258	0.07%	0.0258	0.0258	20.69	0.006
R_c	1	0.0185	0.05%	0.0185	0.0185	14.82	0.012
Square	3	0.0569	0.16%	0.0569	0.019	15.23	0.006
T_{amb}^2	1	0.0564	0.16%	0.0394	0.0394	31.68	0.002
P_{air}^2	1	0.0004	0.00%	0.0003	0.0003	0.24	0.643
R_c^2	1	0.0001	0.00%	0.0001	0.0001	0.05	0.839
Two-way interaction	3	0.0072	0.02%	0.0072	0.0024	1.94	0.242
$T_{amb} \times P_{air}$	1	0.0001	0.00%	0.0001	0.0001	0.11	0.75
$T_{amb} \times R_c$	1	0.0067	0.02%	0.0067	0.0067	5.37	0.068
$P_{air} \times R_c$	1	0.0004	0.00%	0.0004	0.0004	0.33	0.592
Error	5	0.0062	0.02%	0.0062	0.0012		
Total	**14**	**35.282**	**100.00%**				

After neglecting the insignificant terms in the design, the final Equation (5.8) of V_{res} for $R_c < R_{th}$ is given as follows:

$$V_{res} = V_{amb} + 2 = 2.0476 + 1.8753T_{amb,1} - 0.0508P_{air,1} - 0.043R_{c,1} + 0.1301T_{amb,1}^2 \tag{5.8}$$

whereas $T_{amb,1} = \frac{T_{amb} - \frac{273+323}{2}}{\frac{323-273}{2}}$, $P_{air,1} = \frac{P_{air} - \frac{0.6+1}{2}}{\frac{1-0.6}{2}}$, and $R_{c,1} = \frac{R_c - \frac{0.5+1}{2}}{\frac{1-0.5}{2}}$.

The final equation of V_{amb} for $R_c \leq R_{th}$ is given in Equation (5.9) with original factors T_{amb} and P_{air}. The resultant equation has linear and quadratic effects based on T_{amb}, P_{air}, R_c, and T_{amb}^2. The effect of T_{amb} is more prominent than those of P_{air} and R_c, and this result is also proven experimentally in (Hottinen et al., 2003; Werner et al., 2010; Pratt, Brouwer and Samuelsen, 2007).

$$V_{amb} = 0.0476 + 1.8753\frac{(T_{amb}-298)}{25}) - 0.0508\frac{(P_{air}-0.8)}{0.2}) - 0.043\frac{(R_c-0.75)}{0.25}), +$$

$$0.1301\frac{(T_{amb}-298)}{25})^2 = -3.4968 - 0.04905 T_{amb} - 0.254 P_{air} - 0.172 R_c +$$

$$2.0816 \times 10^{-4} T_{amb}^2 \qquad\qquad (5.9)$$

where $R_c \leq R_{th}$.

This empirical model must be validated using experimental chambers where variation of ambient pressure and temperature will be introduced for different loading conditions as future research work.

5.9.3 Proposed electrical equivalent model from empirical model

This estimation of change in PEMFC voltage with respect to change in ambient pressure and temperature based on load resistance can be easily incorporated with the PEMFC electrical equivalent model mentioned in (Aglzim et al., 2014). The model in (Aglzim et al., 2014) estimates the voltage of PEMFC at standard PEMFC ambient temperature and pressure (T_{amb} and P_{air} are 298 K and 1 atm respectively) purely on the basis of output resistance R_c. This additional V_{amb} can be incorporated in the electrical equivalent model as additional voltage source in the design. Figure 48 presents the final form of modified electrical equivalent model.
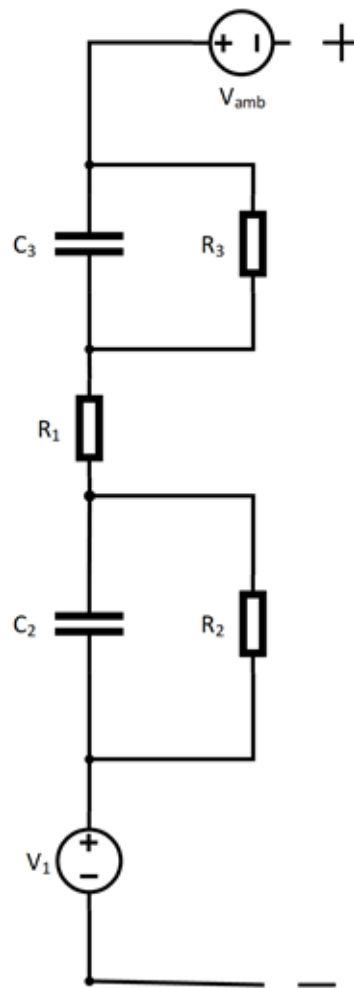
Figure 48: PEMFC stack proposed electrical equivalent model incorporating ambient conditions

Here V_1, C_2, R_2, C_3 and R_3 can be calculated with the help of output resistance R_c using similar Equation (5.10) The coefficients a_i (i= 1 to 6) can vary for each of the variables.

$$[V_1, C_2, R_2, C_3, R_3] = a_6 R_c^6 + a_5 R_c^5 + a_4 R_c^4 + a_3 R_c^3 + a_2 R_c^2 + a_1 R_c \quad (5.10)$$

Table 24 gives the value of coefficients a_i to calculate for all variables V_1, C_2, R_2, C_3 and R_3 using Equation (5.10). R_1 is taken as constant with value of 0.073 ohms. The threshold resistance R_c for (Aglzim et al., 2014) model is 8 ohms.

Table 24: Coefficients a_i for R_2, R_3, C_2, C_3, and V_1

a_i	V1		R2		C2		R3		C3	
	$R_c<8\Omega$	$R_c>8\Omega$	$R_c<8\Omega$	$R_c>8\Omega$	$R_c<8\Omega$	$R_c>8\Omega$	$R_c<8\Omega$	$R_c>8\Omega$	$R_c<8\Omega$	$R_c>8\Omega$
a_6	-11.97×10^{-3}	-16.95×10^{-6}	-86.73×10^{-5}	-29.19×10^{-8}	31.44×10^{-5}	-17.29×10^{-9}	-23.36×10^{-4}	32.63×10^{-9}	54.48×10^{-4}	-51.76×10^{-6}
a_5	31.13×10^{-2}	12.86×10^{-4}	23.47×10^{-3}	22.48×10^{-6}	-82.65×10^{-4}	13.45×10^{-7}	61.29×10^{-3}	-22.18×10^{-7}	-12.63×10^{-2}	37.73×10^{-4}
a_4	-3.21	-30.10×10^{-3}	-25.06×10^{-2}	-54.03×10^{-5}	85.26×10^{-3}	-32.74×10^{-6}	-63.10×10^{-2}	41.01×10^{-6}	1.085	-82.11×10^{-3}
a_3	16.64	22.86×10^{-2}	1.32	43.04×10^{-4}	-43.14×10^{-2}	26.31×10^{-5}	3.18	-16.94×10^{-5}	-4.11	55.20×10^{-2}
a_2	-45.32	0	-3.43	0	1.06	0	-7.87	0	5.95	0
a_1	61.75	0	3.63	0	-1.03	0	7.65	0	-0.31	0

5.10 Chapter summary

This chapter gives details discussion on the voltage and temperature model of PEMFC that were proposed in previous chapters. Both semi-empirical and empirical models have been discussed with results. The fault diagnosis feature of the semi-empirical model has also been discussed with details. The empirical models will help easy estimation of voltage variation of PEMFC in varying ambient conditions.

Chapter 6: Conclusion

6.1 Conclusion

This thesis presents the development of model-based fault diagnosis of PEMFC by incorporating ambient conditions variation. The research has four main objectives (i) to develop the voltage model of PEMFC (ii) to develop the temperature model of PEMFC (iii) to study and model the effects of ambient conditions on PEMFC (iv) to use the developed models for online fault diagnosis.

To accomplish the first objective the novel dynamic semi-empirical voltage model has been developed with parameters are extracted using QLSA. This model satisfies not only on-load voltage variations but also the no-load variations as well. The major inputs are the internal pressure of Hydrogen, current of PEMFC and temperature of PEMFC. The voltage model consists of various voltage drops i.e activation, ohmic and concentration voltage drops. These voltage drops waveform exactly follow the theoretical pattern and also the equations used are not too complex. In Matlab® the computational time to implement all equations is almost 0.05 seconds which makes this model suitable for online monitoring.

The second objective is to develop the temperature model of PEMFC but without using the voltage of PEMFC. The model in this research only takes load current and ambient temperature of PEMFC as input and uses an effective algorithm to predict the online variations of PEMFC through model equations. Here again the parameters are optimized using QLSA. After completion of the temperature model, both PEMFC voltage and temperature can be predicted by using internal pressure of Hydrogen and current of PEMFC under normal ambient conditions.

The third objective is based on the need if ambient conditions vary the PEMFC output voltage and temperature varies. The detailed study has been done and the empirical model of PEMFC voltage has been developed that predicts PEMFC voltage variation for the variations in ambient temperature and pressure empirically. The starting voltage has also been modelled empirically, as starting voltage of PEMFC exhibits different variations with ambient than PEMFC working continuously. At starting the PEMFC temperature is very close to ambient temperature.

For fault diagnostic modelling to achive the fourth objective, it was necessary to upgrade the semi-empirical voltage model towards more generic model and to check the model validity at varying ambient conditions. The developed generatic model was then tested at varying ambient conditions for two different sets of PEMFCs (NEXA 1.2 kW system and Horizon 300 W system). The ambient conditions were incorporated in the model by updating the varying parameters through statistical analysis, and ambient condition-based equations have been proposed. A compensating factor has also been introduced which makes the model more generic and accounts for the change in number of fuel cells in the model. After these modifications the model was again validated experimentally for both PEMFCs system and the results revealed that the RMSE is less than 0.5 and the total computation time for running both voltage and temperature model is 0.08 seconds in Matlab® software. Also the membrane water content λ calculated from the model equations has higher values for humid conditions and the lowest values for dry condition. Now this model was used for fault diagnosis, the harsh ambient conditions have been tested through simulations on Matlab® . The severe dry and humid conditions were tested separately. The membrane water content λ threshold limits have been revealed for the Horizon PEMFC system, the upper limit

is 12.5 while the lower limit is 6.5. Beyond these limits, the flooding and drying faults may occur. It is advised to use PEMFC within these limits. These limits, however, vary based on the maximum current and power ratings.

6.2 Significant contributions of the research

The major contribution of this thesis can be summarized as follows:

1- Developed the semi-empirical voltage model that considers the effect of internal currents, fits the no-load/on-load voltage and reveals the exact theoretical component voltage waveforms simultaneously.

2- Developed the accurate temperature model of PEMFC that only takes the load current and ambient temperature without using complex equations. The temperature model doesn't require a very good sampling rate, all it requires memory for the algorithm, due to the use of memory the complexity of the equations is reduced.

3- Devloped a new electrical equivalent model that inccoperates ambient condition effects on PEMFC based entirely upon the output resistance and ambient conditions.

4- Finally, the model-based fault diagnosis has been proposed which has a computation time of 0.08 seconds and no complex equation involved. The threshold limits of membrane water content are very helpful in fault diagnosis for any PEMFC system. These threshold limits can be found for any PEMFC by plotting the membrane water content from zero to maximum current at severe dry and humid ambient conditions with the help of simulations.

5- Proposed a quick fault diagnosis technique can be very helpful in taking a quick measure to resolve the issue. The steps that can be taken to resolve the issues

are (i) controlling reactant gases humidity (ii) controlling reactant gas flow rate (iii) controlling temperature (iv) controlling the current drawn.

6- Proposed health monitoring feature in the model of PEMFC by analyzing the membrane water content of PEMFC throughout its entire useage.

6.3 Recommendations for future studies

The thesis presents the novel model-based fault diagnosis technique and empirical models for predicting the voltage change in case of ambient condition change. However, this work can be extended in the future if the researchers follow the suggestions given below:

1- The semi-empirical voltage model can be tested on more PEMFC systems other than NEXA 1.2 kW and Horizon 300 W PEMFC system, with a different number of fuel cells, membrane electrode assembly and the systems that use extra humidification for inlet fuel gases. The model can be updated by using new equations through statistical analysis.

2- The temperature model can also be tested with PEMFC systems that use different cooling mechanisms other than simple fan cooling. There are some PEMFC systems that use water cooling tubes and other mechanisms. The model can also be updated by using new differential equations that account for the cooling system.

3- The first proposed empirical model in this thesis has not been tested as the change in ambient pressure requires special chambers. These chambers can change the ambient pressure/temperature, and it can easily be used to validate and update the empirical model.

4- The threshold limits of membrane water content λ can be set experimentally for different commercial PEMFCs system. Though the PEMFC systems may damage permanently by introducing drying and flooding faults, the set limits will avoid a lot of PEMFCs damages in the future.

5- Water management control strategies given in the previous section will be adopted experimentally after the diagnosis of faults. The response time and effectivity for each control strategy will be discussed in detail.

References

Abdollahzadeh, M., Ribeirinha, P., Boaventura M. and Mendes, A. (2018). Three-dimensional modeling of PEMFC with contaminated anode fuel. *Energy* 152: 939–959.

Aglzim, E., Rouane, A. Chrenko, Kourtiche, D. and Nadi, M. (2014). Polymer Electrolyte Fuel Cell stack modelling in VHDL-AMS language with temporal and EIS experimental validations. *J. Energy Power Eng*. 8(2): 343–349.

Andres, H., Hissel, D. and Rachid, O. (2010). Modeling and fault diagnosis of a Polymer Electrolyte Fuel Cell using electrical equivalent analysis. *IEEE Trans. Energy Convers.* 25: 148–160.

Akbari, A. and Dahari, M. (2019). Using ANFIS technique for PEM Fuel Cell electric bicycle prediction model. *International Journal of Environmental Science and Technology* 16: 7319–7326.

Akimoto, Y. and Suzuki, S. (2018). Overpotential evaluation of PEMFC using semi-empirical equation and SEM. *The 3rd International Tropical Renewable Energy Conference. Sustainable Development of Tropical Renewable Energy*, *Indonesia.*

Al-Baghdadi, M. (2005). Modelling of Proton Exchange Membrane Fuel Cell performance based on semi-empirical equations. *Renewable Energy* 30(10): 1587–1599.

Al-Zeyoudi, H., Sasmito, A. and Shamim, T. (2015). Performance evaluation of an open-cathode PEM fuel cell stack under ambient conditions: Case study of United Arab Emirates. *Energy Convers. Manag*. 105: 798–809.

Ali, J., Hannan, A. and Mohamed, A. (2015). A novel Quantum-Behaved Lightning Search Algorithm approach to improve the fuzzy logic speed controller for an induction motor drive. *Energies* 8(11): 13112–13136.

Amphlett, J., et al., (1995). Performance modeling of the Ballard Mark IV solid polymer electrolyte fuel cell mechanistic model development. *J. Electrochem. Soc.* 142(1) : 1–8.

Andrea, E., et al., (2006). A simplified electrical model of small PEM fuel cell. *International Conference on Renewable Energies and Power Quality, Spain.*

Araya, S., Zhou, F., Sahlin, S., Thomas, S. and Jeppesen, C. (2019). Fault characterization of a Proton Exchange Membrane Fuel Cell stack. *Energies* 12 (1): 152–167.

Ariza, H., et al., (2018). Thermal and electrical parameter identification of a Proton Exchange Membrane Fuel Cell using genetic algorithm. *Energies* 11(8): 2099–2114.

Atifi, A., Mounir, H. and El-Marjani, A. (2014). Effect of internal current, fuel crossover, and membrane thickness on a PEMFC performance. *Proceedings of 2014 International Renewable and Sustainable Energy Conference, IRSEC, Morocco.*

Atyabi, S. and Afshari, E. (2019). Three-dimensional multiphase model of Proton Exchange Membrane Fuel Cell with honeycomb flow field at the cathode side. *Journal of Cleaner Production* 214: 738–748.

Ay, M., Midilli, A. and Dincer, I. (2006). Thermodynamic modelling of a Proton Exchange Membrane Fuel Cell. *International Journal of Exergy* 3(1): 16–44.

Azri, M., et al., (2017). Development of PEMFC emulator using electrical equivalent circuit. *6th International Conference on Electrical Engineering and Informatics (ICEEI), Malaysia*.

Barzegari, M., Alizadeh, E. and Pahnabi. A. (2017). Grey-Box modeling and model predictive control for Cascade-Type PEMFC. *Energy* 127: 611–622.

Becherif, M., Hissel, D., Gaagat, S., and Wack M. (2011). Electrical equivalent model of a Proton Exchange Membrane Fuel Cell with experimental validation. *Renewable Energy* 36(10): 2582–2588.

Benmouna, A., et al., (2017). Fault diagnosis methods for Proton Exchange Membrane Fuel Cell system. *International Journal of Hydrogen Energy* 42: 1534–1543.

Belmokhtar, K. and Doumbia, M. (2014). PEM Fuel Cell modelling using artificial neural networks. *Int. J. Renew. Energy Res.* 4(3): 725–730.

Benne, M., Grondin-Perez, B., and Bessa, M. (2015). Polymer Electrolyte Membrane Fuel Cell fault diagnosis based on empirical mode decomposition. *Journal of Power Sources* 299: 596–603.

Bernardi, D. and Verbrugge, M. (1992). A mathematical model of the Solid-Polymer-Electrolyte Fuel Cell. *J. Electrochem. Soc.* 139(9): 2477–2491.

Burheim, O., et al., (2014). Study of thermal conductivity of PEM Fuel Cell catalyst layers. *International Journal of Hydrogen Energy* 39(17): 9397–9408.

Cauffet, G., Chadebec, O. and Rouveyre, L. (2019). Fault detection for Polymer Electrolyte Membrane Fuel Cell stack by external magnetic field. *Electrochimica Acta* 313: 141–150.

Chamagne D., et al., (2018). Characterization of an H_2/O_2 PEMFC short-stack performance aimed to health-state monitoring and diagnosis. *Fuel Cells* 18(3): 279–286.

Chavan S. and Talange, D. (2017). Modeling and performance evaluation of PEM Fuel Cell by controlling its input parameters. *Energy* 138: 437–445.

Choi, W., Howze, J., W. and Enjeti, P. (2006). Development of an equivalent circuit model of a fuel cell to evaluate the effects of inverter ripple current. *Journal of Power Sources* 158(2): 1324–1332.

Correa, J., et al., (2005). Sensitivity analysis of the modeling parameters used in simulation of Proton Exchange Membrane Fuel Cells. *IEEE Transactions on Energy Conversion* 20(1): 211–218.

Dannenberg, K., Ekdunge, P. and Lindbergh, G. (2000). Mathematical model of the PEMFC. *Journal of Applied Electrochemistry* 30(12): 1377–1387.

Del-Real, A., Arce, A. and Bordons, C. (2007). Development and experimental validation of a PEM Fuel Cell dynamic model. *Journal of Power Sources* 173(1): 310–324.

Du, C., Shi, X., Cheng, Q. and Yin, G. (2004). Effective protonic and electronic conductivity of the catalyst layers in Proton Exchange Membrane Fuel Cells. *Electrochemistry Communications* 6(5):435–440.

Dyantyi, N., Parsons, A., Bujlo, P. and Pasupathi, S. (2019). Behavioural study of PEMFC during start- up / shutdown cycling for aeronautic applications. *Materials for Renewable and Sustainable Energy* 8(1): 1–8.

Ettihir, K., et al., (2014). Online identification of semi-empirical model parameters for PEMFCs. *International Journal of Hydrogen Energy* 39(36): 21165–21176.

Fathy, A. and Rezk, H. (2017). Multi-Verse optimizer for identifying the optimal parameters of PEMFC model. *Energy* 143: 634–644.

Forrai, A., Funato, H., Yanagita, Y. and Kato, Y. (2005). Fuel-Cell parameter estimation and diagnostics. *IEEE Trans. Energy Convers.* 20: 668–675.

Fouquet, N., et al., (2006). Model based PEM Fuel Cell state-of-health monitoring via ac impedance measurements. *Journal of Power Sources* 159(2): 905–913.

Gamalath, K., Wijewardena, A. and Peiris, B. (2012). Theoretical approach to the physics of fuel cells. *International Letters of Chemistry, Physics and Astronomy* 2: 15–27.

Geem, Z. and Noh, J. (2016). Parameter estimation for a Proton Exchange Membrane Fuel Cell model using GRG technique. *Fuel Cells* 16(5): 640–645.

Giner-Sanz, J., Ortega, E. and Pérez-Herranz V. (2015). Statistical analysis of the effect of the temperature and inlet humidities on the parameters of a PEMFC Model. *Fuel Cells* 15(3): 479–493.

Görgün, H., Barbir, F. and Arcak, M. (2005). A voltage-based observer design for membrane water content in PEM fuel cells. *Proceedings of the American Control Conference, USA.*

Gurau, V., Liu, H. and Kakaç S. (1998). Two-Dimensional model for Proton Exchange Membrane Fuel Cells. *AIChE Journal* 44(11): 2410–2422.

Headley, A., et al., (2016). Development and experimental validation of a physics-based PEM Fuel Cell model for cathode humidity control design. *IEEE/ASME Transactions on Mechatronics* 21(3): 1775–1782.

Hinaje, M., (2012). An equivalent electrical circuit model of Proton Exchange Membrane Fuel Cells based on mathematical modelling. *Energies* 5(8): 2724–2744.

Hogarth, H. and Benziger, J. (2006). Dynamics of autohumidifed PEM Fuel Cell operation. *Journal of The Electrochemical Society* 153(11): A2139–A2146.

Hoon, D., Seung, S., Yoo, R. and Hyun Y. (2019). Real time water contents measurement based on step response for PEM Fuel Cell. *International Journal of Precision Engineering and Manufacturing-Green Technology* 6(5): 883–892.

Hottinen, T., et al., (2003). Effect of ambient conditions on performance and current distribution of a Polymer Electrolyte Membrane Fuel Cell. *Journal of Applied Electrochemistry* 33: 265–271.

Hou, Y., Zhuang, M. and Wan, G. (2007). A transient semi-empirical voltage model of a fuel cell stack. *International Journal of Hydrogen Energy* 32(7): 857–862.

Hyun-Il, et al., (2010). A simple dynamic model for polymer electrolyte membrane fuel cell (PEMFC) power modules: Parameter estimation and model prediction. *International Journal of Hydrogen Energy* 35: 3656-3663.

Hannan, A. (2015) Indoor air quality in UAE office buildings and their effects on occupants' health, comfort, productivity and performance. *MSc Sustainable Design of the Built Environment, The British University in Dubai.*

Ibrahim, M., et al., (2015). Signal-Based diagnostics by wavelet transform for Proton Exchange Membrane Fuel Cell. *Energy Procedia* 74: 1508–1516.

Jee-Hoon, J., Ahmed, S. and Enjeti, P. (2011). PEM Fuel Cell stack model development for real-time simulation applications. *IEEE Transactions on Industrial Electronics* 58(9): 4217–4231.

Ji, M. and Wei, Z. (2009). A review of water management in Polymer Electrolyte Membrane Fuel Cells. *Energies* 2(4): 1057–1106.

Johnsson, F., Kjarstad, J. and Rootzan, J. (2018). The threat to climate change mitigation posed by the abundance of fossil fuels fuels. *Climate Policy* 19(2): 258–274.

Junyan, S. and Shudan, L. (2015). Dynamic window-based adaptive median filter algorithm. *The Open Cybernetics & Systemics Journal* 9: 1502–1506.

Kandlikar, S. and Lu, Z. (2009). Fundamental research needs in combined water and thermal management within a Proton Exchange Membrane Fuel Cell stack under normal and cold-start condition. *Journal of Fuel Cell Science and Technology* 6(4): 044001–044014.

Kim, B., Cha, D. and Kim, Y. (2015) .the effects of air stoichiometry and air excess ratio on the transient response of a PEMFC under load change conditions. *Applied Energy* 138: 143–149.

Kim, H., et al., (2010). A simple dynamic model for Polymer Electrolyte Membrane Fuel Cell (PEMFC) power modules: parameter estimation and model prediction. *International Journal of Hydrogen Energy* 35(8): 3656–63.

Kumar, P., et al., (2017). Electric power components and systems genetic algorithm-based modeling of pem fuel cells suitable for integration in DC microgrids Genetic Algorithm-based modeling of PEM Fuel Cells suitable for integration in DC microgrids. *Electric Power Components and Systems* 45(10): 1152–1160.

Kurz, T., et al., (2008). An impedance-based predictive control strategy for the state-of-health of PEM Fuel Cells Stacks. *Journal of Power* Sources 180(2): 742–747.

Labach, I., Rallières O. and Turpin C. (2017). Steady-state semi-empirical model of a single Proton Exchange Membrane Fuel Cell (PEMFC) at varying operating conditions. *Fuel Cells* 17(2): 166–177.

Laribi, S., Mammar, K., Sahli, Y. and Koussa, K. (2019). Analysis and diagnosis of PEM Fuel Cell failure modes (flooding & drying) across the physical parameters of electrochemical impedance model: using neural networks method. *Sustainable Energy Technologies and Assessments* 34: 35–42.

Larminie, J. and Dicks, A. (2003). *Fuel Cell Systems Explained*, J. Wiley, United Kingdom.

Le, M., et al., (2012). AThree Dimensional Electrical Model of PEMFC Stack. *Fuel Cells* 12: 225-238.

Lechartier, B., et al., (2014). Static and Dynamic Modeling of a PEMFC for Prognostics Purpose. *2014 IEEE Vehicle Power and Propulsion Conference, VPPC, Portugal.*

Le-Canut, J., Abouatallah, R. and Harrington D. (2006). Detection of membrane drying, fuel cell flooding, and anode catalyst poisoning on PEMFC stacks by

electrochemical impedance spectroscopy. *J. Electrochem. Soc.* 153(5): A857–864.

Li, Z., et al., (2018) .Fault diagnosis for PEMFC systems in consideration of dynamic behaviors and spatial inhomogeneity. *IEEE Transactions on Energy Conversion* 34: 3–11.

Lim, B., et al., (2019). Three-Dimensional study of stack on the performance of the Proton Exchange Membrane Fuel Cell. *Energy* 169: 338–43.

Liu, J., Li, Q., Chen, W. and Yan, Y. (2018). A fast fault diagnosis method of the PEMFC system based on extreme learning machine and dempster - shafer evidence theory. *IEEE Transactions on Transportation Electrification* 5(1): 271–284.

Lu, H., et al., (2019). On-Line fault diagnosis for Proton Exchange Membrane Fuel Cells based on a fast electrochemical impedance spectroscopy measurement. *Journal of Power Sources* 430: 233–43.

Maggio, G., Recupero, V. and Pino L. (2001). Modeling Polymer Electrolyte Fuel Cells: an innovative approach. *Journal of Power Sources* 101(2): 275–86.

Mennola, T. (2004). Mass transport in Polymer Electrolyte Membrane Fuel Cells using natural convection for air supply. *Ph.D. Thesis of the University of Technology of Helsinki*.

Maizia, R., et al., (2017). Statistical short-time analysis of electrochemical noise generated within a Proton Exchange Membrane Fuel Cell. *Journal of Solid State Electrochemistry* 22(6):1649–1660.

Manoharan Y., Hosseini, S., Butler, B. and Alzhahrani, H. (2019). Hydrogen fuel cell vehicles; current status and future prospect. *Appl. Sci.* 9(11): 2296–2300.

Mao, L., Jackson, L. and Davies, B. (2017). Investigation of PEMFC fault diagnosis with consideration of sensor reliability. *International Journal of Hydrogen Energy* 43(35): 16941–16948.

Marr, C. and Li, X. (1999). Composition and performance modelling of catalyst layer in a Proton Exchange Membrane Fuel Cell. *Journal of Power Sources* 77(1): 17–27.

Martín, I., Ursúa, A. and Sanchis, P. (2014). Modelling of PEM Fuel Cell performance: steady-state and dynamic experimental validation. *Energies* 7(2): 670–700.

Mo, Z., Zhu, X.,Wei, L. and Cao G. (2006). Parameter optimization for a PEMFC model with a hybrid genetic algorithm. *International Journal of Energy Research* 30(8): 585–97.

Montgomery, D. (2013) *Design and Analysis of Experiments*. John Wiley & Sons, USA.

Moore, A., et al., (2018). High fidelity model for Proton Exchange Membrane Fuel Cell power module considering internal power losses. *Fuel Cells* 18 (1): 63–72.

Moreira, M. and Da-Silva, G. (2009). A practical model for evaluating the performance of Proton Exchange Membrane Fuel Cells. *Renewable Energy* 34(7): 1734–1741.

Motapon, S., N., Tremblay, O. and Dessaint, L. (2012). Development of a generic fuel cell model: application to a fuel cell vehicle simulation. *International Journal of Power Electronics* 4(6): 505–522.

Murugesan, K. and Senniappan V. (2013) .Investigation of water management dynamics on the performance of a Ballard-Mark-V Proton Exchange Membrane Fuel Cell stack system. *International Journal of Electrochemical Science* 8(6): 7885–7904.

Nalbant, Y., Colpan, C. and Devrim, Y. (2018). Development of a one-dimensional and semi-empirical model for a high temperature Proton Exchange Membrane Fuel Cell. *International Journal of Hydrogen Energy* 43(11): 5939–5950.

Nishida, K., Hosotani, T. and Asa M. (2019). Evaluation of two water transports through electrolyte membrane of Polymer Electrolyte Fuel Cell based on water visualization and current measurement. *Fuel Cells* 19(1): 60–70.

Panos, C., Kouramas, K., Georgiadis, M. and Pistikopoulos, E. (2012). Modelling and explicit model predictive control for PEM Fuel Cell systems. *Chemical Engineering Science* 67(1): 15–25.

Pessot, A., et al., (2018). Contribution to the modelling of a low temperature PEM Fuel Cell in aeronautical conditions by design of experiments. *Mathematics and Computers in Simulation* 158: 179–198.

Pucheng, P., Yuehua, L., Huachi, X. and Ziyao, W. (2016). A review on water fault diagnosis of PEMFC associated with the pressure drop. *Applied Energy* 173: 366–385.

Petrone, R., et al., (2013). A review on model-based diagnosis methodologies for PEMFCs. *International Journal of Hydrogen Energy* 38(17): 7077–7091.

Pisani L., et al., (2002). A new semi-empirical approach to performance curves of Polymer Electrolyte Fuel Cells. *Journal of Power Sources* 108: 192–203.

Pratt, J., W., Brouwer, J. and Scott, S. (2007). Performance of Proton Exchange Membrane Fuel Cell at high-altitude conditions. *Journal of Propulsion and Power* 23(2): 437–444.

Puranik, S., V., Keyhani, A. and Khorrami, F. (2010). Neural network modeling of Proton Exchange Membrane Fuel Cell. *IEEE Transactions on Energy Conversion* 25(2): 474–483.

Qun, Y., et al., (2014). Temperature modeling of PEM Fuel Cell based on fuzzy strategy. *The 26th Chinese Control and Decision Conference, China.*

Ralph, T. and Hogarth, M. (2002). Catalysis for low temperature fuel cells. *Platinum Metals Review* 46:117–135.

Restrepo, C., Konjedic, T., Garces, A., Calvente, J. and Giral, R. (2015). Identification of a Proton-Exchange Membrane Fuel Cell's model parameters by means of an evolution strategy. *IEEE Trans. Ind. Informatics* 11(2) : 548–559.

Restrepo, C., Garcia, G., Calvente, J., Giral, R. and Martínez-Salamero, L. (2016). Static and dynamic current-voltage modeling of a Proton Exchange Membrane Fuel Cell using an input-output diffusive approach. *IEEE Transactions on Industrial Electronics* 63(2): 1003–15.

San, F., B., Dursun, S. and Yazici, M. (2019). Optimization of the PEMFC operating parameters for cathode in the presence of PtCo/CVD graphene using factorial design. *International Journal of Energy Research* 43(9): 4506–4519.

Said, Z., Alshehhi, A. and Mehmood, A. (2018). Predictions of UAE's renewable energy mix in 2030. *Renewable Energy* 118: 779–789.

Salim, R., Noura, H. and Fardoun, A. (2017). Fault diagnosis of a commercial PEM Fuel Cell system using LMS AMESim. *7th International Conference on Modeling, Simulation, and Applied Optimization (ICMSAO), UAE.*

Salim, R., Nabag, M., Noura, H. and Fardoun, A. (2015). The parameter identification of the Nexa 1.2kW PEMFC's model using particle swarm optimization. *Renewable Energy* 82: 26–34.

Shareef, H., Ibrahim, A. and Mutlag, A. (2015). Lightning Search Algorithm. *Applied Soft Computing Journal* 36: 315–333.

Sharma, A., Birgersson, E. and Khor, S. (2014). Computationally-Efficient hybrid strategy for mechanistic modeling of fuel cell stacks. *Journal of Power Sources* 247: 481–488.

Soltani, M. and Bathaee, S. (2008). A new dynamic model considering effects of temperature, pressure and internal resistance for PEM Fuel Cell power modules. *3rd International Conference on Deregulation and Restructuring and Power Technologies, DRPT, China.*

Springer, T., Zawodzinski, T. and Gottesfeld S. (1993). Polymer Electrolyte Fuel Cell Model. *J. Electrochem. Soc.* 138(8): 2334–2342.

Steiner N., Y., Hissel, D., Moçotéguy, P. and Candusso D. (2011). Non intrusive diagnosis of Polymer Electrolyte Fuel Cells by wavelet packet transform. *International Journal of Hydrogen Energy* 36(1): 740–746.

Sun, Z., Wang, N., Bi, Y. and Srinivasan, D. (2015). Parameter identification of PEMFC model based on hybrid adaptive differential evolution algorithm. *Energy* 90: 1334–1341.

Taieb, A., Mukhopadhyay, B. and Al-Othman, Z. (2019). Dynamic model of a Proton-Exchange Membrane Fuel Cell using equivalent electrical circuit. *Advances in Science and Engineering Technology International Conferences (ASET), UAE.*

Tao, S., Si-Jia, Y., Guang-yi, C. and Xin-Jian Z. (2005). Modelling and control PEMFC using fuzzy neural networks. *Journal of Zhejiang University-Science A* 6(10): 1084–1089.

Um, S., Wang, C. and Chen K. (2000). Computational fluid dynamics modeling of Proton Exchange Membrane Fuel Cells. *J. Electrochem. Soc.* 147 (12) 4485-4493.

Ustinov, A., Khayrullina, A., Sveshnikova, A. and Abrosimov, A. (2016). Effect of inlet air temperature and relative humidity on performance of PEM Fuel Cell. *12th International Conference on Heat Transfer, Fluid Mechanics and Thermodynamics, Spain.*

Werner, C., et al., (2015). Characteristics of PEMFC operation in ambient and lowpressure environment considering the fuel cell humidification. *CEAS Aeronautical Journal* 6(2): 229–243.

Wishart, J., Dong, Z. and Secanell, M. (2006). Optimization of a PEM Fuel Cell system based on empirical data and a generalized electrochemical semi-empirical model. *Journal of Power Sources* 161(2): 1041–1055.

Wong, K., et al., (2011). A theoretical study of inlet relative humidity control in PEM Fuel Cell. *International Journal of Hydrogen Energy* 36(18): 11871–11885.

Wu, B., et al., (2006). An improved dynamic model considering effects of temperature and equivalent internal resistance for PEM Fuel Cell power modules. *Journal of Power Sources* 161 (2): 1062–1068.

Wensheng, H., Guangyu L. and Nguyen T. (2004). Diagnostic tool to detect electrode flooding in Proton-Exchange-Membrane Fuel Cells. *Materials, Interfaces, and Electrochemical Phenomena* 49:3221–3228.

Xing, J., et al., (2017). Two-Dimensional analytical model of a Proton Exchange Membrane Fuel Cell. *Energy* 119: 299–308.

Xu, S., Wang, Y. and Wang, Z. (2019). Parameter estimation of Proton Exchange Membrane Fuel Cells using eagle strategy based on JAYA Algorithm and Nelder-Mead Simplex Method. *Energy* 173: 457–467.

Yan, Q., Qing, L., Peichang, Z. and Datai, Y. (2014). Temperature modeling of PEM Fuel Cell based on fuzzy strategy. *The 26th Chinese Control and Decision Conference, China.*

Yang, Z., et al., (2019). Effects of operating conditions on water and heat management by a transient multi-dimensional PEMFC system model. *Energy* 183 : 462–476.

Yousfi-Steiner, N., et al., (2008). A review on PEM voltage degradation associated with water management: impacts, influent factors and characterization. *Journal of Power Sources* 183: 260–274.

Yildiz, B. and Kazimi, M. (2006). Efficiency of hydrogen production systems using alternative nuclear energy technologies. *International Journal of Hydrogen Energy*, 31: 77–92.

Zhang, G., and Xie, J. (2019). Three-Dimensional multi-scale simulation for large-scale Proton Exchange Membrane Fuel Cell. *WCX SAE World Congress Experience, USA.*

Zhang, J., et al., (2008). PEM Fuel Cell relative humidity (RH) and its effect on performance at high temperatures. *Electrochimica Acta* 53(16): 5315–5321.

Zheng, Z., et al., (2013). A review on non-model based diagnosis methodologies for PEM Fuel Cell stacks and systems. *International Journal of Hydrogen* energy 38: 8914–8926.

Živko D. and Bilas, V. (2006). Analysis of individual PEM Fuel Cell operating parameters for design of optimal measurement and control instrumentation, *IMEKO Event Proceedings, Brazil.*

List of publications

Journals Published:

Saad Saleem Khan, Hussain Shareef et al., (2018). Novel dynamic semiempirical proton exchange membrane fuel cell model incorporating component voltages, *International Journal of Energy Research* 42 (8): 2615-2630. (Journal Impact Factor: 3.343)

Saad Saleem Khan, Hussain Shareef et al., (2019). Influences of ambient conditions on the performance of proton exchange membrane fuel cell using various models. *Energy and Environment* 30 (6): 1087–1110. (Journal Impact Factor: 1.092)

Saad Saleem Khan, Hussain Shareef et al., (2019). Dynamic temperature model for proton exchange membrane fuel cell using online variations in load current and ambient temperature. *International Journal of Green Energy* 16(5): 361-370. (Journal Impact Factor: 1.302)

Saad Saleem Khan, Hussain Shareef et al., (2019). Membrane-hydration-state detection in proton exchange membrane fuel cells using improved ambient-condition-based dynamic model. International Journal of Energy Research *Status: Published online, yet to come in volume*. (Journal Impact Factor: 3.343)

Journal accepeted:

Saad Saleem Khan, Hussain Shareef et al., (2019). Improved Semi-Empirical Model of Proton Exchange Membrane Fuel Cell Incorporating Fault Diagnostic Feature. Journal of Modern Power Systems and Clean Energy *Status: accepted, will publish soon (Manuscript ID :MPCE-D-19-00179R2).* (Journal Impact Factor: 2.848)

Conferences Published:

Saad Saleem Khan, Awais Rafiq, Hussain Shareef et al., (2018). Parameter optimization of PEMFC model using backtracking search algorithm. 5th International Conference on Renewable Energy: Generation and Applications (ICREGA), UAE.

Saad Saleem Khan, Hussain Shareef et al., (2018). An Improved No-load Voltage Model for Proton Exchange Membrane Fuel Cell Systems using Curve Fitting Method. 6th International Renewable and Sustainable Energy Conference (IRSEC), UAE.

Saad Saleem Khan, Vikram B., Hussain Shareef et al., (2019). Effect of ambient conditions on water management and faults in PEMFC systems: A Review. The annual IEEE Canadian conference on electrical and computer engineering, Canada.